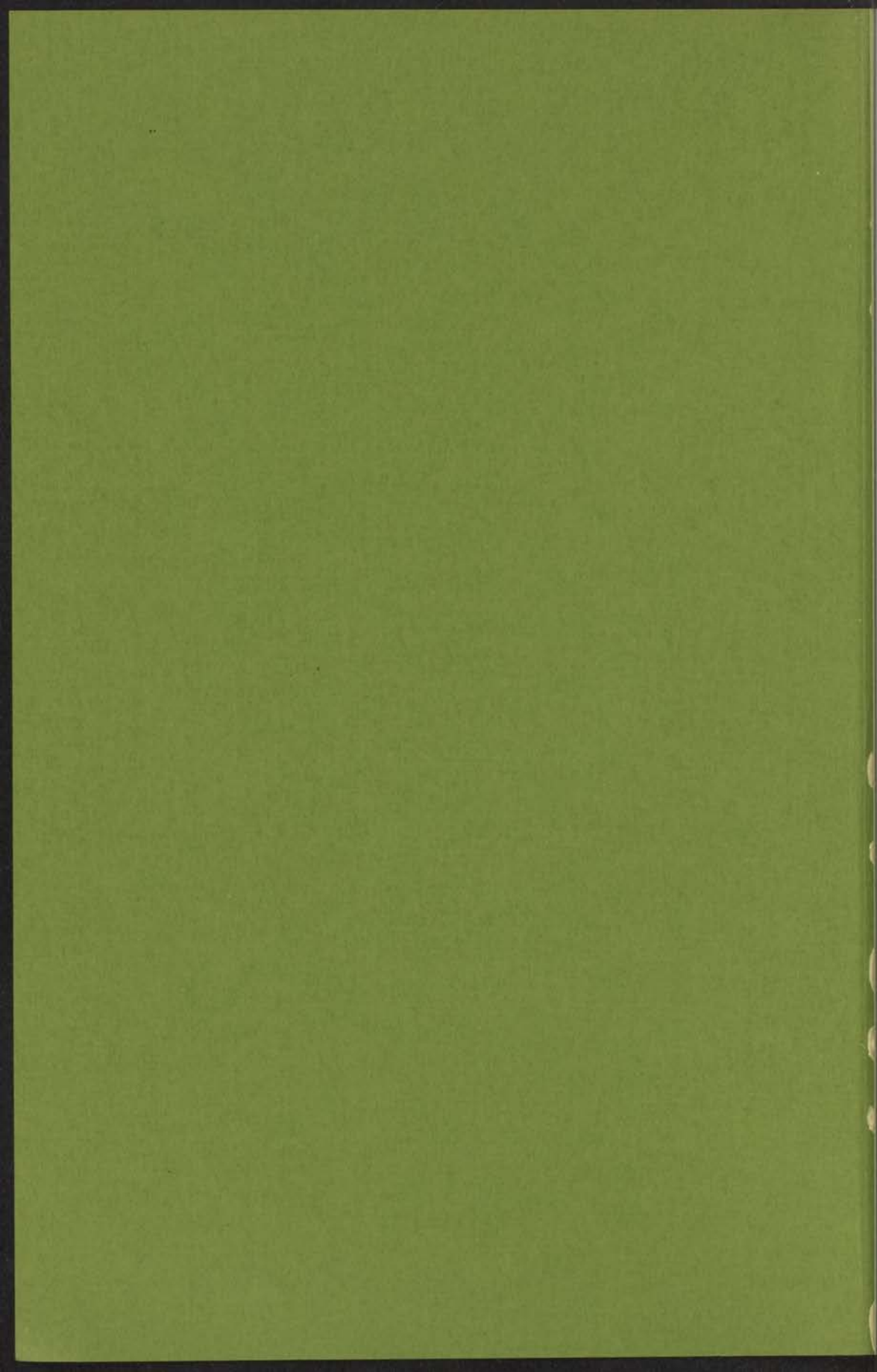


THE VISCOMAGNETIC EFFECT

INSTITUUT-LABORIJN
voor theoretische natuurkunde
Nieuwsteeg 16-Leyden-Nederlands

H. HULSMAN



22 APR. 1974

THE VISCOMAGNETIC EFFECT

PROEFSCHRIJF

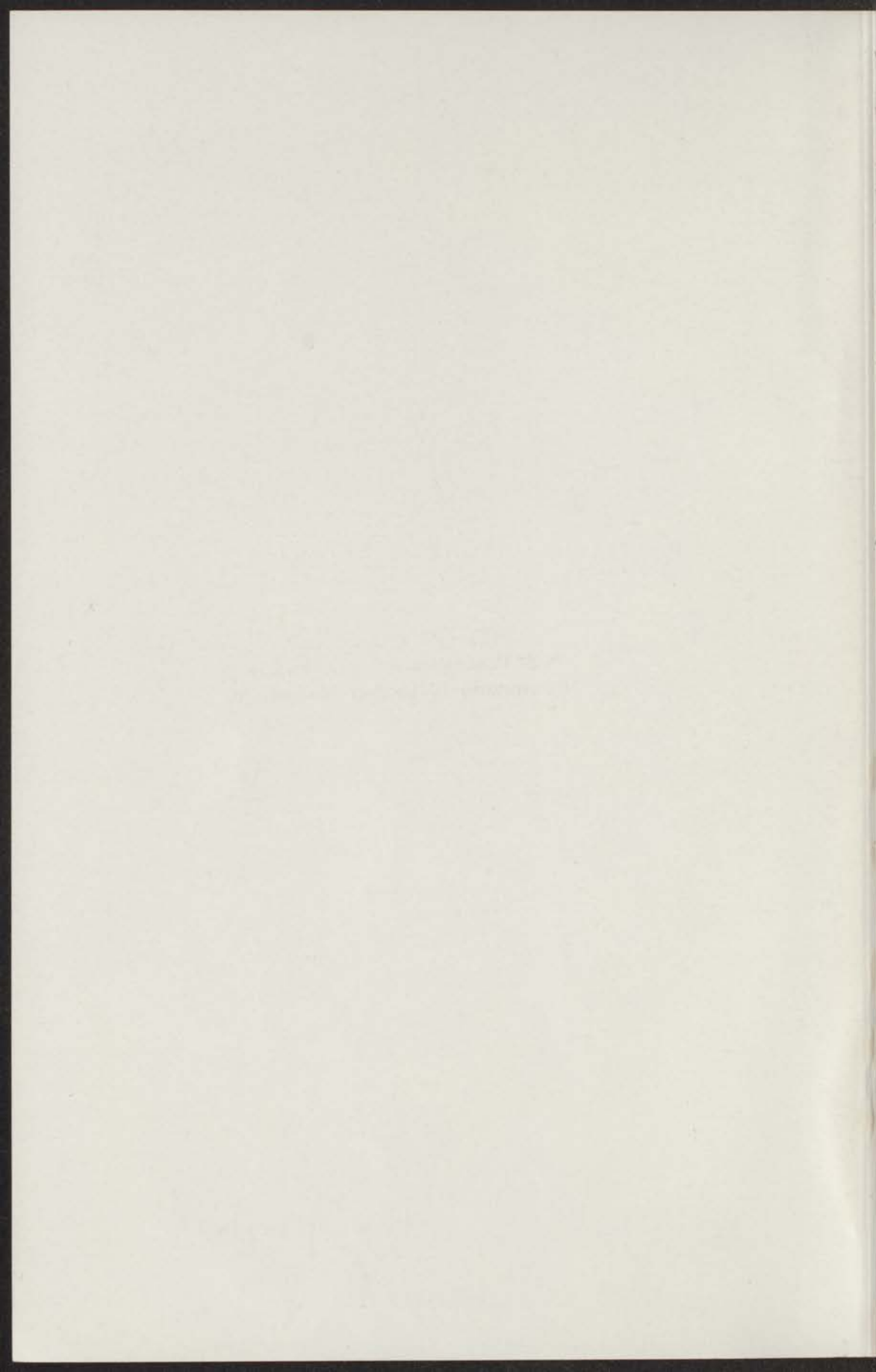
TEGEN AANVAARDING VAN DE GRADE VAN DOCTOR
IN DE WISSENSCHAP VAN NADONANDETSCHAPPER VAN DE
UNIVERSITEIT VAN LEIDEN
AANVAARDING VAN DE DOCTOR WAGNERING VAN DE
UNIVERSITEIT VAN LEIDEN
IN DE FACULTEIT DER WISSENSCHAPEN
TEGEN AANVAARDING VAN DE GRADE VAN DOCTOR
IN DE WISSENSCHAP VAN NADONANDETSCHAPPER VAN DE
UNIVERSITEIT VAN LEIDEN

THE VISCOMAGNETIC EFFECT

INSTITUUT-LORENTZ

voor theoretische natuurkunde
Nieuwsteeg 18-Leiden-Nederland

kast dissertaties



THE VISCOMAGNETIC EFFECT

PROEFSCHRIFT

TER VERKRIJGING VAN DE GRAAD VAN DOCTOR
IN DE WISKUNDE EN NATUURWETENSCHAPPEN AAN DE
RIJKSUNIVERSITEIT TE LEIDEN,
OP GEZAG VAN DE RECTOR MAGNIFICUS DR. W. R. O. GOSLINGS,
HOOGLEERAAR IN DE FACULTEIT DER GENEESKUNDE,
TEN OVERSTAAN VAN EEN COMMISSIE UIT DE SENAAAT
TE VERDEDIGEN OP WOENSDAG 13 OKTOBER 1971
TE KLOKKE 15.15 UUR

DOOR

HERMAN HULSMAN

GEBOREN TE DEN HAAG IN 1940

1971

KONINKLIJKE DRUKKERIJ VAN DE GARDE N.V.
ZALTBOMMEL

THE VISCOMAGNETIC EFFECT

PROEFSCHRIFT

TER VERKRIJGING VAN DE GRAAD VAN DOCTOR
IN DE WISNETHEDE EN NATUURWETENSCHAPPEN VAN DE
RYSCH-ROSSISCHE UNIVERSITEIT VAN LEIDEN
OP VERZAAK VAN DE RECTOR-MAGISTRUS DE W. A. BOUWMEESTER
HIERVOR VERZAAKT DE CANDIDAAT DER WETENSCHAPPEN
DE OVERSTAAFT VAN DE UNIVERSITEIT VAN DE BRUSSEL
DE VERBODENDE DE WETENSCHEDE 13 OKTOBER 1910

Promotor: PROF. DR. J. J. M. BEENAKKER

Dit proefschrift is tot stand gekomen mede onder leiding van
DR. H. F. P. KNAAP

HERMAN HUISMAN

LEIDEN IN DEN MAI VAN 1910

1910
WETENSCHEDELIJKE BOEKVERHANDELING VAN DE WETENSCHEDE
VAN LEIDEN

STELLINGEN

I

Door in één apparaat zowel een even als een oneven viscositeits-coëfficiënt te meten, kan men reorientatie-cross-secties bepalen voor een aantal gassen, waarvoor dit tot op heden niet mogelijk was.

Dit proefschrift.

II

Het is gewenst om de door Parson en Lee op grond van bundeexperimenten voorgestelde potentiaal te testen door berekening van zowel evenwichts- en transporteigenschappen als van kristaleigenschappen.

J. M. Parson en Y. T. Lee, 3e symp. int. jets moléculaires, Cannes 1971.

III

De spin-rooster relaxatie van Mn^{2+} in $ZnSiF_6 \cdot 6H_2O$ beneden 5 K wordt door Thompson en Nolle geïnterpreteerd als een direct proces. Deze interpretatie vindt onvoldoende steun in hun experimenten.

B. C. Thompson en A. W. Nolle, Phys. Rev. **180** (1969) 396.

IV

De door Moraal en McCourt voorgestelde methode voor het bepalen van moleculaire g -factoren is onbetrouwbaar.

H. Moraal en F. R. McCourt, Phys. Rev. **A4** (1971) 511.

Bij thermodiffusie-experimenten bepaalt men meestal de thermodiffusieverhouding k_T . In aanwezigheid van een magnetisch veld wordt dit een tweedegrads tensor, die drie verschillende elementen bevat: k_T^{\parallel} , k_T^{\perp} en k_T^{tr} . Voor het aantonen van een veld-effect is k_T^{tr} te prefereren; in een apparaat zoals beschreven in hoofdstuk V van dit proefschrift kan voor k_T^{tr} een gevoeligheid bereikt worden die een factor 10 tot 100 groter is dan die bereikt is in de tot op heden verrichte experimenten aan k_T^{\perp} .

A. Tip, A. E. de Vries en J. Los, *Physica* **32** (1966) 1429.

M. A. Hidalgo, J. M. Savirón en D. González, *Physica* **46** (1970) 41.

VI

De overgangspunten van $\text{ErCl}_3 \cdot 6\text{H}_2\text{O}$ en $\text{DyCl}_3 \cdot 6\text{H}_2\text{O}$ kunnen op een relatieve temperatuurschaal eenvoudig bepaald worden met een nauwkeurigheid van 10^{-4} K. Zij kunnen gebruikt worden als vaste punten in een praktische temperatuurschaal beneden 1 K.

E. Lagendijk, R. F. Wielinga en W. J. Huiskamp, *Phys. Letters* **31A** (1970) 375.

VII

Het valt te betreuren dat Foch en Ford bij hun wens naar nauwkeurige acoustische metingen aan edelgassen, geen rekening gehouden hebben met de ongevoeligheid van hun theoretische berekeningen voor de precieze vorm van realistische moleculaire wisselwerkingspotentialen.

J. D. Foch en G. W. Ford, "The dispersion of sound in monoatomic gases" in *Studies in Statistical Mechanics*, edited by J. de Boer and G. E. Uhlenbeck (North-Holland Publ. Comp., Amsterdam, 1970) Vol. V, p. 216.

VIII

Voor de interpretatie van experimenten met supersone bundels van meeratomige moleculen dient men te beschikken over gegevens betreffende de bezetting van de inwendige toestanden van de moleculen in de bundel.

IX

Er zijn aanwijzingen dat bij vorming van moleculaire waterstof aan koude oppervlakken ($H + H \rightarrow H_2$) een belangrijk deel van de reactiewarmte wordt afgevoerd door het gevormde molecuul in de vorm van inwendige (vibratie) energie. In interstellaire wolken zullen aldus gevormde moleculen door straling deëxciteren. Het is zeer wel mogelijk dat deze straling van voldoende intensiteit is om waargenomen te kunnen worden.

X

De gebruikelijke manier waarop voor meer-atomige gassen uit viscositeitsmetingen de parameters van het hoek-onafhankelijke deel van de potentiaal bepaald worden, houdt ten onrechte geen rekening met de bijdrage van inelastische botsingen.

stand met behulp van de methode van de vloeistof- of gaschromatografie met een detector van de type kathodische straal. De vloeistofchromatografie werd toegepast op de analyse van de vloeistofoplossingen van de reactieproducten. De gaschromatografie werd toegepast op de analyse van de gaseuze reactieproducten. De vloeistofchromatografie werd toegepast op de analyse van de vloeistofoplossingen van de reactieproducten. De gaschromatografie werd toegepast op de analyse van de gaseuze reactieproducten.

A. T. P. N. K. J. van der Vliet en J. van der Vliet, *J. Chem. Phys.* 43 (1965) 1327.

W. A. Pryor, J. W. Szwarc, en D. L. Buehler, *J. Am. Chem. Soc.* 87 (1965) 1111. De auteurs hebben de reactie van $\text{C}_2\text{H}_5\text{I}$ met $\text{C}_2\text{H}_5\text{MgBr}$ in een aantal oplosmiddelen onderzocht. De reactie wordt beschreven als een $\text{S}_{\text{N}}2$ -proces. De reactie wordt beschreven als een $\text{S}_{\text{N}}2$ -proces. De reactie wordt beschreven als een $\text{S}_{\text{N}}2$ -proces.

VI

protonen uitwisseling

De overgangspunten van $\text{Et}_2\text{O} \cdot \text{CH}_2\text{O}$ en $\text{Et}_2\text{O} \cdot \text{OH}_2$ kunnen op een relative temperatuurschaal verweerd bepaald worden met een nauwkeurigheid van 10^{-4} K. Zij kunnen gebruikt worden als vaste punten in een nauwkeurige temperatuurschaal bereikend 1 K.

K. L. Boring, W. F. Winters en W. J. Bartok, *Phys. Letters* 20 (1966) 325.

VII

Het valt te betwijfelen dat Fock en Ford bij hun studie naar interacties van moleculaire bewegingen met elektronen geen rekening gehouden hebben met de aanwezigheid van hun theoretische berekeningen van de positieve en negatieve ionisatiepotentiaal van moleculaire wisselwerkingspotentiaal.

J. D. Fock en G. W. Ford, "The Spectrum of a Bonded Electron," *J. Chem. Phys.* 43 (1965) 1111. De auteurs hebben de reactie van $\text{C}_2\text{H}_5\text{I}$ met $\text{C}_2\text{H}_5\text{MgBr}$ in een aantal oplosmiddelen onderzocht. De reactie wordt beschreven als een $\text{S}_{\text{N}}2$ -proces. De reactie wordt beschreven als een $\text{S}_{\text{N}}2$ -proces.

VIII

Voor de interpretatie van experimenten met organische moleculen moet men de beschikbare gegevens over de reactie van de moleculen met de reagenten nauwkeurig bekijken.

CONTENTS

Preface	v
Chapter I—Experimental methods	1
1. Introduction	2
2. The apparatus of author	4
3. The flow through a cylindrical capillary	5
4. Applications	9
Chapter II—The oil-filled multi-capillary and its	11
1. Introduction	11
2. Experimental method and apparatus	11
2.1. General	11
2.2. Apparatus	12
3. Measuring procedure and calculation of viscosity	14
3.1. Measurement of different capillaries of the multi-capillary	14
3.2. Determination of the pressure gradient along the capillary	16
3.3. Source of systematic errors	17
3.3.1. Expansion of the gas	18
3.3.2. Pressure at the inlet side	18
3.3.3. Short-circuiting by the ends of the capillary	18
3.3.4. Variation of the pressure along the capillary	20
3.3.5. Interogeneity of the flow resistance	21
Aan mijn ouders	25
Aan Greet	25

Het in dit proefschrift beschreven onderzoek werd uitgevoerd als onderdeel van het programma van de werkgemeenschap voor Molecuulfysica van de Stichting voor Fundamenteel Onderzoek der Materie (F.O.M.) met financiële steun van de Nederlandse Organisatie voor Zuiver Wetenschappelijk Onderzoek (Z.W.O.)

CONTENTS

PREFACE	1
CHAPTER I - <i>Experimental methods</i>	3
1. Introduction	3
2. The equations of motion	4
3. The flow through a rectangular capillary	5
4. Applications	9
CHAPTER II - <i>The odd-in-field coefficients η_4 and η_5</i>	11
1. Introduction	11
2. Experimental method and apparatus	11
2.1 General	11
2.2 Apparatuses	12
3. Measuring procedure and calculation of the results	14
3.1 Measurements for different orientations of the magnetic field	14
3.2 Determination of the pressure gradient along the capillary	15
3.3 Sources of systematic errors	17
3.3.1 Expansion of the gas	18
3.3.2 Presence of the short sides	18
3.3.3 Short-circuiting by the ends of the capillary	18
3.3.4 Variation of the pressure along the capillary	20
3.3.5 Inhomogeneity of the flow resistance	21
3.4 Knudsen corrections	21
3.5 Comparison and combination of the results of the two capillaries	23
4. Experimental results and discussion	25

CHAPTER III – <i>The odd-in-field coefficients η_4 and η_5 for O_2</i>	35
1. Introduction	35
2. Experiment	36
3. Experimental results and discussion	36
3.1 The dependence on H/p	37
3.2 The deviations from H/p	39
CHAPTER IV – <i>The even-in-field coefficients η_1, η_2 and η_3</i>	42
1. Introduction	42
2. Experimental method	43
3. Corrections.	45
3.1 Presence of the short sides	45
3.2 Deviations from the ideal Poiseuille flow.	47
3.2.1 Reynolds correction	47
3.2.2 Expansion correction	48
3.2.3 Knudsen corrections	48
3.3 Stray fields	49
4. Experimental results and discussion	49
Appendix	60
CHAPTER V – <i>Thermomagnetic slip in rarefied polyatomic gases</i>	63
SAMENVATTING	67

For reference purposes it may be useful to note that the work reported in this thesis is also published in *Physica*:

- Chapter I: *Physica* 50 (1970) 565
- Chapter II: *Physica* 50 (1970) 53
- Chapter III: *Physica* 50 (1970) 558
- Chapter IV: *Physica*, in print
- Chapter V: *Physica*, in print

PREFACE

In this thesis experiments are described which measure the influence of an external magnetic field on the viscosity, η , of polyatomic gases. In the general case of a viscous medium the momentum fluxes and the velocity gradients are connected through a fourth rank viscosity tensor. For a gas in a homogeneous magnetic field it can be shown by symmetry arguments that this tensor contains only seven independent elements. Five of these elements are shear viscosity coefficients and are called η_1, \dots, η_5 . The coefficients η_1, η_2 and η_3 are even functions of the field and become in the absence of a field equal to η_0 , the field free shear viscosity coefficient. The coefficients η_4 and η_5 are odd functions of the field and are zero in the field free case.

In chapter I it is shown that the five coefficients may be separately determined by using two experimental arrangements. In each apparatus the flow of gas through a flat capillary is studied and the (changes of) pressure differences, which occur under the influence of the field are measured. The odd-in-field coefficients are determined by measuring transverse pressure differences that occur under the influence of the field. It is possible to determine η_4 and η_5 separately under nearly the same experimental conditions by performing measurements for different orientations of the field. In the second type of experiment one measures the change of the pressure difference over the length of the capillary. By measuring these changes for different orientations of the field with respect to the capillary it is possible to determine η_1, η_2 and η_3 separately.

Results of experiments on the odd-in-field coefficients are given in chapters II and III. First the calculation of η_4 and η_5 from the observed transverse pressure differences is treated in some detail. Experiments on the dependence of the pressure difference on the dimensions of the capillary are

described, several corrections are determined and systematic errors are estimated. Results are presented for the gases N_2 , CO, HD and CH_4 at room temperature. Comparing the results with theory it is found that the dominant contribution to the effect stems from the $[J]^{(2)}$ anisotropy of the distribution of angular momentum J . In chapter III the results for η_4 and η_5 for O_2 are given. These coefficients show a complicated dependence on field and pressure.

Experiments on the even coefficients are described in chapter IV. The coefficients η_1 , η_2 and η_3 are determined for the gases N_2 , CO, HD, CH_4 and CF_4 ; the results appear to be consistent with those for η_4 and η_5 . The $[J]^{(2)}$ contribution is again found to be dominant and the values for the effective cross sections, in terms of which the results can be expressed, are in very good agreement with the values derived from η_4 and η_5 . The small deviations from a pure $[J]^{(2)}$ behaviour that have been found in all cases are discussed. In an appendix some remarks are made on the use of effective cross sections.

In chapter V some preliminary results are reported of measurements of a new phenomenon: thermomagnetic slip. It appears that in a rarefied gas the combined action of a temperature gradient and a magnetic field can give rise to a slip velocity along the wall.

CHAPTER I

EXPERIMENTAL METHODS

Synopsis

In the presence of a magnetic field the ordinary Navier-Stokes equations for a polyatomic gas are replaced by more complicated expressions, in which five independent shear-viscosity coefficients appear. It is shown that all five coefficients can be determined separately by using two experimental arrangements.

1. *Introduction.* In the presence of a magnetic field the stress tensor for a gas of rotating molecules loses its isotropic character¹). As a consequence the ordinary Navier-Stokes equations are replaced by more complicated equations of motion, in which seven - rather than two - independent viscosity coefficients appear^{2,3}). Careful consideration of these equations allows the determination of simple conditions under which the five shear-viscosity coefficients can be obtained. The present paper describes experimental arrangements which allow the determination of these coefficients.

A discussion (see section 2) of the generalized Navier-Stokes equations in the presence of a magnetic field requires a knowledge of certain general properties of the magnetic field viscosity effects in polyatomic gases. For this purpose, the relevant experimental facts are summarized as follows.

- a) The effects of the field on the viscosity coefficients are small, at most of the order 10^{-2} of the field-free viscosity coefficient.
- b) The effect is a unique function of H/p (H = field strength, p = pressure) for a given gas at a fixed temperature.
- c) For an experimental investigation values of H/p as high as 10^4 Oe/torr are required for most gases. Due to this last-mentioned fact, high fields and/or low pressures are required. These features restrict the choice of possible experimental arrangements.

The methods for measuring viscosity of fluids fall into two groups:

firstly the flow-through viscometers and secondly the viscometers with rotating, oscillating or falling bodies in the fluid. For the measurement of the magnetic field effects both methods have their drawbacks: low-pressure measurements in flow-through viscometers are unreliable because of Knudsen effects, while the viscometers of the second group are easily disturbed by high magnetic fields. Since the effects to be measured in a magnetic field are small, a differential measuring arrangement is preferable. This is done most easily with flow-through viscometers. Almost all measurements have been performed using this type of experimental setup and therefore what follows will also be limited to such arrangements.

2. *The equations of motion.* In its general form, the viscous pressure tensor \mathbf{II} is linked to the velocity gradient tensor $\mathbf{V}\mathbf{v}$ by a fourth-rank viscosity tensor. For an isotropic fluid symmetry arguments require that this tensor contains only two independent elements: the shear-viscosity coefficient η coupling the symmetric traceless pressure tensor $\overset{\circ}{\mathbf{II}}^s$ to the symmetric traceless velocity gradient tensor $(\mathbf{V}^{\circ}\mathbf{v})^s$ and the volume viscosity coefficient η_v coupling the trace \mathbf{II} to the divergence of the flow velocity, *viz.*,

$$\overset{\circ}{\mathbf{II}}^s = -2\eta(\mathbf{V}^{\circ}\mathbf{v})^s, \quad \mathbf{II} = -\eta_v \mathbf{V} \cdot \mathbf{v}. \quad (1)$$

The application of an external magnetic field lowers the spatial symmetry so that a more complex behaviour may be expected. This problem has been treated by De Groot and Mazur in their book on non-equilibrium thermodynamics³). They show that when an external magnetic field influences an originally isotropic fluid, seven independent coefficients are needed to describe the viscous behaviour. If the external field is chosen in the x direction, the scheme I connecting $\overset{\circ}{\mathbf{II}}^s$ and \mathbf{II} to $(\mathbf{V}^{\circ}\mathbf{v})^s$ and $\mathbf{V} \cdot \mathbf{v}$ was obtained³):

SCHEME I

	$(\mathbf{V}^{\circ}\mathbf{v})_{xx}^s$	$(\mathbf{V}^{\circ}\mathbf{v})_{yy}^s$	$(\mathbf{V}^{\circ}\mathbf{v})_{zz}^s$	$(\mathbf{V}^{\circ}\mathbf{v})_{yz}^s$	$(\mathbf{V}^{\circ}\mathbf{v})_{zx}^s$	$(\mathbf{V}^{\circ}\mathbf{v})_{xy}^s$	$\mathbf{V} \cdot \mathbf{v}$
$\overset{\circ}{\mathbf{II}}_{xx}^s$	$-2\eta_1$	0	0	0	0	0	-2ζ
$\overset{\circ}{\mathbf{II}}_{yy}^s$	0	$-2\eta_2$	$-2(\eta_1 - \eta_2)$	$-2\eta_4$	0	0	ζ
$\overset{\circ}{\mathbf{II}}_{zz}^s$	0	$-2(\eta_1 - \eta_2)$	$-2\eta_2$	$2\eta_4$	0	0	ζ
$\overset{\circ}{\mathbf{II}}_{yz}^s$	0	η_4	$-\eta_4$	$2\eta_1 - 4\eta_2$	0	0	0
$\overset{\circ}{\mathbf{II}}_{zx}^s$	0	0	0	0	$-2\eta_3$	$-2\eta_5$	0
$\overset{\circ}{\mathbf{II}}_{xy}^s$	0	0	0	0	$2\eta_5$	$-2\eta_3$	0
\mathbf{II}	-2ζ	ζ	ζ	0	0	0	$-\eta_v$

In this scheme η_1 , η_2 , η_3 , ζ and η_v are even functions of the magnetic field, while η_4 and η_5 are odd. The coefficients $\eta_1, \eta_2, \dots, \eta_5$ are shear-viscosity coefficients, because they connect the components of $\overset{\circ}{\mathbf{II}}^s$ to the components

of $(\nabla \circ \mathbf{v})^s$. The coefficient η_v connects the traces Π and $\nabla \cdot \mathbf{v}$ and is therefore the volume viscosity, while ζ describes a cross effect between shear and volume viscosities. This scheme can be utilized to write down the equations of motion which, in the absence of external forces* and neglecting the dependence of the coefficients on the space coordinates**, have the forms:

$$\begin{aligned}
 \rho \frac{dv_x}{dt} + \frac{\partial p}{\partial x} &= (2\eta_1 - \eta_3 + 3\zeta) \frac{\partial^2 v_x}{\partial x^2} + \eta_3 \frac{\partial^2 v_x}{\partial y^2} + \eta_3 \frac{\partial^2 v_x}{\partial z^2} \\
 &+ \eta_5 \frac{\partial^2 v_y}{\partial x \partial z} - \eta_5 \frac{\partial^2 v_z}{\partial x \partial y} + (\eta_3 - \frac{2}{3}\eta_1 + \zeta + \eta_v) \frac{\partial}{\partial x} (\nabla \cdot \mathbf{v}), \\
 \rho \frac{dv_y}{dt} + \frac{\partial p}{\partial y} &= + \eta_3 \frac{\partial^2 v_y}{\partial x^2} + (2\eta_2 - \eta_3 - 3\zeta) \frac{\partial^2 v_y}{\partial y^2} + (2\eta_2 - \eta_1) \frac{\partial^2 v_y}{\partial z^2} \\
 &- \eta_5 \frac{\partial^2 v_z}{\partial x^2} + \eta_4 \frac{\partial^2 v_z}{\partial y^2} + \eta_4 \frac{\partial^2 v_z}{\partial z^2} \\
 &- \eta_5 \frac{\partial^2 v_x}{\partial x \partial z} + (\eta_1 - \eta_3 - 3\zeta) \frac{\partial^2 v_z}{\partial y \partial z} + (\eta_3 - \frac{2}{3}\eta_1 + \zeta + \eta_v) \frac{\partial}{\partial y} (\nabla \cdot \mathbf{v}), \\
 \rho \frac{dv_z}{dt} + \frac{\partial p}{\partial z} &= + \eta_3 \frac{\partial^2 v_z}{\partial x^2} + (2\eta_2 - \eta_1) \frac{\partial^2 v_z}{\partial y^2} + (2\eta_2 - \eta_3 - 3\zeta) \frac{\partial^2 v_z}{\partial z^2} \\
 &+ \eta_5 \frac{\partial^2 v_y}{\partial x^2} - \eta_4 \frac{\partial^2 v_y}{\partial y^2} - \eta_4 \frac{\partial^2 v_y}{\partial z^2} \\
 &+ \eta_5 \frac{\partial^2 v_x}{\partial x \partial y} + (\eta_1 - \eta_3 - 3\zeta) \frac{\partial^2 v_y}{\partial x \partial z} + (\eta_3 - \frac{2}{3}\eta_1 + \zeta + \eta_v) \frac{\partial}{\partial z} (\nabla \cdot \mathbf{v}).
 \end{aligned} \tag{2}$$

In the field-free case $\eta_1 = \eta_2 = \eta_3 = \eta_0$ and $\eta_4 = \eta_5 = \zeta = 0$, and these equations reduce to the well-known Navier-Stokes equations:

$$\rho \frac{d\mathbf{v}}{dt} + \nabla p = \eta_0 \nabla^2 \mathbf{v} + (\frac{1}{3}\eta_0 + \eta_v) \nabla (\nabla \cdot \mathbf{v}). \tag{3}$$

In view of the complexity of the equations of motion [eqs. (2)], it is useful to seek simple experimental situations, *i.e.*, situations where in the absence of the field only a few of the second derivatives $\partial^2 v_\alpha / \partial x_\beta \partial x_\gamma$ are of importance.

3. *The flow through a rectangular capillary.* The most simple situation is found in the case of a straight capillary with a rectangular cross section (length l , width w and thickness t) as illustrated in fig. 1. When the dimensions are chosen such that $l \gg w \gg t$, only one velocity component

* *e.g.*, gravitation and magnetic field gradients.

** For actual experiments this assumption is not trivial: the coefficients are functions of H/p and so even in a homogeneous field a pressure gradient makes the coefficients dependent on the space coordinates. Terms with $\nabla \eta(H/p)$ will, however, be neglected.

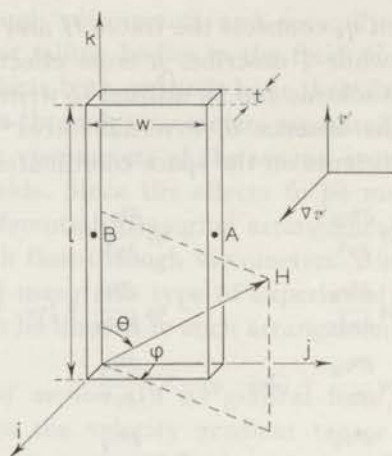


Fig. 1. Schematic diagram of a capillary with a rectangular cross section.

(along l) and one velocity-gradient component (along t) are of importance. The influence of the magnetic field on the flow through this slit can be studied as a function of the orientation of the field. Two essentially different types of experiments can be carried out with such a capillary: a) "Longitudinal experiments" in which the change of the flow resistance is followed, *e.g.*, by monitoring the change in the pressure gradient along the capillary when the flow is kept constant. This is done most elegantly by placing the capillary with three other capillaries in a "Wheatstone-bridge" arrangement (see *e.g.* ref. 4). b) "Transverse experiments" in which transverse pressure gradients caused by the field are observed, *e.g.*, by connecting a differential manometer across two tiny holes A and B in the narrow sides of the capillary (see fig. 1) and thereby measuring the pressure difference over the width of the capillary. In principle, yet a third type of experiment can be imagined, *viz.*, the measurement of pressure gradients arising in the direction of the gradient of the velocity. This is, however, experimentally unfeasible as the resulting pressure difference over the small dimension t is too small. Furthermore, the holes in these walls needed for the pressure measurement would disturb the flow pattern rather drastically.

It will be shown here that by measuring with the field in different orientations with respect to the capillary it is possible to determine separately all five shear viscosity coefficients with the above-mentioned two types of experiments.

In the absence of a field all second derivatives of the velocity in the capillary of fig. 1 can be neglected except $\partial^2 v_k / \partial i^2$. Since all field effects are small (at most 10^{-2} of η_0), this remains true even in the presence of a field. Furthermore the changes in all coefficients are of the same order of magni-

tude. Thus the changes caused by the field will be connected with the derivative $\partial^2 v_k / \partial i^2$ only.

In eqs. (2) the equations of motion are given in the (x, y, z) coordinate system with the field in the x direction. For the description of the experiment, however, it is preferable to have these equations in the capillary-fixed (i, j, k) system (see fig. 1). The desired forms can be obtained by transforming eqs. (2) to the (i, j, k) system. With this transformation and retaining only $\partial^2 v_k / \partial i^2$, the results are

$$\begin{aligned} \frac{\partial p}{\partial k} &= \left\{ \sin^2 \varphi \left[\left(\frac{\eta_1 + \eta_2}{2} \right) \sin^2 2\theta + \eta_3 \cos^2 2\theta \right] \right. \\ &\quad \left. + \cos^2 \varphi \left[(2\eta_2 - \eta_1) \sin^2 \theta + \eta_3 \cos^2 \theta \right] \right\} \frac{\partial^2 v_k}{\partial i^2} \\ \frac{\partial p}{\partial j} &= \left\{ \sin \varphi \sin \theta \left[\eta_4 + \eta_5 - (\eta_4 + 2\eta_5) \sin^2 \varphi \sin^2 \theta \right] \right. \\ &\quad \left. + \cos \varphi \cos \theta \sin \theta \left[\eta_3 - (2\eta_2 - \eta_1) \right. \right. \\ &\quad \left. \left. - 4 \left(\eta_3 - \frac{\eta_1 + \eta_2}{2} \right) \sin^2 \varphi \sin^2 \theta \right] \right\} \frac{\partial^2 v_k}{\partial i^2}, \end{aligned} \quad (4)$$


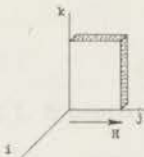
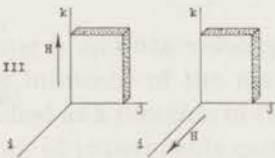
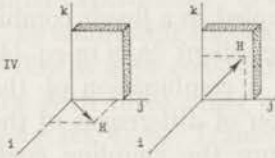
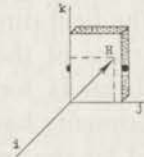
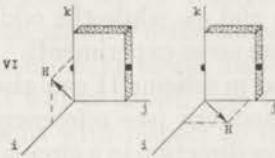
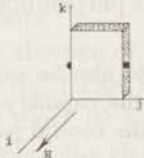
with φ and θ as given in fig. 1. It is seen from these equations that the pressure gradient $\partial p / \partial k$ ("longitudinal effect") is coupled to a linear combination of $\frac{1}{2}(\eta_1 + \eta_2)$, $2\eta_2 - \eta_1$ and η_3 . The pressure gradient $\partial p / \partial j$ in eq. (4) ("transverse effect")[†] can be split into two parts: a combination of the odd-in-field coefficients η_4 and η_5 and a combination of differences of the even-in-field coefficients. In this experimental setup the coupling coefficient ζ between shear and volume viscosity does not appear.

From eqs. (4) it can be seen that by proper choice of the field direction, as determined by the angles θ and φ , specific combinations of the coefficients are measured. This has been summarized in scheme II for some simple cases, where also a literature survey on the experiments has been given. It appears that the longitudinal effects can be used for the separate determination of the even-in-field coefficients η_1 , η_2 and η_3 , while the odd-in-field coefficients η_4 and η_5 can be measured in transverse experiments.

Some of the combinations of coefficients mentioned in scheme II can also be determined using capillaries with circular cross sections (see references with * in scheme II). When the field is parallel to the flow direction in a circular capillary, η_3 can be determined¹⁰⁻¹²), while when the field is perpendicular to

[†] In eq. (4b) terms involving the velocity component v_j would also be expected, since transverse flow must occur at the beginning and end of the capillary in the building-up of $\partial p / \partial j$; these terms, however, can be neglected in the central part of a long capillary.

SCHEME II

The shear viscosity coefficients obtained for different orientations of the field. References with * correspond to experiments done with circular capillaries.		
field - slit arrangement	equation (5) reduces to :	refs.
Longitudinal effect:		
I  $\left. \begin{aligned} \theta &= \frac{\pi}{4} \\ \varphi &= \frac{\pi}{2} \end{aligned} \right\}$	$\frac{\partial p}{\partial k} = \frac{\eta_1 + \eta_2}{2} \frac{\partial^2 v_k}{\partial i^2}$	5
II  $\left. \begin{aligned} \theta &= \frac{\pi}{2} \\ \varphi &= 0 \end{aligned} \right\}$	$\frac{\partial p}{\partial k} = (2\eta_2 - \eta_1) \frac{\partial^2 v_k}{\partial i^2}$	5
III  $\left. \begin{aligned} \theta &= 0 \\ \varphi &= \frac{\pi}{2} \end{aligned} \right\} \left. \begin{aligned} \theta &= \frac{\pi}{2} \\ \varphi &= \frac{\pi}{2} \end{aligned} \right\}$	$\frac{\partial p}{\partial k} = \eta_3 \frac{\partial^2 v_k}{\partial i^2}$	10*, 11*, 12*
IV  $\left. \begin{aligned} \theta &= \frac{\pi}{2} \\ \varphi &= \frac{\pi}{4} \end{aligned} \right\} \left. \begin{aligned} \theta &= \frac{\pi}{4} \\ \varphi &= 0 \end{aligned} \right\}$	$\frac{\partial p}{\partial k} = \frac{\eta_3 + (2\eta_2 - \eta_1)}{2} \frac{\partial^2 v_k}{\partial i^2}$	4*, 13*
Transverse effect:		
V  $\left. \begin{aligned} \theta &= \frac{\pi}{4} \\ \varphi &= 0 \end{aligned} \right\}$	$\frac{\partial p}{\partial J} = \frac{\eta_3 - (2\eta_2 - \eta_1)}{2} \frac{\partial^2 v_k}{\partial i^2}$	7, 11*, 12*
VI  $\left. \begin{aligned} \theta &= \frac{\pi}{4} \\ \varphi &= \frac{\pi}{2} \end{aligned} \right\} \left. \begin{aligned} \theta &= \frac{\pi}{2} \\ \varphi &= \frac{\pi}{4} \end{aligned} \right\}$	$\frac{\partial p}{\partial J} = \frac{\eta_4}{2/2} \frac{\partial^2 v_k}{\partial i^2}$	5, 9 5, 9
VII  $\left. \begin{aligned} \theta &= \frac{\pi}{2} \\ \varphi &= \frac{\pi}{2} \end{aligned} \right\}$	$\frac{\partial p}{\partial J} = -\eta_5 \frac{\partial^2 v_k}{\partial i^2}$	5, 6, 7, 8

the flow direction, the combination $\frac{1}{2}(\eta_3 + 2\eta_2 - \eta_1)$ is obtained^{4,13}). Measurements for the (difference) combination $\frac{1}{2}(\eta_3 - 2\eta_2 + \eta_1)$ have been carried out using both rectangular and circular capillaries: Kikoin⁷) measured this combination of even-in-field coefficients as a transverse pressure difference in a rectangular capillary (situation V in scheme II) and called it the "even planar effect", while Korving^{11,12}) obtained the same combination by using a Wheatstone bridge arrangement of circular capillaries having different orientations with respect to the field.

4. *Applications.* In a rectangular capillary several coefficients can be determined in the course of one experiment by rotating the magnet around the capillary, provided an appropriate orientation of the capillary is chosen with respect to the plane of rotation of the magnetic field. In particular, η_1 and η_2 can be extracted from the combinations $\frac{1}{2}(\eta_1 + \eta_2)$ and $2\eta_2 - \eta_1$ which are found by measuring the change of the flow resistance for the two field directions given in scheme II as situations I and II. In the plane defined by these two field directions the dependence of the effect on the orientation of the field is found to be

$$\frac{\partial p}{\partial k} = \left[\frac{\eta_1 + \eta_2}{2} \sin^4 \omega + (2\eta_2 - \eta_1) \cos^2 \omega + \eta_3 \sin^2 \omega \cos^2 \omega \right] \frac{\partial^2 v_k}{\partial i^2}, \quad (5)$$

where ω is the angle between the field direction and the j axis. Thus it is seen that all three coefficients η_1 , η_2 and η_3 can be determined by measuring as a function of ω , *i.e.*, by turning the magnet around the inclined capillary. The advantage of this method lies in the fact that, since these coefficients are measured under exactly the same conditions, the systematic measuring errors will be the same. This allows data for the different coefficients to be compared confidently. Results of such experiments are given in chapter IV.

Similarly, the odd-in-field coefficients η_4 and η_5 can both be measured in one experimental run by turning a magnet around the capillary. As can be seen from scheme II (situations VI and VII) there are two planes suited for a separate determination of these coefficients, *viz.* the ij plane and the ik plane. In both cases the angular dependence of the transverse pressure gradient is

$$\frac{\partial p}{\partial j} = \left[\frac{1}{2}\eta_4 \sin 2\chi \sin \chi - \eta_5 \cos 2\chi \cos \chi \right] \frac{\partial^2 v_k}{\partial i^2},$$

where χ is the angle between the field direction and the i axis. Results of such experiments are discussed chapter II⁹).

REFERENCES

- 1) Beenakker, J. J. M. and McCourt, F. R., *Ann. Rev. Phys. Chem.* **21** (1970) 47.
- 2) Hooyman, G. J., Mazur, P. and De Groot, S. R., *Physica* **21** (1955) 355.
- 3) De Groot, S. R. and Mazur, P., *Non-equilibrium Thermodynamics*, (North-Holland Publishing Comp., Amsterdam, 1962) p. 311.
- 4) Korving, J., Hulsman, H., Scoles, G., Knaap, H. F. P. and Beenakker, J. J. M., *Physica* **36** (1967) 177 (Commun. Kamerlingh Onnes Lab., Leiden No. 357b).
- 5) Hulsman, H. and Burgmans, A. L. J., *Phys. Letters* **29A** (1969) 629.
- 6) Korving, J., Hulsman, H., Knaap, H. F. P. and Beenakker, J. J. M., *Phys. Letters* **21** (1966) 5.
- 7) Kikoin, I. K., Balashov, K. I., Lasarev, S. D. and Neushtadt, R. E., *Phys. Letters* **24A** (1967) 165.
- 8) Kikoin, I. K., Balashov, K. I., Lasarev, S. D. and Neushtadt, P. E., *Phys. Letters* **26A** (1968) 650.
- 9) Hulsman, H., Van Waasdijk, E. J., Burgmans, A. L. J., Knaap, H. F. P. and Beenakker, J. J. M., *Physica* **50** (1970) 53 (Commun. Kamerlingh Onnes Lab., Leiden No. 381c); this thesis, chapter II.
- 10) Engelhardt, H. and Sack, H., *Phys. Z.* **33** (1932) 724.
- 11) Korving, J., *Physica* **46** (1970) 619 (Commun. Kamerlingh Onnes Lab., Leiden No. 376d).
- 12) Korving, J., *Physica* **50** (1970) 27 (Commun. Kamerlingh Onnes Lab., Leiden No. 381b).
- 13) Trautz, M. and Fröschel, E., *Phys. Z.* **33** (1932) 947.

CHAPTER II

THE ODD-IN-FIELD COEFFICIENTS η_4 AND η_5

Synopsis

Measurements are reported of the two "odd in field" viscosity coefficients η_4 and η_5 for the gases N_2 , CO, CH_4 and HD. Comparing the experimental data with theory it is found that for the gases studied, the $[\mathbf{J}]^{(2)}$ anisotropy of the non-equilibrium distribution function gives a dominant contribution. Cross-sections for the reorientation of the angular momenta are determined.

1. *Introduction.* The transport properties of dilute gases of polyatomic molecules are influenced by external fields. For paramagnetic gases in a magnetic field this effect has been known for a long time. In 1930 Senftleben¹⁾ discovered that the heat conductivity of gaseous O_2 decreases slightly in a magnetic field. Further studies showed that the viscosity is also affected^{2,3)}. Extensive investigations on these effects were made for nearly a decade for the paramagnetic gases O_2 , NO and NO_2 . In 1962 Beenakker *et al.*⁴⁾ proved that diamagnetic polyatomic gases also show these effects. Since then much work, both experimental and theoretical, has been published on this subject. For a survey see refs. 5 and 6.

In this paper we present experiments on the influence of a magnetic field on the shear viscosity. For the description of the shear viscosity in the presence of a magnetic field five coefficients are needed⁷⁾: η_1, \dots, η_5 . In this paper measurements are reported on the odd-in-field coefficients η_4 and η_5 . In a previous article⁸⁾ it has been shown how these coefficients can be determined by studying the gas flow through a capillary with a rectangular cross-section, where these coefficients give rise to a transverse pressure difference analogous to the transverse voltage which is measured in Hall experiments.

2. *Experimental method and apparatuses.* 2.1. General. The measurement of the viscosity coefficients η_4 and η_5 is in principle very simple.

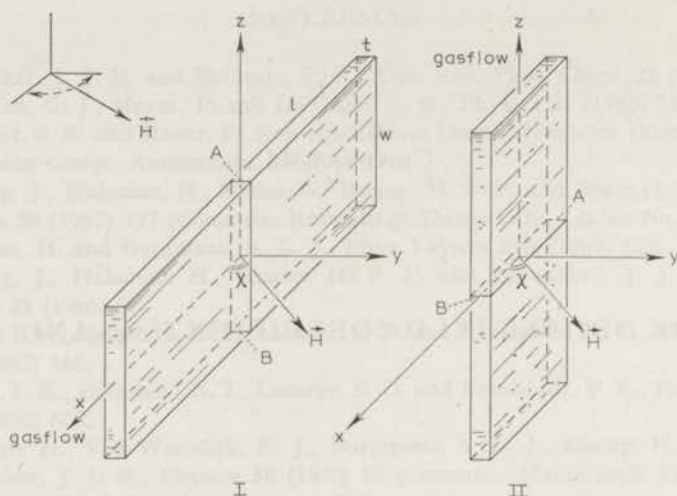


Fig. 1. Schematic diagram of the two capillaries used for the determination of η_4 and η_5 . The xy plane is the horizontal plane in which the magnet is rotated.

Through a capillary of rectangular cross-section a constant gas flow is maintained (see fig. 1). Two small holes A and B opposite to each other in the narrow sides of the capillary are connected with a differential manometer. When a magnetic field is applied a pressure gradient in the A-B direction arises. The resulting pressure difference $p_A - p_B$ over the width (w) of the capillary is measured with the differential manometer. For a given orientation of the field with respect to the capillary this pressure gradient is proportional to a particular (combination of) viscosity coefficient(s). To measure at different field orientations the magnet is rotated around the capillary. For experimental reasons this rotation is in a horizontal plane.

In this research two apparatuses have been used, to be denoted by #I and #II, with different dimensions and a different orientation as shown in fig. 1. According to ref. 8 the pressure difference $p_A - p_B$ is in both configurations given as a function of the angle χ between field and apparatus by:

$$\frac{p_A - p_B}{w(\nabla p)_{AB}} = \frac{\frac{1}{2}\eta_4 \cos \chi \sin 2\chi + \eta_5 \cos 2\chi \sin \chi}{\eta_0}, \quad (1)$$

where w is the width of the capillary, $(\nabla p)_{AB}$ the pressure gradient along the length of the capillary in the plane of A and B, η_0 the field-free viscosity coefficient and η_4 and η_5 the coefficients to be determined.

2.2. Apparatuses. The dimensions of the shorter #I capillary are: length $l = 35$ mm, width $w = 15$ mm and thickness $t = 0.50$ mm, while for the longer #II capillary: $l = 100$ mm, $w = 10$ mm and $t = 0.50$ mm.

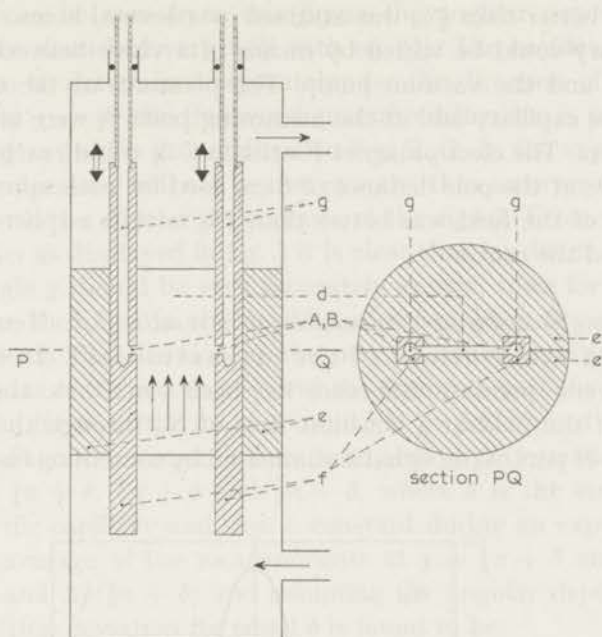


Fig. 2. Apparatus # II.

Schematic cross-sections through A and B parallel and perpendicular to l .

In the capillary I the positions of the measuring points A and B are fixed halfway along the capillary. In the apparatus II the positions of A and B can be chosen freely along the length of the capillary.

In fig. 2 the construction of the capillary #II is schematically shown. Two solid half-cylinders e are held together inside a long cylindrical vessel. Between the half cylinders a slit d with a rectangular cross-section is left open (the actual capillary). The short sides of the cross-section of this slit are formed by long rectangular rods f . The rods, which are hollow, fit closely in channels in the half cylinders and can be moved from outside. At the centre of the rods in the sides facing the slit small holes are made (A and B respectively) leading to the differential manometer via the bores g .

For the measurement of the transverse pressure differences one needs a differential manometer with a high sensitivity. In these experiments an Atlas Membran Micro Manometer (Fried. Krupp MAT) was used. The output of this instrument was displayed on a chart recorder. Pressure differences as small as 10^{-5} torr could be detected. The limitation of the sensitivity was in most cases caused by noise in the gas flow rather than by the instrument.

The gasflow through the capillary was adjusted by means of a needle valve upstream. A flow controller (Moore 63 BDL) was used to keep the flow constant, independent of the pressure in the gas storage vessel. Thus

a stability of better than $\frac{1}{2}\%$ was attained over several hours. The pressure in the capillary could be varied by means of a valve between the exit of the capillary and the vacuum pump. The pressures at the entrance and the exit of the capillary and at the measuring point A were measured with oil manometers. The electromagnet (Oerlikon C 3) could reach a maximum field of 27 kOe at the pole distance of 8 cm used for both apparatuses. The homogeneity of the field was better than 1% within a sphere of 5 cm diameter around the centre.

3. *Measuring procedure and calculation of the results.* 3.1. Measurements for different orientations of the magnetic field. In fig. 3 the observed transverse pressure difference has been plotted vs. the angle χ for two values of the field at a constant flow of N_2 through the capillary (a small even-in- H part of the signal is eliminated by combining results for χ and

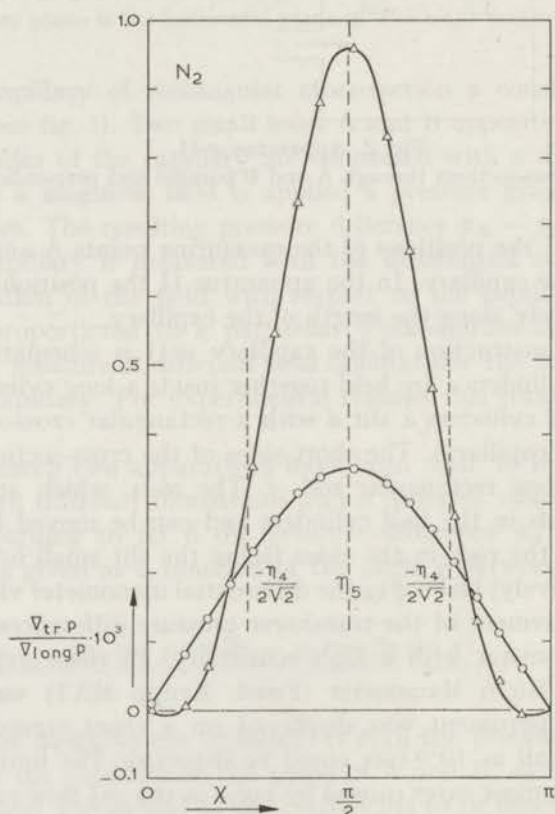


Fig. 3. The ratio of the transverse to the longitudinal pressure gradients as a function of the orientation of the field with respect to the capillary, for N_2 at $p = 6.75$ torr.

\circ $H/p = 0.46 \times 10^3$ Oe/torr, Δ $H/p = 2.3 \times 10^3$ Oe/torr.

The solid lines correspond to the angular dependence according to eq. (1).

$\chi + \pi$). As can be seen from this figure the angular dependence of the results can be described very well with eq. (1). The coefficients η_4 and η_5 can therefore be determined separately: for the direction of the magnetic field given by $\chi = \frac{1}{2}\pi$ the transverse pressure difference is proportional to $-\eta_5$ and at $\chi = \frac{1}{4}\pi$ it is proportional to $+\eta_4/2\sqrt{2}$. In the experiment, however, these values of χ will not be met exactly, thus an error will be present connected with the angular dependence of the signal. From the characteristic examples as displayed in fig. 3 it is clear that for direct determination of η_4 the angle χ should be very accurately known, since for the high field in this figure the slope in the neighbourhood of $\frac{1}{4}\pi$ is 5% per degree. In our experiments the direction of the magnet could be adjusted with an accuracy of one tenth of a degree, but the orientation of the capillary with respect to the frame of the magnet could not be determined to better than one degree. Therefore measurements were always performed for the orientations $\chi = \frac{1}{4}\pi + \delta$, $\frac{1}{2}\pi + \delta$ and $\frac{3}{4}\pi + \delta$, where δ is the error in the positioning of the capillary and thus a constant during an experimental run. Taking the average of the measurements at $\chi = \frac{1}{4}\pi + \delta$ and $\frac{3}{4}\pi + \delta$, *i.e.* $\Delta p(\frac{1}{4}\pi + \delta)$ and $\Delta p(\frac{3}{4}\pi + \delta)$ and assuming the angular dependence of eq. (1), the resulting deviation for small δ is found to be:

$$\begin{aligned} \frac{1}{2}[\Delta p(\frac{1}{4}\pi + \delta) + \Delta p(\frac{3}{4}\pi + \delta)] &= \Delta p(\frac{1}{4}\pi)[1 - \delta^2\{4\eta_5/\eta_4 + 3\}], \\ \Delta p(\frac{1}{2}\pi + \delta) &= \Delta p(\frac{1}{2}\pi)[1 - \delta^2\{\eta_4/\eta_5 + 3\}]. \end{aligned} \quad (2)$$

Since in the present experiments $-2 < \eta_4/\eta_5 < -\frac{1}{2}$, the resulting error can be neglected. Also in each measurement the even part of the transverse pressure difference was eliminated using opposite orientations of the magnet. Therefore each value of η_4 and η_5 corresponds to measurements in respectively 4 and 2 orientations of the magnet. With this measuring procedure the other possible errors in the orientation of the capillary can also only give rise to small deviations that are negligible in view of the other sources of inaccuracy.

3.2. Determination of the pressure gradient along the capillary. To be able to calculate from the observed pressure differences the magnitude of the corresponding viscosity coefficients, let us first briefly treat the gasflow in the absence of a field.

The streamline flow of an incompressible fluid through a pipe of rectangular section has been treated by Cornish⁹). Assuming that the velocity is zero at the walls (no slip) the following formula is derived for the velocity pattern:

$$\begin{aligned} v_x = & -\frac{1}{2\eta_0} \frac{dp}{dx} \left[\left(\frac{t}{2} \right)^2 - y^2 - \frac{8t^2}{\pi^3} \left\{ \frac{\cosh(\pi z/t)}{\cosh(\pi w/2t)} \cos(\pi y/t) \right. \right. \\ & \left. \left. - \frac{1}{3^3} \frac{\cosh(3\pi z/t)}{\cosh(3\pi w/2t)} \cos(3\pi y/t) + \dots \right\} \right], \end{aligned} \quad (3)$$

where the meaning of the symbols is the same as in fig. 1, I. By integration the total volume flow per unit time V is found:

$$V = - \frac{wt^3}{12\eta_0} \frac{dp}{dx} \left[1 - \frac{192}{\pi^5} \frac{t}{w} \left\{ \tanh \frac{\pi w}{2t} + \frac{1}{3^5} \tanh \frac{3\pi w}{2t} + \dots \right\} \right]. \quad (4)$$

This is the equivalent of the well-known Poiseuille formula for a circular tube. For capillaries with $w > 4t$ this becomes to a good approximation

$$V = - \frac{wt^3}{12\eta_0} \frac{dp}{dx} \left(1 - 0.630 \frac{t}{w} \right). \quad (5)$$

Incorporating a number of corrections to be discussed below, the equivalent of the Hagen-Poiseuille flow equation is found for a capillary with rectangular cross-section:

$$\frac{(\phi_C + K_\alpha)^2 - (\phi_D + K_\alpha)^2}{2} = \frac{12\eta_0 l}{wt^3} \frac{G}{\rho_0} \frac{[1 + \frac{1}{20}\{m + \ln(\phi_C/\phi_D)\}(t/l) Re]}{[1 - 0.630t/w]}, \quad (6)$$

where ϕ_C and ϕ_D are the pressures at the entrance and the exit of the capillary; $K_\alpha = \phi n_\alpha \xi / t$ with n_α a number around 6 and ξ is the mean free path of the gas molecules; l , w and t are respectively the length, width and thickness of the capillary; G is the mass flow per unit time; ρ_0 the density at unit pressure; Re the Reynolds number defined as $2G/w\eta$; and m a number of the order unity depending on the shape of the entrance of the capillary (Hagenbach).

Note that the pressure drop along the capillary is quadratic. This is a consequence of the expansion of the gas; along the length of the capillary the mass transport is constant and so $\phi \partial\phi/\partial x$ is constant. The constant K_α describing the Knudsen effect on the gasflow will be considered in section 3.4. The factor

$$1 + \frac{1}{20} \left(m + \ln \frac{\phi_C}{\phi_D} \right) \frac{t}{l} Re$$

arises from the pressure losses caused by the acceleration of the gas at the orifice and in the capillary. For the #I capillary the constant m has been assumed 0.6. For the #II capillary m has been determined experimentally; studying the pressure drop at the entrance a value of 0.57 has been found. In the present experiments the Reynolds number was always low ($Re < 40$) and this correction is at most of the order of 2%.

Analogous to the situation for capillaries with a circular cross-section¹⁰), it can be assumed that the velocity profile is fully developed for distances from the entrance $z \gtrsim (l/10)Re$. This distance being negligible as compared to l , the pressure gradient at the position of the measuring point A can be calculated with:

$$\left[\frac{\partial(p + \rho v^2)}{\partial z} \right]_A = \frac{\Delta p}{l} \frac{p_C + p_D + 2K_\alpha}{2p_A + 2K_\alpha} \left[1 + \frac{1}{20} \left(m + \ln \frac{p_C}{p_D} \right) \frac{l}{l} Re \right]^{-1}. \quad (7)$$

For the measurements with the #I capillary the pressure gradient has been calculated with this formula. As in this way a systematic error may be introduced (see 3.3.5), another procedure has been used for the measurements with the #II capillary: as was described in 2.2, the position of the measuring points A and B can be varied independently while a gasflow is running. So the pressure drop in the capillary can easily be studied. The flow resistance per unit length as a function of the distance to the entrance l_{AB} was determined the following way: for different values of l_{AB} A and B are placed opposite each other. Then one of these points is displaced over a small accurately known distance (0.5 or 1.0 mm). The resulting pressure difference $p_A - p_B$ is measured with the differential manometer. This change in static pressure can also be calculated using the pressures at entrance, exit and measuring point. The ratio of the measured to the calculated pressure difference at a certain position appeared to be – within a few parts per thousand – independent of pressure, pressure gradient and gas. Using this ratio (which varies with position from 0.92 to 1.03) in the calculation of η_4 and η_5 , the error in the calibration of the differential manometer (of the order 2%) is also eliminated, because the same instrument is used for the determination of the longitudinal and the transverse pressure gradient. This error is in fact replaced by the error in the displacement of the measuring point. This error corresponding to inhomogeneity of the screwthread is less than 1%.

3.3. Sources of systematic errors. For the calculation of η_4 and η_5 we have used eq. (1). This equation has been derived from the equations of motion using a number of simplifying assumptions: Compared to the leading term $\partial v_x / \partial y$ (see fig. 1, I) all terms in the equations of motion have been discarded that involve the velocity components v_y or v_z or velocity gradients in x or z direction. It can be shown that this is justified when the experimental situation satisfies the following conditions:

- 1° The capillary should have dimensions such that $l \gg w \gg t$.
- 2° The position of the measuring points should be far from the ends of the capillary.

3° The pressure gradient along the capillary and the coefficients η_4 and η_5 should be constant over the capillary.

In the following we shall first discuss the errors caused by deviations from this ideal situation in actual experiments.

3.3.1. Expansion of the gas. From the quadratic pressure drop along the capillary [see eq. (6)] one can estimate $\partial^2 v_x / \partial x^2$ and show that under the experimental conditions where $l \gg t$ this quantity is very small as compared to $\partial^2 v_x / \partial y^2$.

3.3.2. Presence of the short sides. In addition to the leading second derivative $\partial^2 v_x / \partial y^2$ one has also $\partial^2 v_x / \partial z^2$ as a consequence of the presence of the short sides. From eq. (3) these derivatives, averaged over the cross-section of the capillary, are found to be for capillaries with $w > 4t$

$$\begin{aligned} \frac{\overline{\partial^2 v_x}}{\partial y^2} &= \frac{1}{\eta_0} \frac{\partial p}{\partial x} \left(1 - 0.543 \frac{t}{w} \right); \\ \frac{\overline{\partial^2 v_x}}{\partial z^2} &= \frac{1}{\eta_0} \frac{\partial p}{\partial x} 0.543 \frac{t}{w}. \end{aligned} \quad (8)$$

Therefore under the experimental conditions $\partial^2 v_x / \partial z^2$ is only 2% of $\partial^2 v_x / \partial y^2$. Both second derivatives now contribute to the transverse effect, giving for the orientations of the field in which η_4 and η_5 are determined, respectively

$$\begin{aligned} \chi = \frac{\pi}{4}: \quad 2^1 \frac{\partial p}{\partial z} &= \eta_4 \frac{\partial^2 v_x}{\partial y^2} + 2\eta_4 \frac{\partial^2 v_x}{\partial z^2}; \\ \chi = \frac{\pi}{2}: \quad \frac{\partial p}{\partial z} &= -\eta_5 \frac{\partial^2 v_x}{\partial y^2} + \eta_4 \frac{\partial^2 v_x}{\partial z^2}. \end{aligned} \quad (9)$$

Thus this would lead to corrections for the measurements of η_4 and η_5 of the order of 2%. However, these corrections will not be applied for the following reason: the velocity derivative $\partial^2 v_x / \partial z^2$ is present in the neighbourhood of the short sides. In these short sides holes are made for the measurement of the transverse pressure difference. Thus exactly at the position where the effects are measured, the flow pattern near the short sides is disturbed in an unknown way. So it seems more correct to say that in these measurements an uncertainty of 2% exists than to apply these corrections.

3.3.3. Short-circuiting by the ends of the capillary. The measurement of transverse pressure differences has a strong resemblance to the determination of the electrical Hall coefficient, where a transverse voltage is measured. The experimental situation analogous to ours is a rectangular

plate with the current electrodes extending along two opposite edges. In that case¹¹⁾ a short-circuiting effect of the current electrodes diminishes the observed transverse voltage; this effect becomes large for samples with a ratio of length to width less than 2. For the gasflow through a capillary the same kind of boundary condition is imposed: at the entrance and the exit of the capillary no transverse pressure difference can exist. From the equations of motion⁸⁾ it is clear that qualitatively the effect of this boundary conditions will be the same as in the electrical case. However, because of the complicated nature of the equations it is not feasible to solve this problem mathematically as could be done in the electric case. Hence an experimental approach was chosen.

In the capillary #II ($l/w = 10$) the transverse pressure difference can be measured at arbitrary positions along the capillary. To get information on the end effects, measurements were performed at different distances from the entrance (l_{AB}) under experimental conditions that were otherwise the same; the gasflow was adjusted in such a way that each time the same values were obtained for the pressure and the pressure gradient at the measuring point. The results of an experiment for N_2 at $H/p = 2.1 \times 10^3$ Oe/torr are shown in fig. 4 for the two measuring situations from which η_4 and η_5 are obtained.

It is seen that for the central part of this capillary ($l = 100$ mm, $w =$

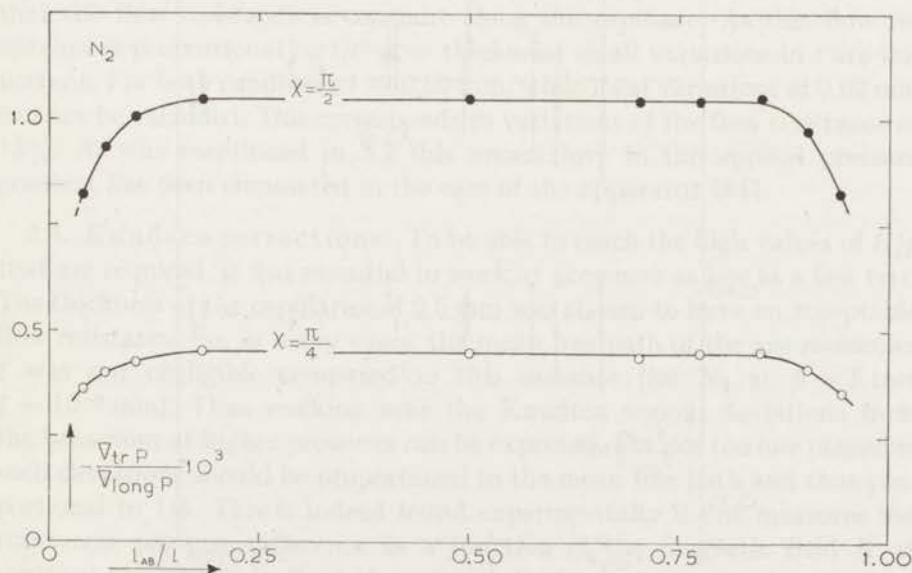


Fig. 4. The ratio of the transverse to the longitudinal pressure gradients $\nabla_{tr} p / \nabla_{long} p$ for N_2 as a function of l_{AB} , the distance from the entrance of the capillary. The pressure at the measuring position p_{AB} is 10 torr and $H/p_{AB} = 2.1 \times 10^3$ Oe/torr.

$\chi = \frac{1}{2}\pi$ corresponds to η_5 and $\chi = \frac{1}{4}\pi$ corresponds to $-\eta_4/2^{\frac{1}{2}}$.

= 10 mm) the signal is constant, but that for distances from the ends smaller than $0.15l$ the measured signal diminishes drastically. As should be expected for such a short-circuiting effect, the decrease is almost equal for the entrance and the exit of the capillary and the relative influence is the same for the η_4 and η_5 measurements. One may conclude that results obtained with capillaries with a small ratio of length over width ($l/w < 3$) are too small by a factor which only depends on l/w . This factor can be estimated by adding the decreases caused by the entrance and by the exit of the capillary. *E.g.*, for the capillary #1 of this work ($l/w = 2.33$) the decrease will be of the order of 7% and the experimental results for this capillary will therefore be corrected by this amount. For the capillary used by Kikoin *et al.* described in ref. 12 ($l/w = 1.33$) the results may be affected by a decrease of the order of 25%.

3.3.4. Variation of the pressure along the capillary. Another complication arises from the fact that in many experiments one has to work with large pressure gradients at low pressures. The consequences are firstly that the pressure gradient and secondly the viscosity coefficients η_4 and η_5 (through their dependence on H/p) will vary drastically along the capillary. In all foregoing considerations it was tacitly assumed either that these quantities

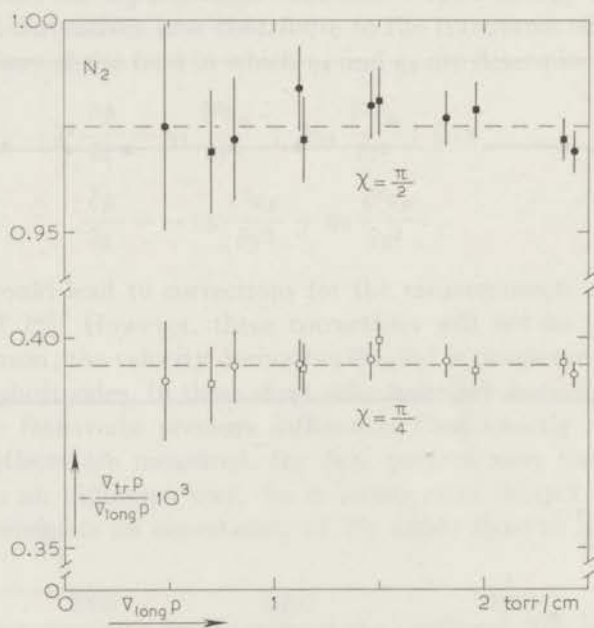


Fig. 5. The ratio of the transverse to the longitudinal pressure gradient $\nabla_{tr} p / \nabla_{long} p$ for N_2 , as a function of the longitudinal pressure gradient at $H/p = 2.25 \times 10^3$ Oe/torr, $p = 11.5$ torr.

$$\chi = \frac{1}{2}\pi \text{ corresponds to } \eta_5, \quad \chi = \frac{1}{4}\pi \text{ corresponds to } -\eta_4/2^{\frac{1}{2}}.$$

were constants over the whole capillary, or that the effects as measured were only dependent on the local values of these quantities. However, in the preceding section it was found that the boundary (where the transverse pressure difference should be zero) influences the observed pressure difference even at considerable distances from this point. So it can be expected that at any point in a capillary the situation in the neighbourhood of that point will also be of importance for the observed effect. When in that neighbourhood both, pressure gradient and H/p value vary drastically, this may cause deviations in the observed effect. As an exact mathematical solution of this problem seems unfeasible, the possible error has been estimated studying the influence of large pressure gradients. In the #I capillary the transverse pressure difference was measured as a function of increasing longitudinal pressure difference, each time with the same field and the same pressure at the measuring point. As is shown in fig. 5 the ratio of the transverse to the longitudinal pressure gradients is found constant within the measuring accuracy for both field orientations corresponding to η_4 and η_5 . Thus one estimates the error involved to be at most of the order of one percent.

3.3.5. Inhomogeneity of the flow resistance. Besides the preceding sources of error connected with the approximate nature of eq. (1), a systematic error may be present in the values of the pressure gradient along the capillary as calculated with eq. (7). In the derivation of this equation it was assumed that the flow resistance is constant along the capillary. As this flow resistance is proportional to $1/t^3$ (t = thickness) small variations in t are important. For both capillaries $t = 0.50$ mm, while local variations of 0.02 mm can not be excluded. This corresponds to variations of the flow resistance of 12%. As was mentioned in 3.2 this uncertainty in the applied pressure gradient has been eliminated in the case of the apparatus #II.

3.4. Knudsen corrections. To be able to reach the high values of H/p that are required, it was essential to work at pressures as low as a few torr. The thickness of the capillaries of 0.5 mm was chosen to have an acceptable flow resistance. So, in many cases, the mean free path of the gas molecules ξ was not negligible compared to this distance (for N_2 at $p = 5$ torr $\xi = 10^{-2}$ mm). Thus working near the Knudsen region, deviations from the behaviour at higher pressures can be expected. For not too low pressures such deviations should be proportional to the mean free path and thus proportional to $1/p$. This is indeed found experimentally if one measures the transverse pressure difference as a function of the magnetic field H at constant pressure p . In fig. 6 the ratio of the transverse to the longitudinal pressure gradient as a function of H/p is plotted for three pressures of HD.

On a double logarithmic scale it appears that all curves obtained at different pressures for a given gas have the same shape and can be brought

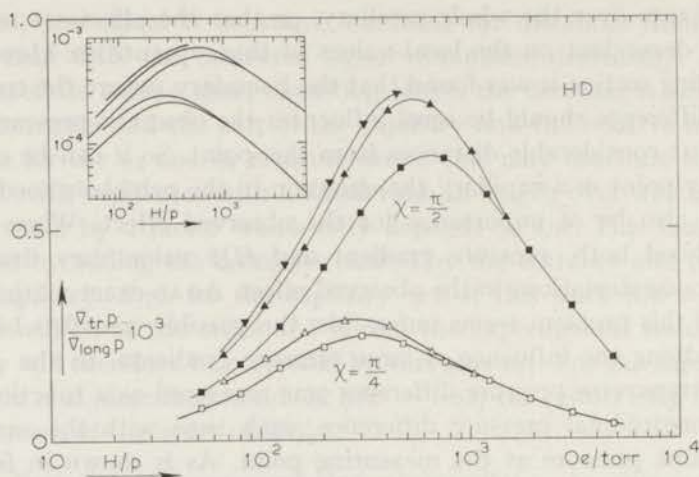


Fig. 6. The ratio of the transverse to the longitudinal pressure gradient as a function of H/p for HD at three different pressures.

▼ 51 torr, ▲ 16.3 torr, ■ 5.5 torr.

$\chi = \frac{1}{2}\pi$ corresponds to $-\eta_5$, $\chi = \frac{1}{4}\pi$ corresponds to $\eta_4/2^{\frac{1}{2}}$.

to coincidence by shifts in both the vertical and the horizontal directions. The shifts required to bring the low-pressure curves to coincidence with the high-pressure curve can indeed be described with corrections of the form $1 + K_\beta/p$ and $1 + K_\gamma/p$. The values obtained for K_β and K_γ are given in table I. With these values of K_β and K_γ the idealised η_4 and η_5 for a

TABLE I

	Knudsen correction parameters						
	$(K_\alpha)_{calc}$ (torr)	$(K_\alpha)_{exp}$ (torr)	K_β (torr)	K_γ (torr)	n_α	n_β	n_γ
N ₂	0.58		1.00	0.2	6	10	2
CO	0.58	0.60	1.04	0.2	6	10	2
CH ₄	0.47	0.40	0.70	0.2	6	10	3
HD	1.09	0.96	1.61	1.9	6	10	12

situation without Knudsen effects is obtained from the observed ratio of the transverse to the longitudinal pressure gradient $\nabla_{tr} p / \nabla_{long} p$ in the following way:

$$\frac{\eta_4}{\eta_0} = 2^{\frac{1}{2}} \left[\frac{\nabla_{tr} p}{\nabla_{long} p} \right]_{\chi=\frac{1}{4}\pi} \left(1 + \frac{K_\beta}{p} \right), \quad \text{at} \quad \frac{H}{p} = \frac{(H/p)_{exp}}{1 + K_\gamma/p}; \quad (10)$$

$$\frac{\eta_5}{\eta_0} = - \left[\frac{\nabla_{tr} p}{\nabla_{long} p} \right]_{\chi=\frac{1}{2}\pi} \left(1 + \frac{K_\beta}{p} \right), \quad \text{at} \quad \frac{H}{p} = \frac{(H/p)_{exp}}{1 + K_\gamma/p}.$$

Under these circumstances the gasflow through the capillary also is affected by Knudsen effects and one has [see eq. (6)]

$$\Delta p(1 + K_\alpha/p) = VR, \quad (11)$$

where V is the volume flow and R the resistance of the capillary. Measuring gasflows at different pressures, K_α has been experimentally determined. With the conventional assumption for the slip at the wall the correction K_α/p is found to be equal to $6\xi/t$, where ξ is the mean free path of the gas molecules. Thus K_α can be calculated using $\xi = (2^{1/2}n\pi\sigma^2)^{-1}$ and taking for σ the rigid-sphere diameters derived from the ordinary viscosity coefficients (in accordance with table 8.3-1 of ref. 13). The measured and the calculated values of K_α are given in table I. As the correspondence of K_α to $6\xi p/t$ seems to hold reasonably for these experiments, it is useful to express the other correction factors K_β and K_γ as $n_\beta\xi p/t$ and $n_\gamma\xi p/t$, since in this way quantities are obtained that do not depend on the dimensions of the apparatus. These numbers, obtained comparing K_β and K_γ with the measured values of K_α , are given in table I. It appears that for these four gases n_β is equal within the measuring accuracy. The explanation of this fact is not clear.

The interpretation of n_γ , the correction for the H/p scale, is more obvious. As is well known, the H/p scale is in fact a scale of $\omega_{\text{prec}}\tau$ where ω_{prec} is the precession frequency and τ the order of time in which the angular momenta of the molecules reorient. It is plausible to assume that the wall is effective in reorienting the molecular axis. At low pressures the collisions with the wall become more and more important, so the effective reorientation time becomes shorter. Hence higher fields are needed, which corresponds to the observed shift to the right in fig. 6. The fact that for HD the mean-free-path effects on H/p are so much larger than for the other gases ($n_\gamma = 12$ compared to 2) can easily be explained. It is well known that in HD the time for reorientation of angular momenta is exceedingly large: about 10 times the time between elastic collisions (*vs.* 2 for N_2). So it is obvious that the influence of the wall will be more pronounced in the case of HD than for N_2 .

3.5. Comparison and combination of the results of the two capillaries. Measurements were performed in the two capillaries #I and #II as described in section 2.2.

At lower pressures the measurements become less accurate; the pressure gradient that can be applied is small, so the transverse pressure difference will also be small. Knudsen effects will reduce this signal and moreover the stability of the gasflow also appears to become worse at lower pressures. Since at each pressure the measurements with the #I capillary showed much less scattering than those with the #II, the measurements with the #I could be extended to much higher H/p using lower pressures.

On the other hand the absolute magnitude of the effect can only be determined accurately using the #II capillary, for the following two reasons: 1° As discussed in section 3.3.3 the short-circuiting effect of the ends of the capillary can be neglected for measurements in the central part of the #II capillary, while the correction for the #I measurements is rather uncertain ($7 \pm 3\%$). 2° As discussed in section 3.2 the longitudinal pressure gradient at the position of the measuring points can be determined very accurately for the capillary #II, while for the #I systematic errors of the order of 10% cannot be excluded (section 3.3.5). Because of these two errors the magnitude of the effects as measured may be different for the two capillaries by a constant factor independent of gas or H/p .

Indeed it appears that after application of the 7% correction for the short-circuiting effect a further correction of 6% to the #I results gives a complete agreement of the results for the two capillaries for both coefficients, for all gases and for all H/p values. This correction – not unreasonable in view of the uncertainties mentioned above – has been applied to all results with the #I capillary.

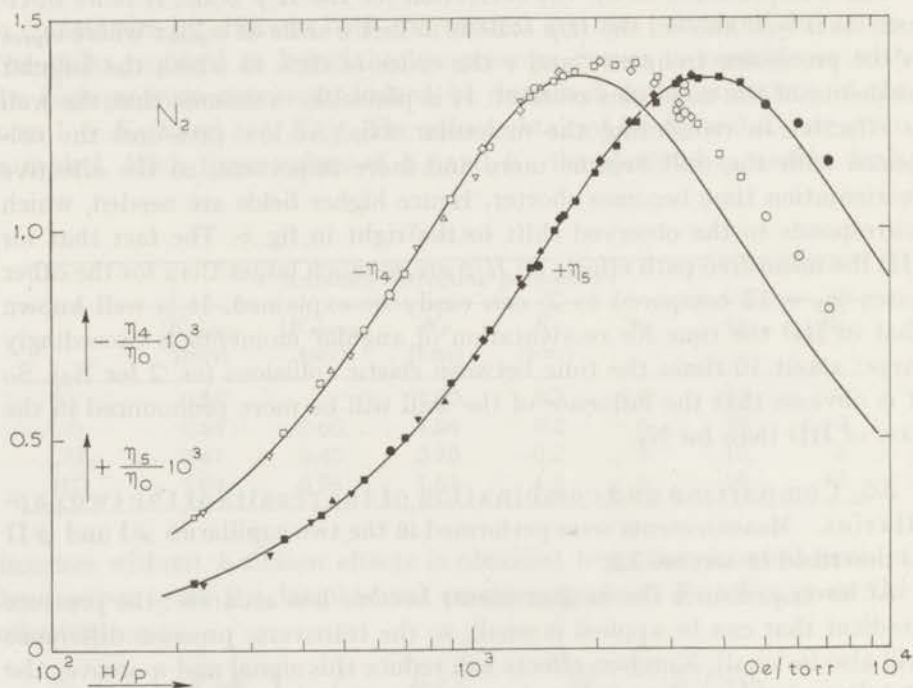
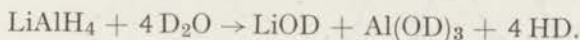


Fig. 7. $-\eta_4/\eta_0$ and $+\eta_5/\eta_0$ as functions of H/p for N_2 .

○● 3.5 torr, □■ 5.8 torr, ◇◆ 7.0 torr, ▲▲ 14.1 torr, ▼▼ 15.8 torr.
 η_4 open symbols, η_5 solid symbols.
 ——— theory: H/p dependence for $[J]^{(2)}$ term.

4. *Experimental results and discussion.* The viscosity coefficients η_4 and η_5 have been measured at room temperature for the gases N_2 , CO , CH_4 and HD . The purity of the gases was better than 99.9% for N_2 and CO and 98% for CH_4 . The HD gas has been prepared using the chemical reaction:



In this process small amounts H_2 and D_2 are also formed. Mass-spectrometer analysis showed that under our conditions a mixture was produced that consisted – apart from traces of air that were frozen out at liquid-hydrogen temperature – of 94% HD and almost equal fractions H_2 and D_2 . All measurements on HD have been performed with such a mixture.

In figs. 7 and 8 the values of $-\eta_4/\eta_0$ and $+\eta_5/\eta_0$ are plotted as a function of H/p for N_2 and CO . In figs. 9 and 10 $+\eta_4/\eta_0$ and $-\eta_5/\eta_0$ are plotted for CH_4 and HD . Note that the signs of the effects for N_2 and CO are opposite to those of CH_4 and HD . As will be seen later this is related to the opposite signs of the magnetic moments [see *e.g.* eq. (12)]. It appears that for these gases the curves for η_4 and η_5 resemble two absorption curves that are shifted by a factor two along the H/p axis. The maxima for the two coef-

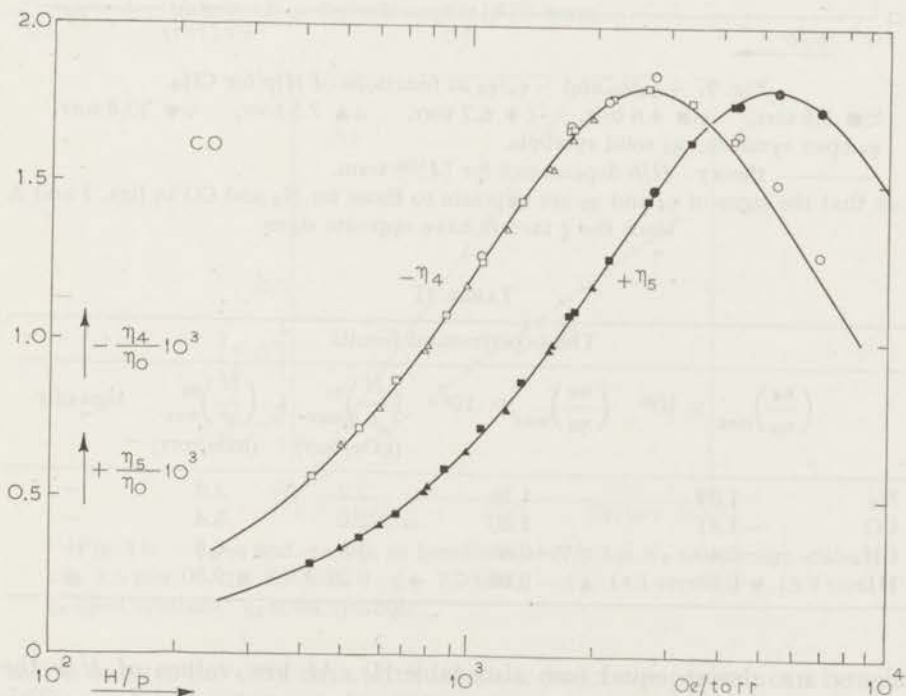


Fig. 8. $-\eta_4/\eta_0$ and $+\eta_5/\eta_0$ as functions of H/p for CO .

○● 3.7 torr, □■ 6.0 torr, △▲ 13.3 torr.

η_4 open symbols, η_5 solid symbols.

— theory: H/p dependence for $[J]^{(2)}$ term.

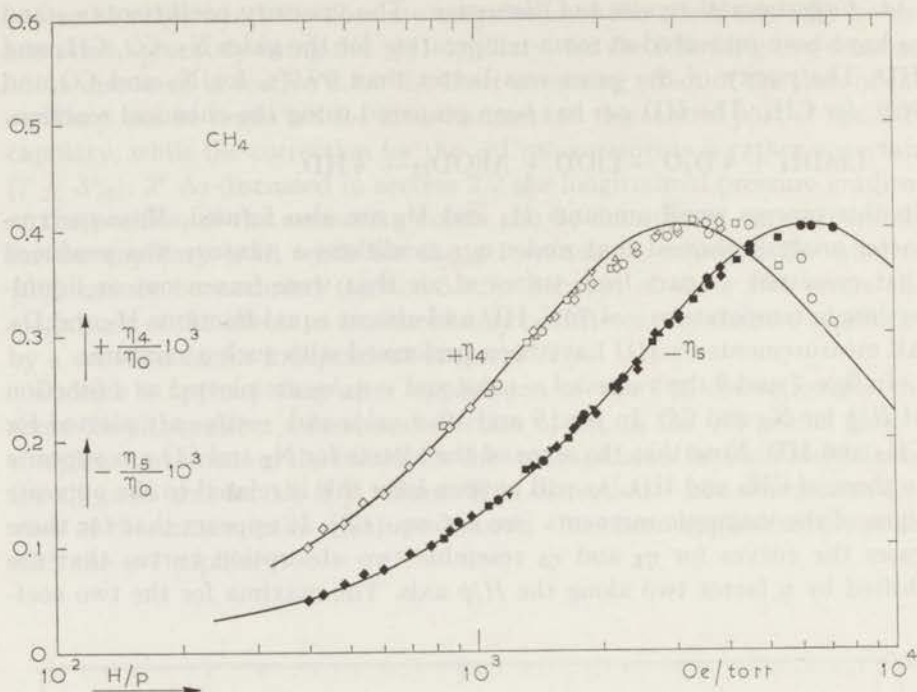


Fig. 9. $+\eta_4/\eta_0$ and $-\eta_5/\eta_0$ as functions of H/p for CH_4 .

○● 3.5 torr, □■ 4.6 torr, ◇◆ 6.7 torr, △▲ 7.5 torr, ▽▼ 13.8 torr.
 η_4 open symbols, η_5 solid symbols.

— theory: H/p dependence for $[J]^{(2)}$ term.

Note that the signs of η_4 and η_5 are opposite to those for N_2 and CO in figs. 7 and 8, since the g factors have opposite signs.

TABLE II

The experimental results

	$\left(\frac{\eta_4}{\eta_0}\right)_{\max} \times 10^3$	$\left(\frac{\eta_5}{\eta_0}\right)_{\max} \times 10^3$	$\left(\frac{H}{p}\right)_{\max}^{\eta_4}$ (kOe/torr)	$\left(\frac{H}{p}\right)_{\max}^{\eta_5}$ (kOe/torr)	sign of g
N_2	-1.39	1.36	2.2	3.8	-
CO	-1.81	1.80	2.8	5.4	-
CH_4	0.40	-0.40	3.6	6.6	+
HD	0.88	-0.88	0.27	0.50	+

ficients are almost equal (see also table II). At low values of H/p the dependence on H/p is linear, the slope for η_4 being twice that for η_5 . This is shown for N_2 in fig. 11.

Earlier measurements on η_5 have been reported in letters by Korving *et al.*¹⁴) and by Kikoin *et al.*^{12,15}). The results of Korving being of quali-

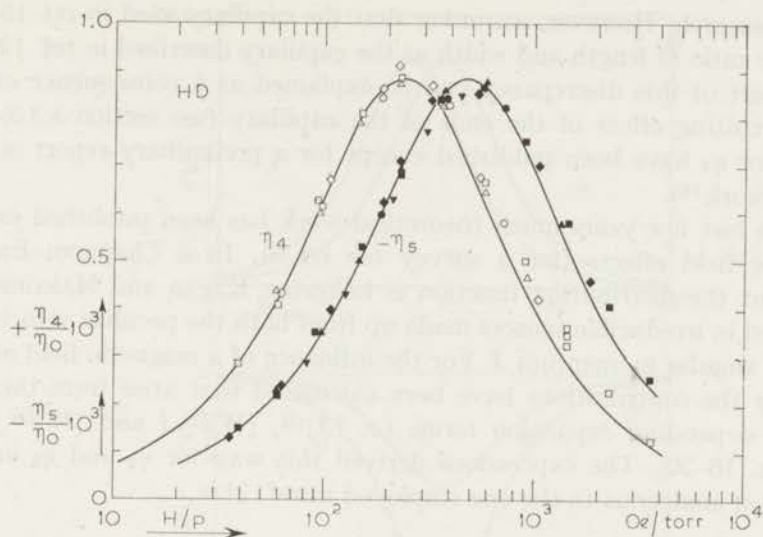


Fig. 10. $+\eta_4/\eta_0$ and $-\eta_5/\eta_0$ as functions of H/p for HD (94% purity).
 ○● 4.0 torr, □■ 5.5 torr, ◇◆ 10.9 torr, △▲ 16.3 torr, ▼ 51 torr.
 η_4 open symbols, η_5 solid symbols.
 — theory: H/p dependence for $[J]^{(2)}$ term.

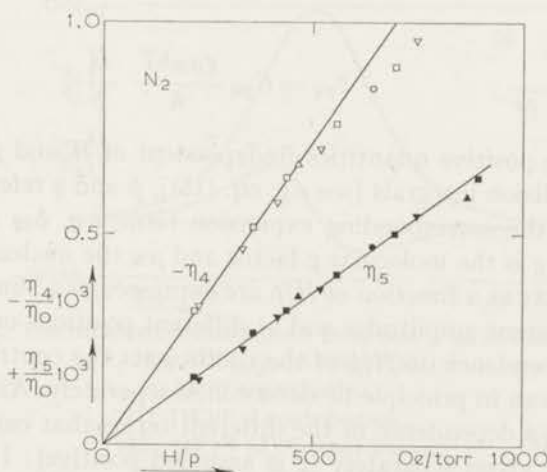


Fig. 11. $-\eta_4/\eta_0$ and $+\eta_5/\eta_0$ as functions of H/p for N_2 on a linear scale.
 ○● 3.5 torr, □■ 5.8 torr, ◇◆ 7.0 torr, △▲ 14.1 torr, ▼ 15.9 torr.
 η_4 open symbols, η_5 solid symbols.

tative nature, the only data with which a direct comparison can be made are the measurements on η_5 for N_2 by Kikoin¹⁵).

For the position of the maximum on the H/p axis the agreement is excellent, but for the magnitude of the effect the difference is considerable. The maximum of η_5/η_0 for N_2 as found by Kikoin is 0.99×10^{-3} vs. 1.36×10^{-3}

in this research. However, assuming that the capillary used in ref. 15 had the same ratio of length and width as the capillary described in ref. 12, the major part of this discrepancy can be explained as a consequence of the short-circuiting effect of the ends of the capillary (see section 3.3.3). No results for η_4 have been published except for a preliminary report on the present work¹⁶).

In the last few years much theoretical work has been published on the magnetic field effects (for a survey see ref. 6). In a Chapman-Enskog treatment the distribution function is following Kagan and Maksimov¹⁷) expanded in irreducible tensors made up from both the peculiar velocity \mathbf{W} and the angular momentum \mathbf{J} . For the influence of a magnetic field on the viscosity the contributions have been calculated that arise from the first three \mathbf{J} depending expansion terms *i.e.* $[\mathbf{J}]^{(2)}$, $[\mathbf{W}]^{(2)}\mathbf{J}$ and $[\mathbf{W}]^{(2)}[\mathbf{J}]^{(2)}$ (see refs. 18-20). The expressions derived this way for η_4 and η_5 are, in a notation analogous to the one employed in ref. 21†:

$$\begin{aligned} \frac{\eta_4}{\eta_0} &= \psi_{02}g(2\xi_{02}) - \frac{3}{2}\psi_{21}g(\xi_{21}) + \frac{1}{24}\psi_{22}[4g(2\xi_{22}) + 6g(\xi_{22})]; \\ -\frac{\eta_5}{\eta_0} &= \psi_{02}g(\xi_{02}) - \frac{3}{4}\psi_{21}g(\xi_{21}) + \frac{1}{24}\psi_{22}[6g(2\xi_{22}) - 5g(\xi_{22})], \end{aligned} \quad (12)$$

where

$$g(\xi) = \frac{\xi}{1 + \xi^2}; \quad \xi_{pq} = C_{pq} \frac{g\mu_N kT}{\hbar} \frac{H}{p};$$

ψ_{pq} and C_{pq} are positive quantities (independent of H and p) that are determined by collision integrals [see *e.g.* eq. (15)], p and q refer to the degree of \mathbf{W} and \mathbf{J} in the corresponding expansion term, *e.g.* ψ_{02} and C_{02} correspond to $[\mathbf{J}]^{(2)}$, g is the molecular g factor and μ_N the nuclear magneton.

Thus the effects as a function of H/p are expressed as a sum of absorption curves with different amplitudes and at different positions on the H/p axis. So from the dependence on H/p of the coefficients the contributions of the different terms can in principle be determined separately. As an illustration in fig. 12 the H/p dependence of the different terms that can contribute to η_4 and $-\eta_5$ are given separately (g is assumed positive): In I the contribution of the $[\mathbf{J}]^{(2)}$ anisotropy is given (only $\psi_{02} \neq 0$), in II that from $[\mathbf{W}]^{(2)}\mathbf{J}$ (only $\psi_{21} \neq 0$) and in III that from $[\mathbf{W}]^{(2)}[\mathbf{J}]^{(2)}$ (only $\psi_{22} \neq 0$). Comparing these graphs with the measured H/p dependence as given in figs. 7-10 it is clear that for the gases studied the $[\mathbf{J}]^{(2)}$ term is by far the most important. To indicate that this term alone gives already a good description of the measurements, in the figs. 7-10 the curves corresponding

† The ψ_{pq} 's employed here are related to those of ref. 20 by $\psi_{02} = \psi'$, $\psi_{21} = \frac{8}{3}\psi''$ and $\psi_{22} = 24\psi$.

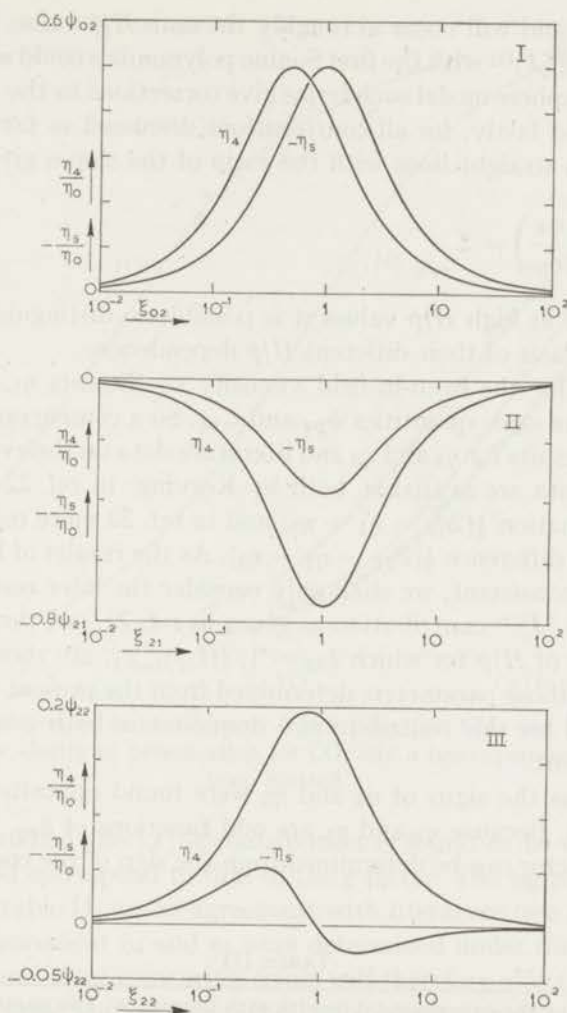


Fig. 12. The different contributions to η_4 and $-\eta_5$ as functions of

$$\xi_{pq} = C_{pq}(g\mu_N kT/\hbar)(H/p).$$

I: $[J]^{(2)}$ contribution,

II: $[W]^{(2)}$ J contribution,

III: $[W]^{(2)}$ $[J]^{(2)}$ contribution.

to $[J]^{(2)}$ have been fitted to the measured points, giving more weight to the points in the low H/p region, using ψ_{02} and C_{02} as adaptable parameters. The values of ψ_{02} and C_{02} obtained this way can differ to some extent from the values that would have been obtained from a fit including all three terms. Such an evaluation of all three contributions appears to be impossible, *i.e.* no meaningful values can be obtained for the four quantities ψ_{21} , C_{21} , ψ_{22} and C_{22} in view of the measuring accuracy for the following reasons: the contributions of the $[W]^{(2)}$ J and the $[W]^{(2)}$ $[J]^{(2)}$ terms have

opposite signs and will occur at roughly the same H/\bar{p} value. Moreover, two terms involving $[J]^{(2)}$ with the first Sonine polynomials could also contribute. For the rough-sphere model such terms give corrections in the order of a few percent²¹). And lastly, for all contributions discussed so far the η_4 and η_5 curves start as straight lines with the ratio of the slopes given by:

$$\lim_{H/\bar{p} \rightarrow 0} \left(-\frac{\eta_4}{\eta_5} \right) = 2. \quad (13)$$

Therefore only at high H/\bar{p} values it is possible to distinguish between the terms on the basis of their different H/\bar{p} dependence.

The effects for the even-in-field viscosity coefficients η_1 , η_2 and η_3 are functions of the same quantities ψ_{pq} and C_{pq} . So a comparison can be made between our results for η_4 and η_5 and literature data on the even coefficients. Two sets of data are available, both by Korving: in ref. 22 measurements for the combination $\frac{1}{2}(2\eta_2 - \eta_1 + \eta_3)$ and in ref. 23 more recent results for η_3 and for the difference $\frac{1}{2}(2\eta_2 - \eta_1 - \eta_3)$. As the results of both references are mutually consistent, we shall only consider the later results. The parameters for the $[J]^{(2)}$ contribution as given in ref. 23, *viz.* the amplitude ψ_{02} and the value of H/\bar{p} for which $\xi_{02} = 1$, $(H/\bar{p})_{\xi_{02}=1}$, are shown in table III together with those parameters determined from the present measurements. It is seen that for this contribution – dominant in both cases – the agreement is excellent.

For each gas the signs of η_4 and η_5 were found opposite, in agreement with eq. (12)[†]. Because η_4 and η_5 are odd functions of ξ_{pq} , the sign of the molecular g factor can be determined from the sign of the coefficients. Since

TABLE III

Comparison of the experimental results with literature: The parameters for the $[J]^{(2)}$ contribution from this research and from ref. 23 (measurements on even-in-field coefficients)				
	$\psi_{02} \times 10^3$		$(H/\bar{p})_{\xi_{02}=1}$ (kOe/torr)	
	this research	ref. 23	this research	ref. 23
N ₂	2.71 ± 0.05	2.7 ± 0.05	3.7 ± 0.1	3.5 ± 0.05
CO	3.60 ± 0.07	3.7 ± 0.03	5.2 ⁵ ± 0.1	5.3 ⁵ ± 0.05
CH ₄	0.81 ± 0.05	0.9 ± 0.03	6.1 ⁵ ± 0.2	6.2 ± 0.1
HD	1.87 ± 0.05		0.48 ± 0.01	

[†] In the introduction of these coefficients in ref. 7 the signs of η_4 and η_5 could be chosen freely. The choice made there causes η_4 and η_5 to have opposite signs in eq. (12).

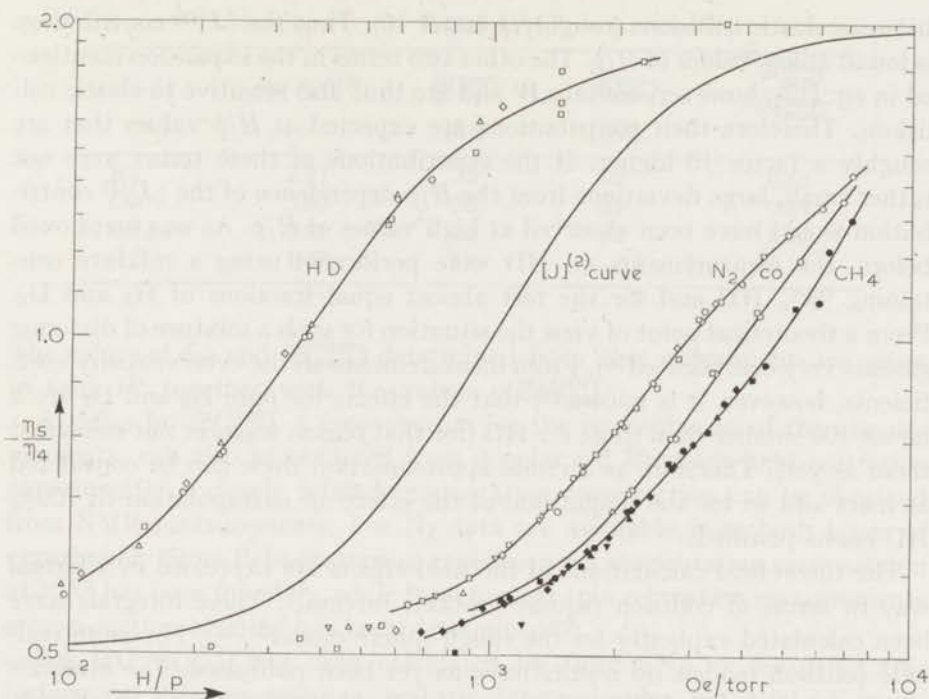


Fig. 13. The ratio $-\eta_5/\eta_4$ as functions of H/p for N_2 , CO , CH_4 and HD (symbols as in figs. 7-11). For clarity of presentation for CO only a few experimental points have been plotted.

for the gases studied the $[J]^{(2)}$ contribution is found to be dominant, the sign of η_4 should correspond to that of the g factor. The signs obtained in this way, shown in table II, are in agreement with literature (see e.g. ref. 24).

At each measurement η_4 and η_5 were determined under the same experimental conditions. Most measuring errors will therefore affect the two coefficients in the same way, leaving the ratio $-\eta_5/\eta_4$ unaffected. In fig. 13 this ratio is plotted vs. H/p for all four gases on a double logarithmic scale. For comparison the theoretical curve corresponding to a pure $[J]^{(2)}$ behaviour has been drawn at an arbitrary position on the H/p axis. Comparing in this graph the results for the different gases, it is seen that the (small) deviations from the $[J]^{(2)}$ shape are definitely different for these gases. This points to different contributions of the higher terms and can also be considered as an argument that these deviations are not caused by systematic measuring errors.

The effects for HD occur at much lower values of H/p than for the other gases. As has been pointed out before²⁵) this is a consequence of the fact that the $[J]^{(2)}$ anisotropy is sensitive only for collisions in which the angular momentum J is changed. Thus the time scale involved is related to the reorientation of J . For HD this time is appreciably longer than the time

between elastic collisions (roughly a factor 10). Thus the $[J]^{(2)}$ contribution is found at low values of H/p . The other two terms in the expansion mentioned in eq. (12), however, contain W and are thus also sensitive to elastic collisions. Therefore their contributions are expected at H/p values that are roughly a factor 10 higher. If the contributions of these terms were not rather small, large deviations from the H/p dependence of the $[J]^{(2)}$ contribution would have been observed at high values of H/p . As was mentioned before, the measurements on HD were performed using a mixture containing 94% HD and for the rest almost equal fractions of H_2 and D_2 . From a theoretical point of view the situation for such a mixture of diatomic gases is very complicated²⁶). From measurements on the even viscosity coefficients, however, it is known²²) that the effects for pure H_2 and D_2 are a factor 100 smaller than those for HD (for that reason we have not measured them as yet). Therefore as a crude approximation these can be considered as inert and so for the magnitude of the effect an extrapolation to 100% HD seems justified.

The theoretical calculations of the field effects are expressed in a formal way in terms of collision (square-bracket) integrals. These integrals have been calculated explicitly for the rough-sphere model^{21, 27}). For more realistic collision models no results have as yet been published. The integrals connected with the $[J]^{(2)}$ anisotropy can be determined from this work. For the presentation of experimental results in a numerical way the collision integrals do not seem very well suited: These integrals contain trivial factors arising from contraction of isotropic tensors and the integrations over the velocities and the angular momenta. For the "spherical" diagonal collision integrals these factors can be removed by defining generalized cross-sections. In this case the general definition reduces to:

$$\mathfrak{S}_{pq00}^{(pq00)} = \frac{1}{\langle v_{\text{rel}} \rangle} \frac{\langle [W]^{(p)} [J]^{(q)} \odot^{(p+q)} \mathfrak{R}_0 [J]^{(q)} [W]^{(p)} \rangle}{\langle [W]^{(p)} [J]^{(q)} \odot^{(p+q)} [J]^{(q)} [W]^{(p)} \rangle}, \quad (14)$$

where $\langle \rangle$ denotes an average over the equilibrium distribution function, $\langle v_{\text{rel}} \rangle = (8kT/\pi\mu)^{1/2}$ with μ the reduced mass and $\mathfrak{R}_0 = -\mathcal{J}_0/n$; n is the number density and \mathcal{J}_0 is the (dissipative) collision operator as defined in eq. (14) of ref. 28.

The cross-sections defined this way are directly related to the quantities C_{pq} of eq. (12) by

$$\mathfrak{S}_{pq00}^{(pq00)} = C_{pq}^{-1} \langle v_{\text{rel}} \rangle^{-1}, \quad (15)$$

while $\mathfrak{S}_{2000}^{(2000)}$ is related to the field-free viscosity coefficient η_0 by

$$\mathfrak{S}_{2000}^{(2000)} = \frac{kT}{\eta_0 \langle v_{\text{rel}} \rangle}. \quad (16)$$

TABLE IV

	$\psi_{02} \times 10^3$	$\mathcal{E}_{(0200)}^{(2000)}$ (\AA^2)	$\mathcal{E}_{(0200)}^{(0200)}$ (\AA^2)	$\frac{\mathcal{E}_{(0200)}^{(0200)}}{\mathcal{E}_{(0200)}^{(2000)}}$
N ₂	2.71	35	22	0.65
CO	3.60	35	31	0.89
CH ₄	0.81	42	32	0.75
HD	1.87	19	2.3	0.12

The values of ψ_{02} and $\mathcal{E}_{(0200)}^{(2000)}$ determined from this experiment are given in table IV together with the values of $\mathcal{E}_{(0200)}^{(2000)}$.

A value for $\mathcal{E}_{(0200)}^{(0200)}$, a cross-section for the reorientation of the angular momenta, can also be obtained from depolarized Rayleigh light-scattering experiments. A closely related reorientation cross-section can be obtained from NMR measurements. For N₂ data are available from both types of experiment. From light-scattering experiments a reorientation cross-section of 30\AA^2 has been found²⁹, while from nuclear spin relaxation measurements a cross-section of 26\AA^2 has been determined³⁰.

For HD $\mathcal{E}_{(0200)}^{(0200)}$ has been calculated by Gordon³¹) by means of trajectory calculations using a realistic intermolecular potential. A cross-section of 1.6\AA^2 was found. This is, in view of the limitation of the model used in these calculations, in reasonable agreement with the value of 2.3\AA^2 as determined from this experiment.

REFERENCES

- 1) Senftleben, H., Physik. Z. **31** (1930) 822.
- 2) Engelhardt, H. and Sack, H., Physik. Z. **33** (1932) 724.
- 3) Trautz, M. and Fröschel, E., Physik. Z. **33** (1932) 947.
- 4) Beenakker, J. J. M., Scoles, G., Knaap, H. F. P. and Jonkman, R. M., Phys. Letters **2** (1962) 5.
- 5) Beenakker, J. J. M., Festkörperprobleme VIII, (Friedr. Vieweg and Sohn GmbH, Braunschweig, Germany, 1968) p. 276.
- 6) Beenakker, J. J. M. and McCourt, F. R., Ann. Rev. Phys. Chem. **21** (1970) 47.
- 7) De Groot, S. R. and Mazur, P., Non-Equilibrium Thermodynamics, (North-Holland Publ. Comp., Amsterdam, 1962) p. 311.
- 8) Hulsman, H. and Knaap, H. F. P., Physica **50** (1970) 565; this thesis, chapter I.
- 9) Cornish, R. J., Proc. Roy. Soc. **A120** (1928) 691.
- 10) Collins, M. and Schowalter, W. R., Phys. of Fluids **5** (1962) 1122.
- 11) Isenberg, I., Russell, B. R. and Greene, R. F., Rev. sci. Instr. **19** (1948) 685.
- 12) Kikoin, I. K., Balashov, K. I., Lasarev, S. D. and Neushtadt, R. E., Phys. Letters **24A** (1967) 165.
- 13) Hirschfelder, J. O., Curtiss, C. F. and Bird, R. B., Molecular theory of gases and liquids, (John Wiley, New York, 1954).

- 14) Korving, J., Hulsman, H., Knaap, H. F. P. and Beenakker, J. J. M., Phys. Letters **21** (1966) 5.
- 15) Kikoin, I. K., Balashov, K. I., Lazarev, S. D. and Neushtadt, P. E., Phys. Letters **26A** (1968) 650.
- 16) Hulsman, H. and Burgmans, A. L. J., Phys. Letters **29A** (1969) 629.
- 17) Kagan, Yu. and Maksimov, L. A., Soviet Physics - JETP **14** (1962) 604.
- 18) Knaap, H. F. P. and Beenakker, J. J. M., Physica **33** (1967) 643 (Commun. Kamerlingh Onnes Lab., Leiden, Suppl. No. 124a).
- 19) McCourt, F. R. and Snider, R. F., J. chem. Phys. **47** (1967) 4117.
- 20) Levi, A. C. and McCourt, F. R., Physica **38** (1968) 415 (Commun. Kamerlingh Onnes Lab., Leiden, Suppl. No. 126a).
- 21) Moraal, H., McCourt, F. R. and Knaap, H. F. P., Physica **45** (1969) 455 (Commun. Kamerlingh Onnes Lab., Leiden, Suppl. No. 127d).
- 22) Korving, J., Hulsman, H., Scoles, G., Knaap, H. F. P. and Beenakker, J. J. M., Physica **36** (1967) 177 (Commun. Kamerlingh Onnes Lab., Leiden No. 357b).
- 23) Korving, J., Physica **50** (1970) 27 (Commun. Kamerlingh Onnes Lab., Leiden No. 381b).
- 24) Hermans, L. J. F., Fortuin, P. H., Knaap, H. F. P. and Beenakker, J. J. M., Phys. Letters **25A** (1967) 81.
- 25) Korving, J., Knaap, H. F. P., Gordon, R. G. and Beenakker, J. J. M., Phys. Letters **24A** (1967) 755.
- 26) Tip, A., Physica **37** (1967) 411.
- 27) McCourt, F. R., Knaap, H. F. P. and Moraal, H., Physica **43** (1969) 485 (Commun. Kamerlingh Onnes Lab., Leiden, Suppl. No. 127c).
- 28) Levi, A. C., McCourt, F. R. and Tip, A., Physica **39** (1968) 165 (Commun. Kamerlingh Onnes Lab., Leiden, Suppl. No. 126b).
- 29) Cooper, V. G., May, A. D., Hara, E. H. and Knaap, H. F. P., Phys. Letters **27A** (1968) 52.
- 30) Speight, P. A. and Armstrong, R. L., Canad. J. Phys. **47** (1969) 1475.
- 31) Gordon, R. G., Malone, G. and Knaap, H. F. P., J. chem. Phys. to be published.

CHAPTER III

THE ODD-IN-FIELD COEFFICIENTS η_4 AND η_5 FOR O_2

Synopsis

Measurements are reported for O_2 on the two odd-in-magnetic-field viscosity coefficients η_4 and η_5 . The dependence on field and pressure has been investigated for fields from 2 Oe to 25 kOe and pressures between 4 torr and 770 torr. It is found that for low pressures and low fields the coefficients can be described as functions of H/p . For higher values of field strength and pressure large deviations from this behaviour are observed. It is found that these deviations can approximately be described as a unique function of H^2/p .

1. *Introduction.* As is well known the transport properties of polyatomic gases are influenced by external fields. For a survey see ref. 1. To describe the influence of a magnetic field on the shear viscosity five coefficients, labelled η_1 to η_5 , are needed²⁾. As was shown in ref. 3, these coefficients can be determined separately by studying the gas flow through a capillary having a rectangular cross section. The field dependence of the coefficients can, for diamagnetic gases such as N_2 , CO, etc., be described as a unique function of H/p , the magnetic field strength divided by the gas pressure (see, e.g., ref. 4). In this paper measurements will be presented for O_2 on the viscosity coefficients η_4 and η_5 which describe the transverse momentum transport caused by the magnetic field. Large deviations from a H/p law are observed in these experiments. Although small, but significant deviations from a H/p law had previously been observed by Senftleben⁵⁾ for the change of the heat conductivity $\Delta\lambda^+$ of O_2 (see also ref. 6), the first observations of large deviations from a H/p law were made by Kikoin *et al.*⁷⁾ in measurements on the viscosity coefficient η_5 . All measurements on the viscosity coefficients prior to this had overlooked these deviations; e.g., in the first Leiden experiments on η_5 these deviations went undetected because of the large scattering in the data⁸⁾. For the even-in-field viscosity coefficients

η_1 , η_2 and η_3 small deviations from H/p have been observed^{7,9}). In this article a systematic study is presented of the deviations for the coefficients η_4 and η_5 .

2. *Experiment.* The experiments were performed at room temperature on O_2 with a purity of 99%. The experimental setup and the measuring procedure were essentially the same as was used for diamagnetic gases in ref. 4. There are, however, a few minor differences. Firstly, the Knudsen corrections could not be determined experimentally, as was done in ref. 4, since the H/p law is essential in that procedure. Consequently, the Knudsen correction on the magnitude of the effect has been assumed to be $1 + 10\xi/t$, where ξ is the mean free path of the gas molecules and t the thickness of the (rectangular) capillary. This has been done since in ref. 4 this same factor was found for all gases studied. This correction is unimportant for the high-pressure measurements (1.5% at 60 torr) and is rather large for the lowest pressures (25% at 4 torr). For diamagnetic gases another Knudsen correction was found *viz.* for the H/p scale. However, as this correction was dependent on the gas, it has not been applied for O_2 : the error thus made is expected to be at most 5% for the lowest pressure series. Secondly, as a consequence of the large magnetic moment of the O_2 molecule – of the order of a Bohr magneton – the effects occur at values of H/p that are very small compared to those for diamagnetic gases. Thus a much larger range of fields and pressures could be used. In the experiments at the lowest fields a coil magnet was used instead of the usual iron core magnet in order to avoid problems with remanent fields. The earth's magnetic field could be neglected under the experimental conditions. For measurements at high fields magnetostriction can be of importance. However, this effect is even in the magnetic field, while the coefficients η_4 and η_5 are odd functions of H so that this disturbance is easily eliminated by combining the results for fields $+H$ and $-H$.

3. *Experimental results and discussion.* The experimental results for η_4 are presented in fig. 1 where $-\eta_4/\eta_0$ is plotted as a function of H/p for five pressures from 4.1 to 61.3 torr. In fig. 2 $+\eta_5/\eta_0$ is plotted *vs.* H/p for the same set of pressures and, in addition, for 772 torr. It is seen from these figures that neither η_4 nor η_5 can be described as an universal function of H/p (*i.e.*, over the whole range of fields and pressures). However, under certain conditions (low fields and low pressures) a H/p law is found to be a good approximation. Under such circumstances all measurements can be represented by the solid lines in figs. 1 and 2 (to be referred to hereafter as the low-pressure curves). It will be shown later that the deviations from these lines can be described as a function of H^2/p rather than as a function of H or p alone.

Measurements on η_5 have also been published by Kikoin *et al.*⁷). If it is

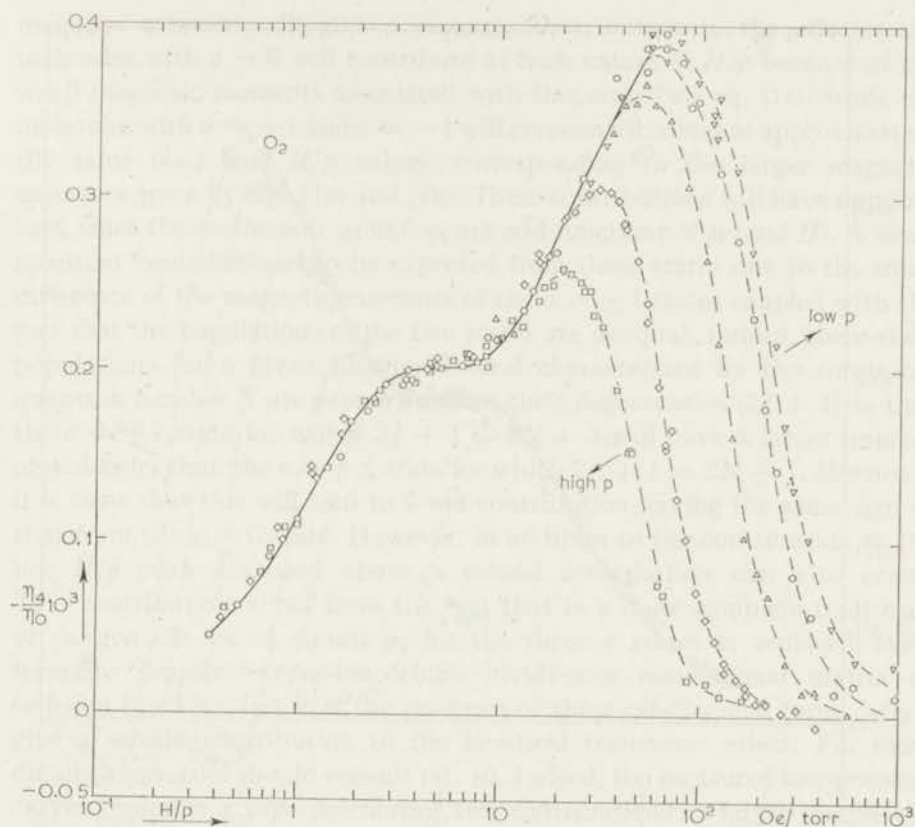


Fig. 1. $-\eta_4/\eta_0$ vs H/p for O_2 .

Δ 4.1 torr, \circ 6.1 torr, \triangle 10.9 torr, \diamond 31.5 torr, \square 61.3 torr.

taken into account that in their work no corrections have been applied for Knudsen effects, their results are not inconsistent with the present ones.

The complicated dependence on field and pressure is basically due to the electronic state of the O_2 molecule, a $^3\Sigma$ ground state. For an explanation of the observed characteristics a detailed theoretical treatment is needed. Such a study is being undertaken¹⁰), but as yet few results are available. Therefore the present discussion will be limited to some general remarks and a phenomenological analysis of the experimental results.

3.1. The dependence on H/p . Using relatively crude models, the dependence on H/p , which is found to be valid for low pressures and low fields, can qualitatively be understood (see also ref. 11). In the $^3\Sigma$ state the spin angular momentum $S(S=1)$ can have three orientations with respect to the total angular momentum J with components $\sigma = +1, -1$ or

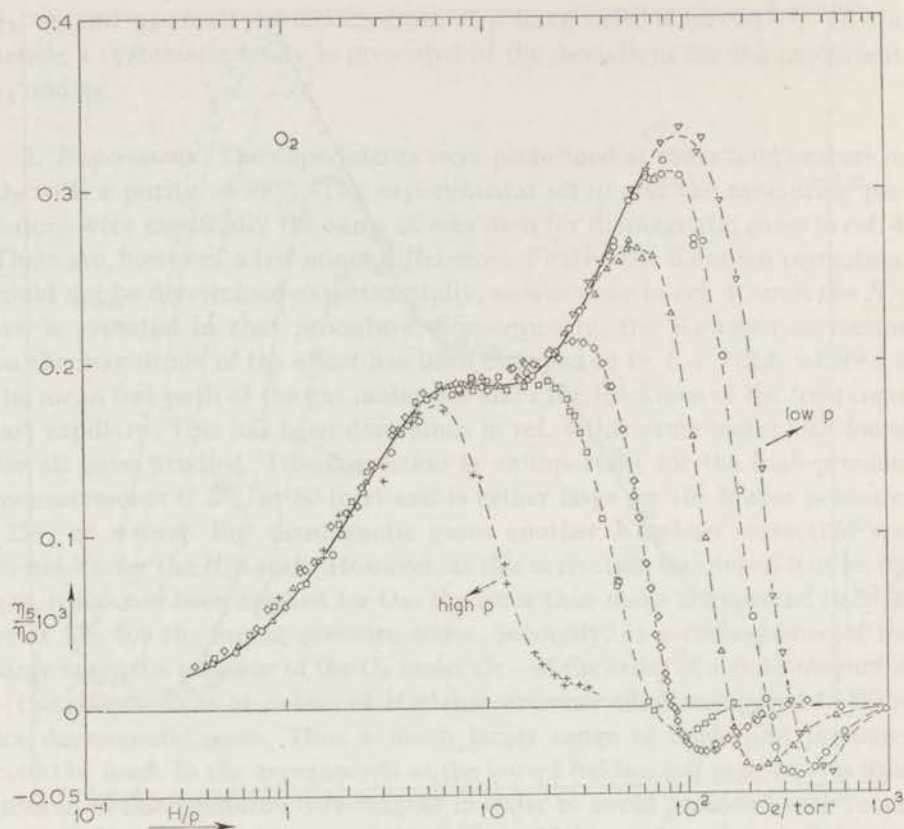


Fig. 2. $+\eta_5/\eta_0$ vs H/p for O_2 .

∇ 4.1 torr, \circ 6.0 torr, Δ 10.9 torr, \diamond 31.6 torr, \square 61.3 torr,
 $+$ 772 torr.

0 along J . Accordingly, the magnetic moments along J are:

$$\mu \approx -2\mu_B J/J \quad (\sigma = +1), \quad (1a)$$

$$\mu \approx +2\mu_B J/J \quad (\sigma = -1), \quad (1b)$$

$$\mu \approx -2\mu_B J/J^2 \quad (\sigma = 0). \quad (1c)$$

In the absence of a magnetic field the σ states can be considered to be well separated when the time of free flight of the molecules is so long that the uncertainty relation does not make the corresponding energy levels overlap, *i.e.* at low pressures. This is still the case in low external fields when the Zeeman levels of the different σ states do not yet overlap. Thus at low fields and low pressures each molecule can be considered to have a magnetic moment as given in eq. (1) and a H/p law will be valid (see *e.g.* eq. (4.2) of ref. 12 and subsequent discussion). Each set of molecules with a particular

magnetic moment will give a separate contribution to the effects: the molecules with $\sigma = 0$ will contribute at high values of H/p because of the small magnetic moments associated with this state [see eq. (1c)] while the molecules with $\sigma = +1$ and $\sigma = -1$ will give contributions at approximately the same (*i.e.*, low) H/p values, corresponding to the larger magnetic moments given by eqs. (1a) and (1b). These contributions will have opposite sign, since the coefficients η_4 and η_5 are odd functions of μ (and H). A small resultant contribution can be expected from these states due to the small difference of the magnetic moments of the $\sigma = \pm 1$ states coupled with the fact that the populations of the two states are unequal. Indeed, the σ -state populations for a given rotational level characterized by the rotational quantum number N are proportional to their degeneracies ($2J + 1$) so that the $\sigma = +1$ state for which $2J + 1 = 2N + 3$ will have a larger number of molecules than the $\sigma = -1$ state for which $2J + 1 = 2N + 1$. Moreover, it is clear that this will lead to a net contribution having the same sign as that from the $\sigma = 0$ state. However, in addition to the contribution to the low H/p peak discussed above a second contribution can also occur. This contribution arises from the fact that in a more complete treatment of oxygen the set of equations for the three σ states is replaced by a formally simpler expression which involves a nondiagonal matrix of collision brackets and it is the presence of these off-diagonal terms which give a second contribution to the low-field transverse effect. For more details, the reader should consult ref. 10. Indeed, the measured low-pressure curves resemble a superposition of two contributions: a larger one at the values of H/p where the contribution of the $\sigma = 0$ molecules would be expected to occur and a smaller one at much lower values of H/p connected with the resultant of the $\sigma = +1$ and the $\sigma = -1$ contributions. Note that the solid curves of figs. 1 and 2 have the same overall shape, displaced by a factor two on the H/p axis, in accordance with the simple single-frequency-double-frequency properties of the coefficients.

3.2. The deviations from H/p . While for low values of field strength and pressure the coefficients can be described as unique functions of H/p - to be denoted by $\eta_{4, \text{lim}}$ and $\eta_{5, \text{lim}}$ - a complicated behaviour is found for high fields and pressures. Still, it appears to be possible to describe the onset of the deviations from $\eta_{4, \text{lim}}$ and $\eta_{5, \text{lim}}$ in a simple way, *viz.*, as a function of H^2/p :

$$\eta_4(H, p) = \eta_{4, \text{lim}}(H/p) - F(H^2/p),$$

$$\eta_5(H, p) = \eta_{5, \text{lim}}(H/p) - F(H^2/p),$$

where $\eta_4(H, p)$ is the value of η_4 as measured for field H and pressure p , $\eta_{4, \text{lim}}(H/p)$ the value of η_4 for the same H/p taken from a smoothed curve through the low-pressure measurements and $F(H^2/p)$ an unknown function

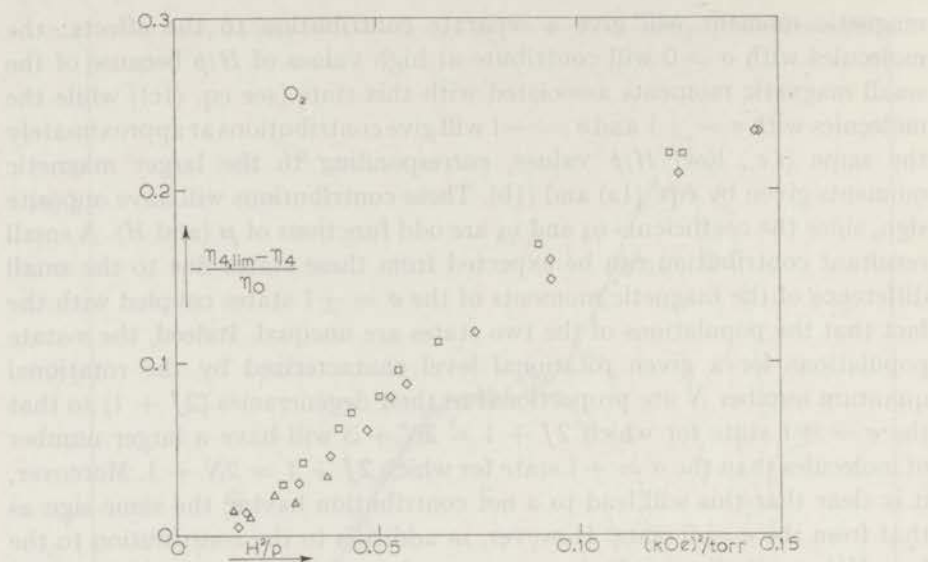


Fig. 3. The difference between the measured values of η_4 at pressure p and the limiting value of η_4 for low pressures $\eta_{4,lim}$ at the same value of H/p (solid line in fig. 1) plotted vs H^2/p .

Δ 10.9 torr, \diamond 31.5 torr, \square 61.3 torr.

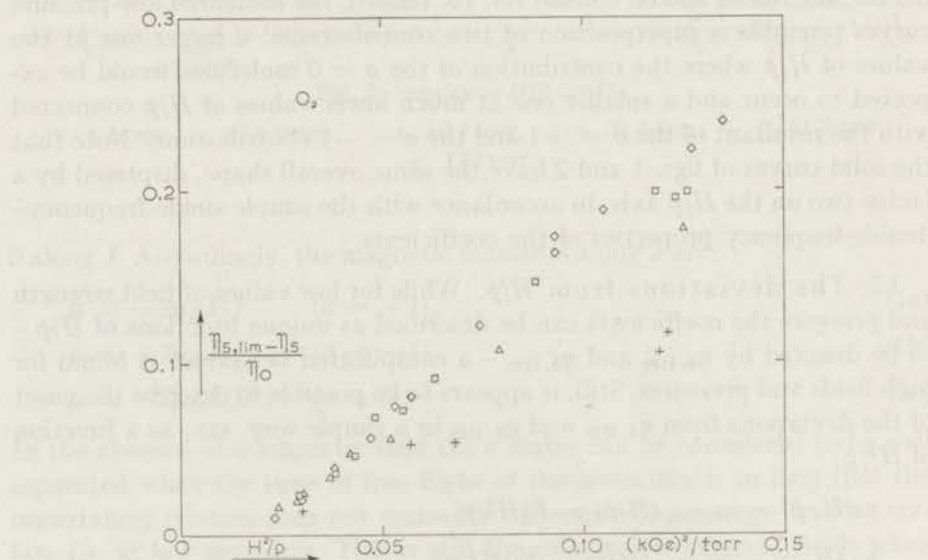


Fig. 4. The difference between the measured values of η_5 at a pressure p and the limiting value of η_5 for low pressures $\eta_{5,lim}$ at the same value of H/p (solid line in fig. 2) plotted vs H^2/p .

Δ 10.9 torr, \diamond 31.6 torr, \square 61.3 torr, $+$ 772 torr.

to be determined from the experiment. The occurrence of the H^2/p term is illustrated in figs. 3 and 4 where the differences $\eta_{4, \text{lim}} - \eta_4$ and $\eta_{5, \text{lim}} - \eta_5$ are plotted *vs.* H^2/p . Note that the same dependence on H^2/p is found both for η_4 and η_5 in contradistinction to the single-frequency-double-frequency behaviour of the corresponding low-pressure curves. This is quite possibly the source of the different behaviour of the various η_4 and η_5 curves in figs. 1 and 2. No statement can be made regarding the precise functional form of the H^2/p dependence due to the fact that the results of this analysis are very sensitive to systematic measuring errors.

Note. Since the first publication of this paper Beenakker, Coope and Snider¹³) have developed a theory that explicitly takes into account the structure of the hamiltonian for O_2 in high magnetic fields. They obtain excellent agreement with the experimental results.

REFERENCES

- 1) Beenakker, J. J. M. and McCourt, F. R., *Ann. Rev. Phys. Chem.* **21** (1970) 47.
- 2) De Groot, S. R. and Mazur, P., *Non-Equilibrium Thermodynamics*, (North-Holland Publ. Comp., Amsterdam, 1962) p. 311.
- 3) Hulsman, H. and Knaap, H. F. P., *Physica* **50** (1970) 565 (Commun. Kamerlingh Onnes Lab., Leiden No. 383*b*); this thesis, chapter I.
- 4) Hulsman, H., Van Waasdijk, E. J., Burgmans, A. L. J., Knaap, H. F. P. and Beenakker, J. J. M., *Physica* **50** (1970) 53 (Commun. Kamerlingh Onnes Lab., Leiden No. 381*c*); this thesis, chapter II.
- 5) Senftleben, H. and Pietzner, J., *Ann. Physik* **27** (1936) 117.
- 6) Hermans, L. J. F., Koks, J. M., Hengeveld, A. F. and Knaap, H. F. P., *Physica* **50** (1970) 410 (Commun. Kamerlingh Onnes Lab., Leiden No. 378*a*).
- 7) Kikoin, I. K., Balashov, K. I., Lasarev, S. D. and Neushtadt, R. E., *Phys. Letters* **24A** (1967) 165.
- 8) Korving, J., Hulsman, H., Knaap, H. F. P. and Beenakker, J. J. M., *Phys. Letters* **21** (1966) 5.
- 9) Hulsman, H., van Kuik, F. G., Walstra, K. W., Knaap, H. F. P. and Beenakker, J. J. M., *Physica* in press; this thesis, chapter IV.
- 10) Coope, J. A. R., Snider, R. F. and McCourt, F. R., *J. chem. Phys.*, **53** (1970) 3358.
- 11) Hermans, L. J. F., Schutte, A., Knaap, H. F. P. and Beenakker, J. J. M., *Physica* **46** (1970) 491 (Commun. Kamerlingh Onnes Lab., Leiden No. 375*b*).
- 12) Moraal, H. and McCourt, F. R., *Physica* **46** (1970) 367 (Commun. Kamerlingh Onnes Lab., Leiden, Suppl. No. 128*b*).
- 13) Beenakker, J. J. M., Coope, J. A. R. and Snider, R. F., *Phys. Rev.* in press.

CHAPTER IV

THE EVEN-IN-FIELD COEFFICIENTS η_1, η_2 AND η_3

Synopsis

Measurements are reported on the influence of a magnetic field on the shear viscosity of the gases N_2 , CO , CH_4 , CF_4 , HD and O_2 at room temperature. The viscosity coefficients η_1 , η_2 and η_3 are determined separately by measuring for different orientations of the field the flow resistance of a capillary with a rectangular cross section. It is found that the change of η_1 is only a few percent of the changes of η_2 and η_3 . The contribution arising from the $[\mathbf{J}]^{(2)}$ anisotropy of the distribution function is found to be dominant. The generalized cross sections connected with this anisotropy are determined.

1. *Introduction.* The viscous behaviour of a gas of polyatomic molecules in a magnetic field can be described with five independent shear viscosity coefficients. According to ref. 1 the symmetric traceless pressure tensor $\overset{\circ}{\Pi}^s$ is related to the symmetric traceless velocity gradient tensor $(\nabla^{\circ}\mathbf{v})^s$ through the following matrix scheme (field in the x direction):

	$(\nabla^{\circ}\mathbf{v})_{xx}^s$	$(\nabla^{\circ}\mathbf{v})_{yy}^s$	$(\nabla^{\circ}\mathbf{v})_{zz}^s$	$(\nabla^{\circ}\mathbf{v})_{yz}^s$	$(\nabla^{\circ}\mathbf{v})_{zx}^s$	$(\nabla^{\circ}\mathbf{v})_{xy}^s$
$\overset{\circ}{\Pi}_{xx}^s$	$-2\eta_1$	0	0	0	0	0
$\overset{\circ}{\Pi}_{yy}^s$	0	$-2\eta_2$	$-2(\eta_1 - \eta_2)$	$-2\eta_4$	0	0
$\overset{\circ}{\Pi}_{zz}^s$	0	$-2(\eta_1 - \eta_2)$	$-2\eta_2$	$2\eta_4$	0	0
$\overset{\circ}{\Pi}_{yz}^s$	0	η_4	$-\eta_4$	$2\eta_1 - 4\eta_2$	0	0
$\overset{\circ}{\Pi}_{zx}^s$	0	0	0	0	$-2\eta_3$	$-2\eta_5$
$\overset{\circ}{\Pi}_{xy}^s$	0	0	0	0	$2\eta_5$	$-2\eta_3$

Of the five independent coefficients, three (η_1, η_2, η_3) are even in the

field and two (η_4, η_5) are odd functions of the field. It is found that the effects of a magnetic field on these coefficients are unique functions of H/p , the ratio of the magnetic field strength to the gas pressure. For a thorough comparison between experiment and theory it appeared necessary to know the behaviour of all five coefficients. In two previous papers^{2,3}) we reported results for the coefficients η_4 and η_5 . In this article experiments will be discussed in which the coefficients η_1, η_2 and η_3 are determined for the same gases.

Although several sets of data on the even coefficients are available, these data are limited to measurements on η_3 and on the combinations of coefficients $\frac{1}{2}(2\eta_2 - \eta_1 + \eta_3)$ and $2\eta_2 - \eta_1 - \eta_3$. (For a survey see ref. 4.) It is obvious that η_1 and η_2 cannot be determined separately from these measurements, as these coefficients occur only in the combination $2\eta_2 - \eta_1$. This is unfortunate, since η_1 is especially interesting for a comparison between theory and experiment: theory predicts that the dominant contribution to the field effect in η_2, η_3, η_4 and η_5 should not contribute to η_1 [see eq. (15)]. Therefore the present experiment was devised to obtain accurate results on η_1 and η_2 separately. Moreover, in the same experiment η_3 can be determined, but only with moderate accuracy.

2. *Experimental method.* As has been discussed in an earlier paper⁵) the viscosity coefficients η_1, η_2 and η_3 can be determined by measuring the flow resistance of a capillary with a rectangular cross section for different orientations of the magnetic field. In the present experiments these different orientations can be realized by rotating an electromagnet around the capillary held in a fixed position as shown in fig. 1. In this arrangement the field lies in the bisector plane of the flow velocity and the velocity gradient of the gas flowing through the capillary. As shown in eq. (5) of ref. 5, the flow through the capillary is in this case determined by

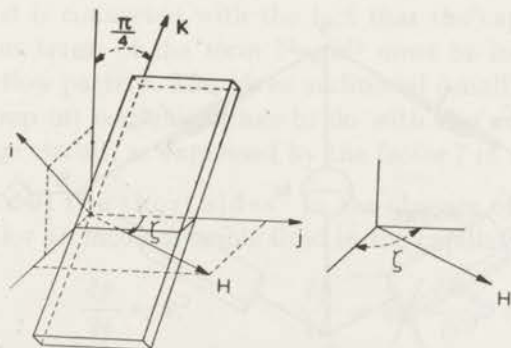


Fig. 1. Schematic diagram of the capillary.

$$\frac{\partial p}{\partial k} = \left[\frac{1}{2}(\eta_1 + \eta_2) \sin^4 \zeta + (2\eta_2 - \eta_1) \cos^2 \zeta + \eta_3 \sin^2 \zeta \cos^2 \zeta \right] \frac{\partial^2 v_k}{\partial i^2}, \quad (1)$$

where (i, j, k) is the capillary-fixed coordinate system and ζ the angle between the field direction and the j axis (see fig. 1). In deriving eq. (1) the effect of the short sides of the capillary on the velocity profile has been neglected. This will be considered in section 3.1. In a typical measurement the same field is applied for three orientations of the magnet, *viz.* $\zeta = 0$, $\frac{1}{4}\pi$ and $\frac{1}{2}\pi$. For these orientations one obtains from eq. (1)

$$\begin{aligned} \zeta = 0: \quad \frac{\partial p}{\partial k} &= (2\eta_2 - \eta_1) \frac{\partial^2 v_k}{\partial i^2}, \\ \zeta = \frac{\pi}{4}: \quad \frac{\partial p}{\partial k} &= \left(\frac{9}{8}\eta_2 - \frac{3}{8}\eta_1 + \frac{1}{4}\eta_3 \right) \frac{\partial^2 v_k}{\partial i^2}, \\ \zeta = \frac{\pi}{2}: \quad \frac{\partial p}{\partial k} &= \left(\frac{1}{2}\eta_1 + \frac{1}{2}\eta_2 \right) \frac{\partial^2 v_k}{\partial i^2}. \end{aligned} \quad (2)$$

By measuring the changes in the pressure drop over the capillary caused by the field, while the flow is kept constant, one can determine the changes of the three combinations of coefficients on the right-hand sides of eqs. (2). From these one can calculate η_1 , η_2 and η_3 .

Because the changes in the pressure drop that are introduced by the field are small, at most of the order of 0.1%, a differential method has been used. The measuring capillary (C_1) is part of a gas-flow Wheatstone bridge. The three other capillaries in the bridge (C_2 , C_3 , C_4) are placed outside the field. A high-sensitivity differential manometer (M) serves as the null detector (see fig. 2). When a field is applied on C_1 the resulting viscosity change causes an unbalance of the bridge that is measured by M.

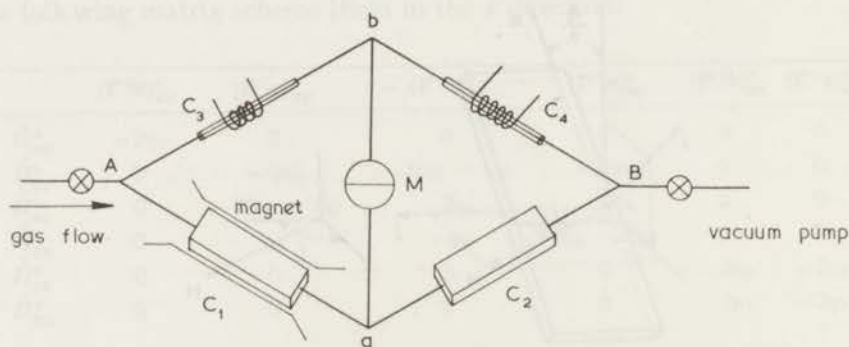


Fig. 2. Schematic diagram of the capillary bridge.

The relative change of the viscosity is calculated from

$$\frac{\Delta\eta}{\eta} = -4 \frac{p_a - p_b}{p_A - p_B} f. \quad (3)$$

The subscripts A, B, a and b refer to different points of the bridge (see fig. 2), while f is a correction factor to account for the deviations from the ideal Poiseuille flow as will be discussed in section 3.2.

The measuring capillary C_1 and the capillary C_2 have rectangular cross sections and have the same dimensions: length $l = 104$ mm, width $w = 15$ mm and thickness $t = 0.75$ mm. Both C_3 and C_4 consist of two parallel capillaries of circular cross section 1 mm in diameter and 62 mm in length. Complete balance of the bridge can be attained by slightly heating either C_3 or C_4 . This varies the effective flow resistance of the capillary by changing the density and the viscosity of the gas.

The gas flow through the bridge is adjusted by means of a needle valve upstream. A flow controller (Moore 63 BDL) is used to keep the flow constant, independent of the pressure in the gas storage vessel. The pressure in the measuring capillary is adjusted by means of a valve between the exit of the bridge and the vacuum pump. Pressures at the points A, B and a (see fig. 2) are measured with oil manometers. The pressure difference $p_a - p_b$ is measured with a differential capacitance manometer with a sensitivity of better than 10^{-5} torr (Atlas Membran Mikro Manometer). The electromagnet is an Oerlikon C 3, used with pole pieces of 18 cm diameter at a distance of 12 cm, giving a maximum field of 22.6 kOe. The homogeneity of the field is sufficient for the present experiments.

A control run has been performed with argon. As should be expected, no field effects could be detected. The long-term reproducibility of the measurements was excellent.

3. *Corrections.* In order to calculate the viscosity coefficients η_1 , η_2 and η_3 from the observed pressure differences, two types of corrections must be applied. The first is connected with the fact that the capillary is not infinitely wide. Thus terms of the form $\partial^2 v_k / \partial j^2$ must be included in the description of the flow pattern. This gives additional (small) terms in eq. (1). The second (group of) corrections has to do with the non-ideal Poiseuille flow in the bridge circuit, as expressed by the factor f in eq. (3).

3.1. *Presence of the short sides.* In the absence of a field the equations of motion for an incompressible fluid in the capillary of fig. 1 are

$$\frac{\partial p}{\partial i} = 0, \quad \frac{\partial p}{\partial j} = 0, \quad \frac{\partial p}{\partial k} = \eta_0 \left(\frac{\partial^2 v_k}{\partial i^2} + \frac{\partial^2 v_k}{\partial j^2} \right), \quad (4)$$

where η_0 is the field-free viscosity coefficient. Assuming that the velocity

is zero at the walls, the resulting flow pattern is given⁶) by

$$v_k = -\frac{1}{2\eta_0} \frac{\partial p}{\partial k} \left[\left(\frac{1}{2}t\right)^2 - i^2 - \frac{8t^2}{\pi^3} \left\{ \frac{\cosh(\pi j/t)}{\cosh(\pi w/2t)} \cos(\pi i/t) - \frac{1}{3^3} \frac{\cosh(3\pi j/t)}{\cosh(3\pi w/2t)} \cos(3\pi i/t) + \dots \right\} \right], \quad (5)$$

where w , t and l are the width, thickness and length of the capillary. By integration one finds V the total volume flow per unit time. For capillaries with $w > 4t$ it is given to a good approximation by

$$V = \frac{\Delta p}{12\eta_0} \frac{wt^3}{l} \left(1 - 0.630 \frac{t}{w} \right). \quad (6)$$

In the presence of a magnetic field the equations of motion are rather complicated: the pressure gradients $\partial p/\partial i$ and $\partial p/\partial j$ of eq. (4) become non-zero. One can argue, however, that the influence of these gradients on the total flow through the capillary is small. Therefore the only gradient of importance is $\partial p/\partial k$, which for the field directions considered can be written as

$$\frac{\partial p}{\partial k} = \eta_i \frac{\partial^2 v_k}{\partial i^2} + \eta_j \frac{\partial^2 v_k}{\partial j^2},$$

with

$$\begin{aligned} \eta_i &= \frac{1}{2}(\eta_1 + \eta_2) \sin^4 \zeta + (2\eta_2 - \eta_1) \cos^2 \zeta + \eta_3 \sin^2 \zeta \cos^2 \zeta, \\ \eta_j &= \frac{1}{2}(\eta_1 + \eta_2) \frac{1}{2} \sin^2 2\zeta + (2\eta_2 - \eta_1) \frac{1}{2} \sin^2 \zeta \\ &\quad + \eta_3 \left(\frac{1}{2} \cos^2 \zeta + \frac{1}{2} \cos^2 2\zeta \right). \end{aligned} \quad (7)$$

The resulting flow velocity pattern [corresponding to eq. (5)] is found with a simple transformation. Then, integrating over the cross section, one finds for the total volume flow:

$$V = \frac{\Delta p}{12\eta_i} \frac{wt^3}{l} \left(1 - 0.630 \frac{t}{w} \sqrt{\frac{\eta_j}{\eta_i}} \right). \quad (8)$$

Comparing eqs. (6) and (8) one finds the following relation for the (small) changes that are introduced by the field when V is kept constant:

$$\begin{aligned} &\frac{\Delta p(H) - \Delta p(H=0)}{\Delta p(H=0)} \\ &= \left(1 - \frac{1}{2} 0.630 \frac{t}{w} \right) \frac{\eta_i - \eta_0}{\eta_0} + \frac{1}{2} 0.630 \frac{t}{w} \frac{\eta_j - \eta_0}{\eta_0}, \end{aligned} \quad (9)$$

where η_i and η_j are the combinations of viscosity coefficients as defined in eq. (7). Thus it appears that in the experiment where $w = 20t$ the contri-

butions related to the presence of $\partial^2 v_k / \partial j^2$ are only 1.5%. Although this correction is small, it is very important for the effects obtained for η_1 , since for all gases studied, the effect for this coefficient is only a few percent of those for η_2 or η_3 (see figs. 5-14). Including this correction, the changes of η_1 , η_2 and η_3 can be calculated from the measurements for $\zeta = 0$, $\frac{1}{4}\pi$ and $\frac{1}{2}\pi$, with

$$\begin{aligned}\Delta\eta_1 &= -0.3387\Delta\eta(\zeta = 0) - 0.0215\Delta\eta(\zeta = \frac{1}{4}\pi) \\ &\quad + 1.3602\Delta\eta(\zeta = \frac{1}{2}\pi), \\ \Delta\eta_2 &= +0.3554\Delta\eta(\zeta = 0) - 0.0441\Delta\eta(\zeta = \frac{1}{4}\pi) \\ &\quad + 0.6887\Delta\eta(\zeta = \frac{1}{2}\pi), \\ \Delta\eta_3 &= -2.0909\Delta\eta(\zeta = 0) + 4.1656\Delta\eta(\zeta = \frac{1}{4}\pi) \\ &\quad - 1.0747\Delta\eta(\zeta = \frac{1}{2}\pi),\end{aligned}\tag{10}$$

where $\Delta\eta(\zeta)$ are the viscosity changes as calculated from the unbalance of the capillary bridge according to eq. (3).

3.2. Deviations from the ideal Poiseuille flow. Incorporating a number of corrections, to be discussed below, the equation (6) for the gas flow through the capillary becomes (see also refs. 2 and 7)

$$\begin{aligned}\frac{(p_A + K_\alpha)^2 - (p_a + K_\alpha)^2}{2} \\ = \frac{12\eta_0 l}{wt^3} \frac{G}{\rho_0} \frac{[1 + \frac{1}{20}\{m + \ln(p_A/p_a)\}(t/l) Re]}{[1 - 0.630t/w]},\end{aligned}\tag{11}$$

where K_α is a constant describing the Knudsen effect on the flow, G is the mass flow per unit time, ρ_0 the density at unit pressure, m a number of the order unity and Re the Reynolds number defined as $2G/w\eta_0$. For the correction factor f in eq. (3) the following form has been used:

$$\begin{aligned}f &= \frac{p_a + K_\alpha}{\frac{1}{2}(p_A + p_B) + K_\alpha} [1 + \frac{1}{20}\{m + \ln(p_A/p_a)\}(t/l) Re] \\ &\quad \times \left[1 + \frac{K_\beta}{\frac{1}{2}(p_A + p_a)} \right],\end{aligned}\tag{12}$$

where K_β is a constant describing the Knudsen effect.

3.2.1. Reynolds correction. The factor $1 + \frac{1}{20}\{m + \ln(p_A/p_a)\}(t/l) Re$ arises from the pressure losses caused by the acceleration of the gas. The constant m , which depends on the shape of the entrance of the capillary, is assumed to be 0.75. This correction is less than 1% for all cases, except for the high-pressure O_2 measurements where it can be as large as 5%.

3.2.2. Expansion correction. According to eq. (11) the pressure drop over the capillary is quadratic. This is caused by the expansion of the gas in the capillary. Along the length of the capillary the mass transport is constant and so $p \partial p / \partial k$ is constant. In eq. (12) the quadratic dependence gives rise to the factor $(p_a + K_\alpha) / (\frac{1}{2}p_A + \frac{1}{2}p_a + K_\alpha)$.

3.2.3. Knudsen corrections. Most experiments have been performed at low pressures, where the mean free path of the gas molecules, ξ , is not negligible as compared to the thickness of the capillary t . Thus deviations from the high-pressure values can be expected. (A detailed theoretical treatment is performed by Vestner⁸.) For not too low pressures such deviations should be proportional to the mean free path and therefore proportional to $1/p$. Indeed, it appears that one has to apply corrections of the form $1 + K/p$. In eqs. (11) and (12) the constant K_α describes the correction of the field-free flow. For a simplified case K_α can be calculated under the assumption that the molecules leave the wall with randomly oriented velocities: one finds

$$K_\alpha = 6\xi p/t. \quad (13)$$

Calculated and measured values of K_α agree within the (moderate) accuracy. Knudsen corrections also have to be applied to the magnetic-field effect. Plotting the effects as functions of H/p , it is found that the curves obtained for different pressures do not coincide completely. As discussed in ref. 2 this is caused by Knudsen effects which affect both the magnitude of $\Delta\eta$ and the position of the curve along the H/p axis. The correction for the magnitude $1 + K_\beta/p$ has been included in eq. (12). The generally small correction for the H/p scale has the form

$$(H/p)_{\text{corr}} = \frac{(H/p)_{\text{exp}}}{1 + K_\gamma/p}. \quad (14)$$

The calculated values of K_α and the experimental values of K_β and K_γ are given in table I. Since eq. (13) appears to hold reasonably well, K_β and K_γ can also be expressed as $n_\beta \xi p/t$ and $n_\gamma \xi p/t$. The quantities n_β and n_γ , which do not depend on the dimensions of the apparatus, have been included in table I.

TABLE I

	Knudsen correction parameters					
	K_α (torr)	K_β (torr)	K_γ (torr)	n_α	n_β	n_γ
N ₂	0.39	0.76	0.27	(6)	12	4
CO	0.39	0.64	0.14	(6)	10	2
CH ₄	0.32	0.50	0.13	(6)	9	3
CF ₄	0.22	0.49	—	(6)	13	—
HD	0.73	0.77	1.72	(6)	6	14

In the present experiments the Knudsen correction to the magnitude of the effects $(1 + K_{\beta}/p)$ is, for the lowest pressures, as large as 35%, whereas for the high-pressure measurements it is of the order of 5%. The correction for the H/p values $(1 + K_{\gamma}/p)$ is always less than 10% with the exception of the HD measurements, where for the lowest pressure it becomes as large as 50%.

3.3. Stray fields. A correction for the stray field at the positions of the other capillaries is applied to the measurements of O₂ and HD at the lowest pressures. At the highest fields a small correction has to be applied for a disturbance of the membrane manometer by the stray field. For all measuring series this correction is less than a few percent of the maximum signal.

4. *Experimental results and discussion.* First of all, measurements have been performed for various magnetic-field directions as indicated by the angle ζ in fig. 1. The observed viscosity changes $\Delta\eta(\zeta)$, normalized to the change for $\zeta = 0$, are plotted in fig. 3 for N₂ at two values of H/p . One can derive four main conclusions from this figure: a. The curve is symmetric around $\zeta = 0$, as should be expected from the symmetry of the experimental setup [cf. fig. 1 and eqs. (1) and (7)]. b. The curves for different values of H/p do not coincide, thus reflecting the different field dependences

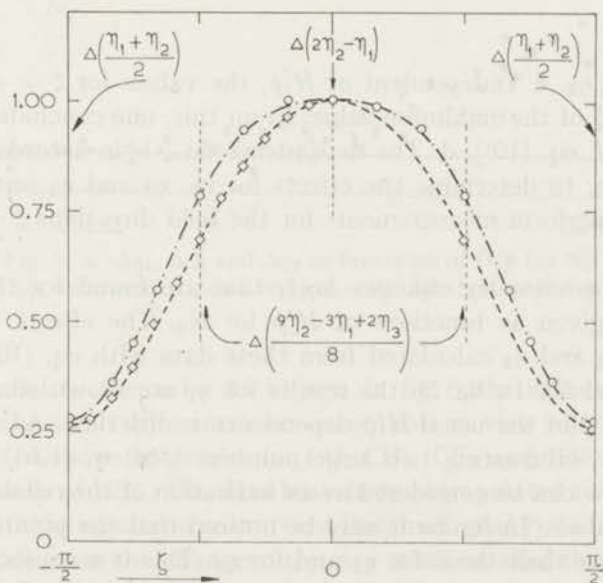


Fig. 3. The viscosity change for N₂ as a function of the field direction ζ normalized to the effect for $\zeta = 0$.

◇ $H/p = 2.0$ kOe/torr; ○ $H/p = 7.7$ kOe/torr.

The lines correspond to the angular dependence given by eq. (7).

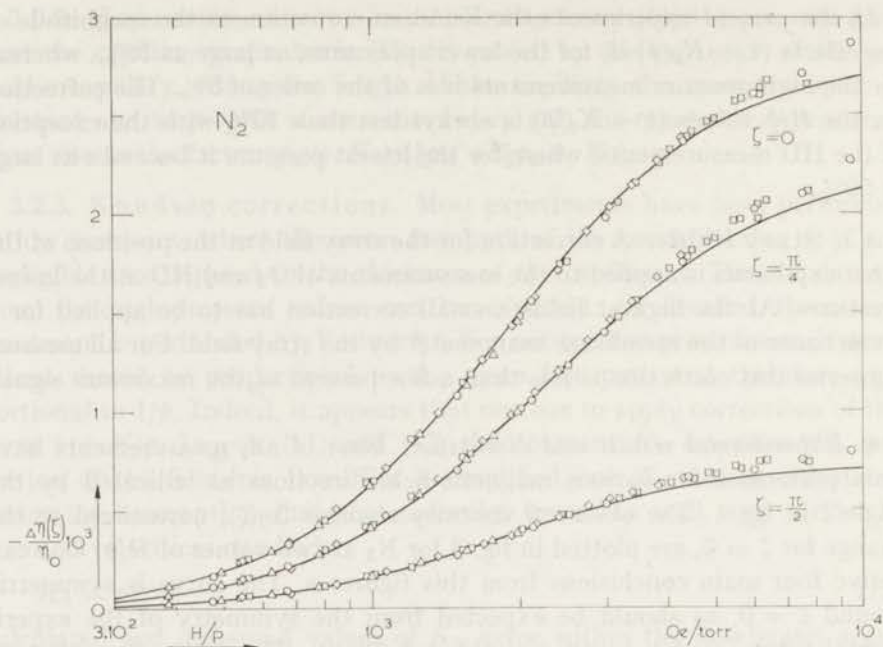


Fig. 4. The viscosity changes for N_2 as functions of H/p for $\zeta = 0, \pi/4$ and $\pi/2$.
 \circ 2.1 torr; \diamond 5.0 torr; \square 3.3 torr; \triangle 11.2 torr;
 ——— theoretical H/p dependence for $[J]^{(2)}$ term.

of η_1 , η_2 and η_3 . c. Independent of H/p , the values for $\zeta = \pm\pi/2$ are approximately $\frac{1}{4}$ of the maximum value. From this, one concludes that $\Delta\eta_1$ is very small [cf. eq. (10)]. d. The dependence on ζ is in accordance with eq. (7). Therefore, to determine the effects for η_1 , η_2 and η_3 separately, it is sufficient to perform measurements for the field directions $\zeta = 0, \pi/4$ and $\pi/2$.

In fig. 4 the viscosity changes $\Delta\eta(\zeta)$ that are found for these field directions are given as functions of H/p for N_2 . The effects for the coefficients η_1 , η_2 and η_3 calculated from these data with eq. (10), are shown in figs. 5a and 5b. In fig. 5b the results for η_1 are shown on an expanded scale. In this plot the usual H/p dependence is observed. As $\Delta\eta_1$ has been calculated by subtracting two large numbers [see eq. (10a)] the validity of the H/p law can be considered as an indication of the reliability of these very small values. In fig. 5a it may be noticed that the points for η_3 show a larger scatter than those for η_1 and for η_2 . This is a consequence of the fact that in this setup the effects as measured for the different orientations depend only weakly on η_3 [see eq. (7)]. In fig. 6 the results for η_3 are compared with the experimental results of ref. 7. In the latter experiment η_3 is obtained directly, using a capillary with a circular cross section and with

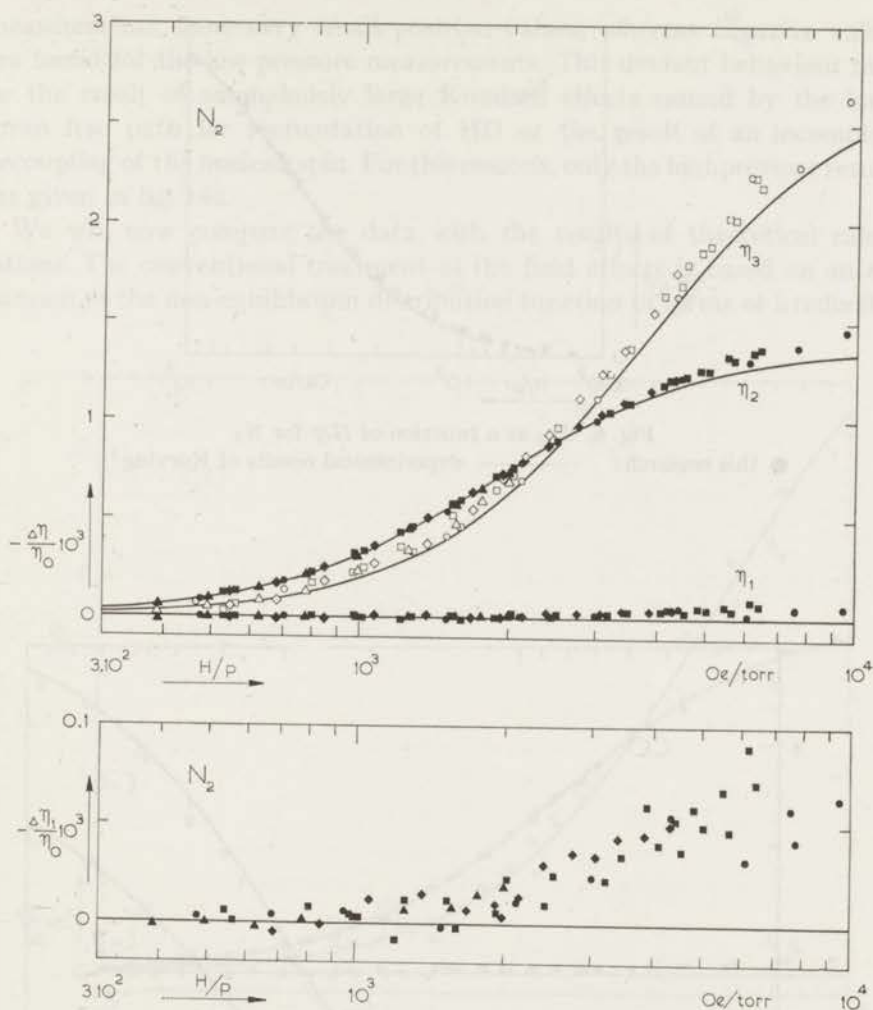


Fig. 5. a. $\Delta\eta_1$, $\Delta\eta_2$ and $\Delta\eta_3$ as functions of H/p for N_2 .
 b. $\Delta\eta_1$ with an expanded vertical scale. Symbols as in fig. 4.

the field parallel to the axis. As is seen in fig. 6 the agreement is quite satisfactory; the small differences are acceptable in view of the accuracies.

The figs. 7-14 show the results for CO, CH_4 , CF_4 and HD. The HD gas used had a purity of 92%. The data have been extrapolated to 100% HD in accordance with the results on mixtures of Burgmans *et al.*⁹⁾ In the figures one sees that for all gases the changes in η_1 are much smaller than those in η_2 and η_3 . While for N_2 and CO the changes in η_1 , η_2 and η_3 are all negative, positive changes in η_1 are found for CH_4 and CF_4 . We shall come back to this point below. The results for η_1 of HD as shown in fig. 14b cannot be described as a unique function of H/p . The most reliable high-pressure

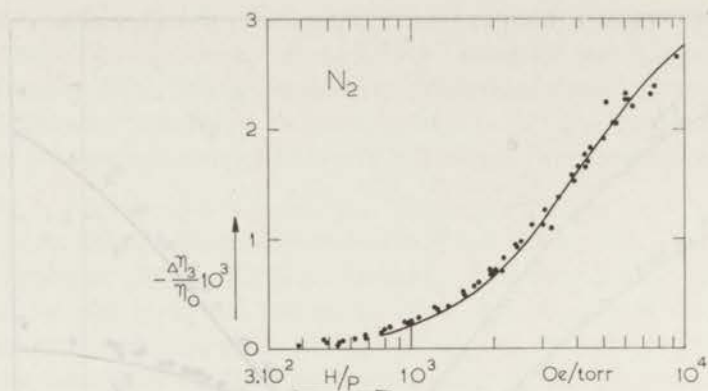


Fig. 6. $\Delta\eta_3$ as a function of H/p for N_2 .

● this research; — experimental results of Korving⁷⁾.

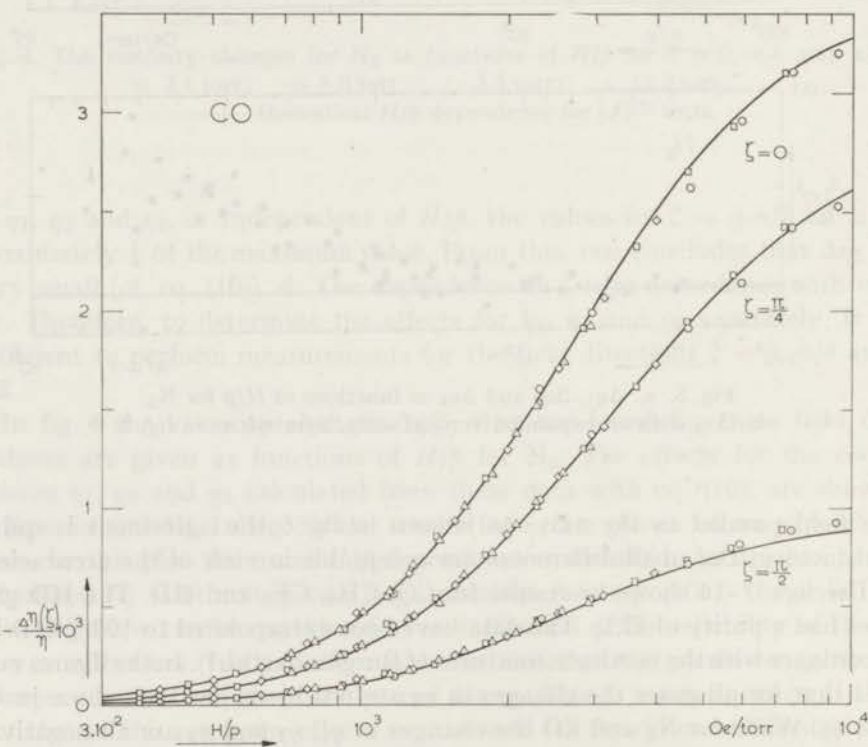


Fig. 7. The viscosity changes for CO as a function of H/p for $\zeta = 0, \pi/4$ and $\pi/2$.

○ 1.8 torr; ◇ 5.5 torr; □ 3.0 torr; △ 7.6 torr;
 — theoretical H/p dependence for $[J]^{(2)}$ term.

measurements show very small positive values, whereas negative values are found for the low-pressure measurements. This deviant behaviour may be the result of anomalously large Knudsen effects caused by the large mean free path for reorientation of HD or the result of an incomplete decoupling of the nuclear spin. For this reasons, only the highpressure results are given in fig. 14a.

We will now compare the data with the results of theoretical calculations. The conventional treatment of the field effects is based on an expansion of the non-equilibrium distribution function in terms of irreducible

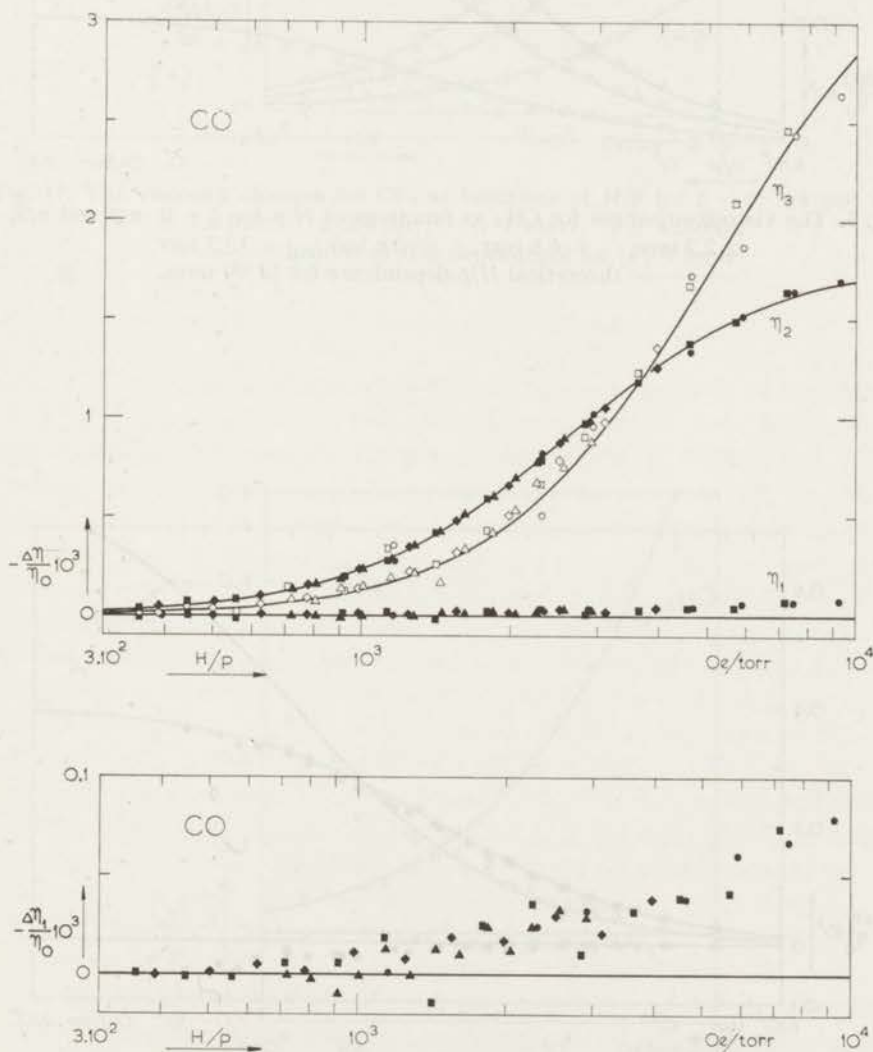


Fig. 8. a. $\Delta\eta_1$, $\Delta\eta_2$ and $\Delta\eta_3$ as functions of H/p for CO.
 b. $\Delta\eta_1$ with an expanded vertical scale. Symbols as in fig. 7.

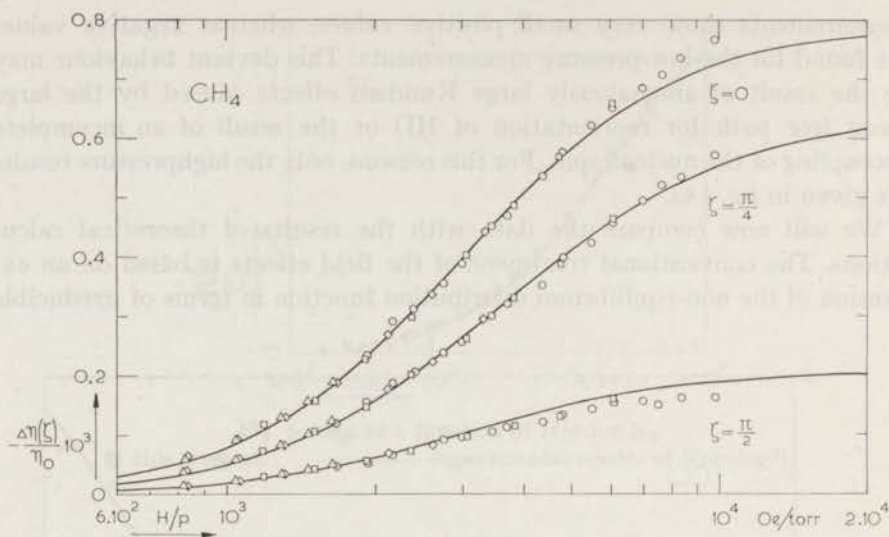


Fig. 9. The viscosity changes for CH_4 as functions of H/p for $\zeta = 0, \pi/4$ and $\pi/2$.
 \circ 2.2 torr; \diamond 6.6 torr; \square 3.6 torr; \triangle 13.7 torr;
 ——— theoretical H/p dependence for $[J]^{(2)}$ term.

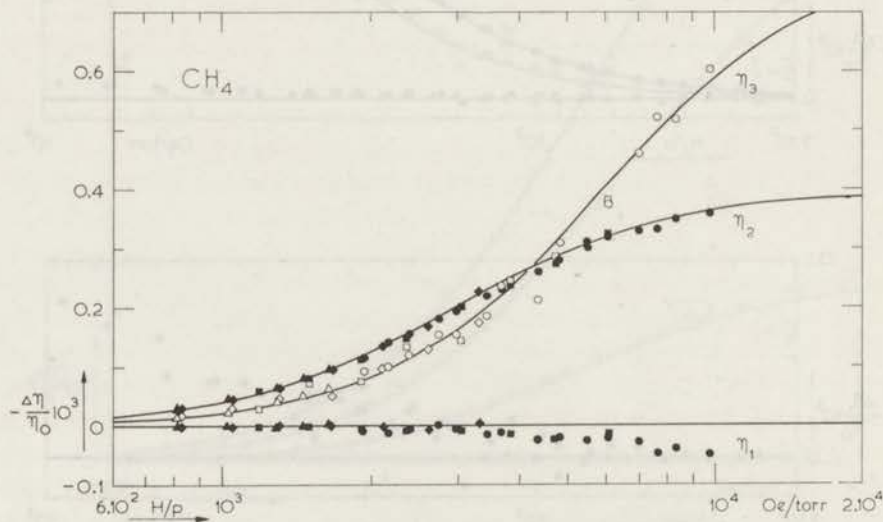


Fig. 10. $\Delta\eta_1$, $\Delta\eta_2$ and $\Delta\eta_3$ as functions of H/p for CH_4 .
 Symbols as in fig. 9.

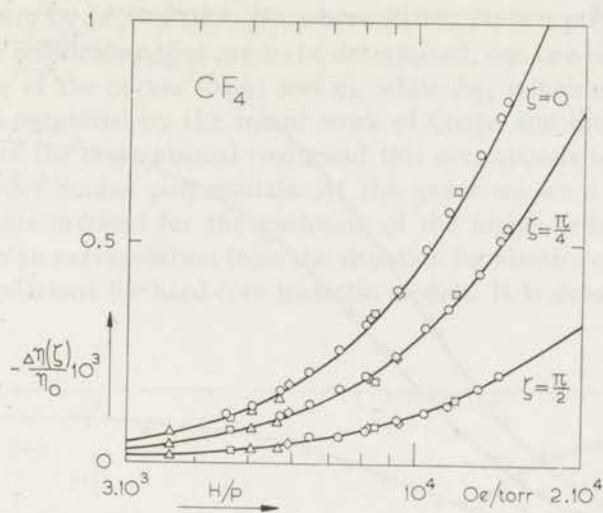


Fig. 11. The viscosity changes for CF_4 as functions of H/p for $\zeta = 0, \pi/4$ and $\pi/2$.
 ○ 1.6 torr; ◇ 2.4 torr; □ 1.9 torr; △ 4.0 torr;
 — theoretical H/p dependence for $[J]^{(2)}$ term.

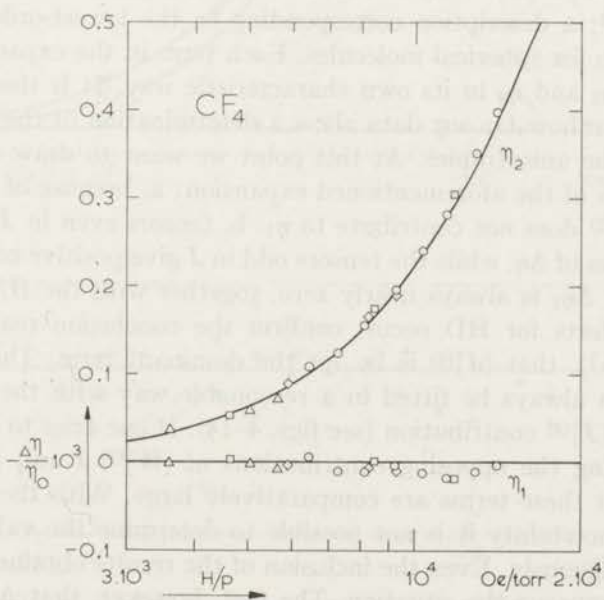


Fig. 12. $\Delta\eta_1$ and $\Delta\eta_2$ as functions of H/p for CF_4 . Symbols as in fig. 11.

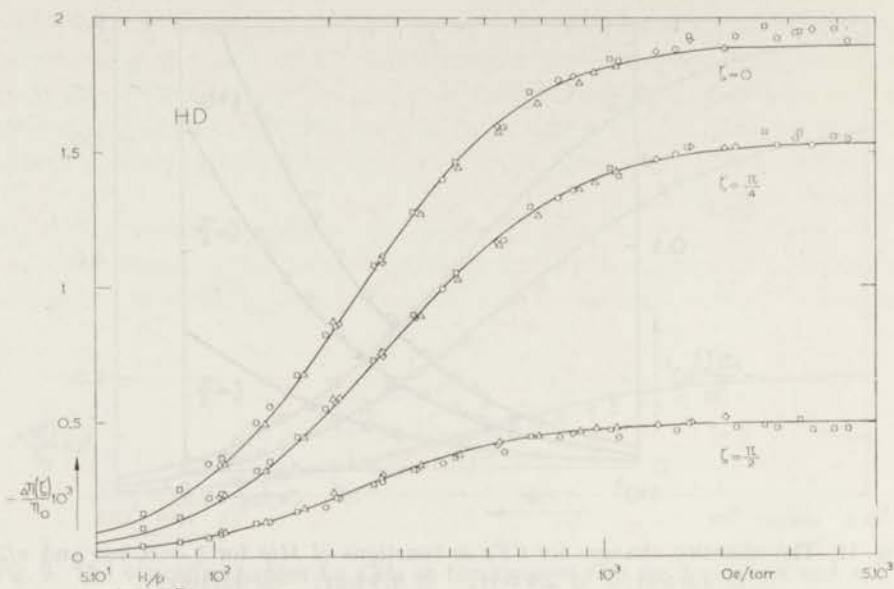


Fig. 13. The viscosity changes for HD as functions of H/p for $\zeta = 0, \pi/4$ and $\pi/2$.
 ○ 3.4 torr; ◇ 8.8 torr; □ 5.1 torr; △ 16.9 torr;
 — theoretical H/p dependence for $[J]^{(2)}$ term.

tensors made up of reduced velocity W and angular momentum J . In this expansion at most three (vector) J -dependent terms are considered: $[J]^{(2)}$, $[W]^{(2)} J$ and $[W]^{(2)} [J]^{(2)}$. The coefficients in the expansion are independent of J^2 and W^2 ; a description corresponding to the lowest-order "Sonine" approximation for spherical molecules. Each term in the expansion contributes to η_1 , η_2 and η_3 in its own characteristic way. It is therefore interesting to see in how far our data allow a determination of the relative importance of the anisotropies. At this point we want to draw attention to two properties of the aforementioned expansion: a. because of its tensorial structure $[J]^{(2)}$ does not contribute to η_1 . b. tensors even in J give rise to negative values of $\Delta\eta$, while the tensors odd in J give positive contributions. The fact that $\Delta\eta_1$ is always nearly zero, together with the H/p values for which the effects for HD occur, confirm the conclusion reached in our earlier work^{2,7}, that $[J]^{(2)}$ is by far the dominant term. The results for η_2 and η_3 can always be fitted in a reasonable way with the expressions valid for the $[J]^{(2)}$ contribution (see figs. 4-14). If one tries to improve the fit by including the opposing contributions of $[W]^{(2)} J$ and $[W]^{(2)} [J]^{(2)}$, one finds that these terms are comparatively large. With the present experimental uncertainty it is not possible to determine the values of these terms unambiguously. Even the inclusion of the results obtained for η_4 and η_5 does not improve the situation. The fact, however, that $\Delta\eta_1$ is almost zero is highly suggestive of another solution to the problem. If one replaces

the $[J]^{(2)}$ term by $[J]^{(2)} P(W^2, J^2)$, where $P(W^2, J^2)$ is a polynomial in W^2 and J^2 with coefficients that are to be determined, one can obtain a change in the shape of the curves for η_2 and η_3 , while $\Delta\eta_1$ remains zero. Such an approach is suggested by the recent work of Coope and Snider¹⁰). In the framework of the conventional treatment this corresponds to the inclusion of higher-order Sonine polynomials. At this point we want to stress that the arguments invoked for the exclusion of the higher-order polynomials are based on an extrapolation from the situation for elastic-collision models, and on calculations for hard-core inelastic models. It is debatable whether

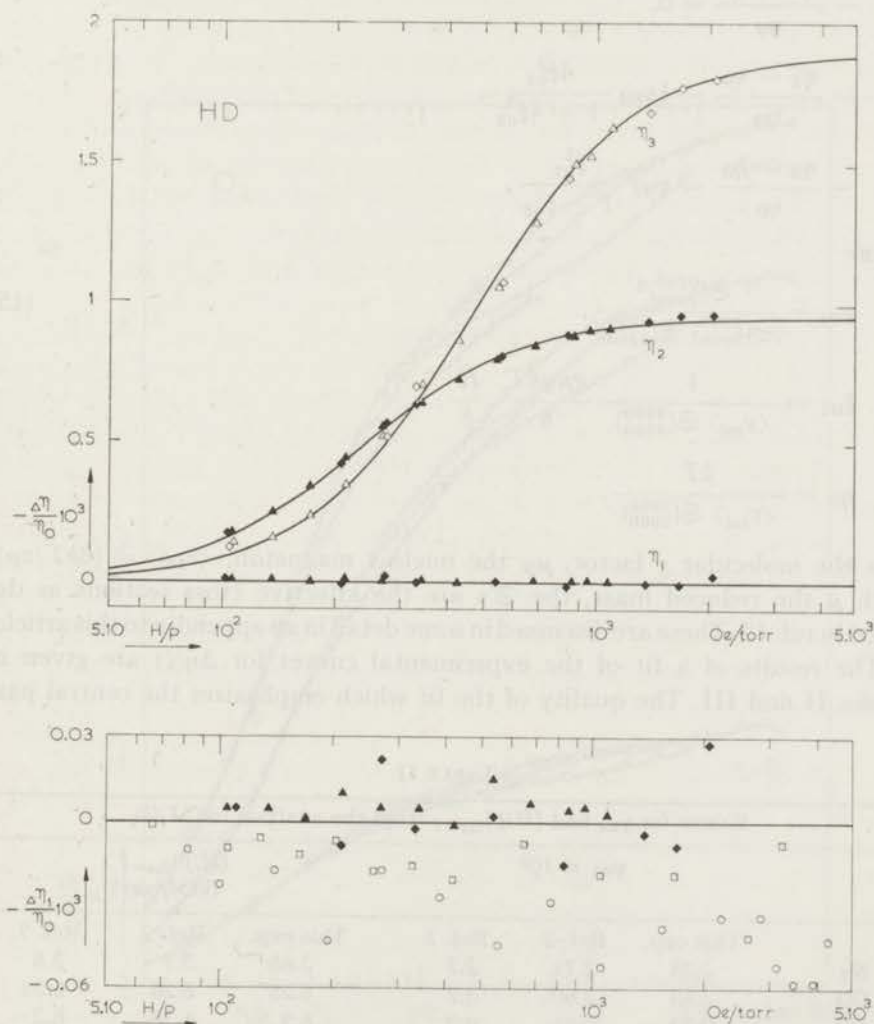


Fig. 14. a. $\Delta\eta_1$, $\Delta\eta_2$ and $\Delta\eta_3$ as functions of H/p for HD.
 b. $\Delta\eta_1$ with an expanded vertical scale. Symbols as in fig. 13.

extrapolation of these last results to more realistic potentials is permissible, especially where the inelastic cross sections are strongly dependent on the energy of the relative motion.

The fact, however, that $\Delta\eta_1$ is definitely nonzero shows that small contributions of different tensorial character are also present. Both $[W]^{(2)} J$ and $[W]^{(2)} [J]^{(2)}$ will be needed because $\Delta\eta_1$ can be both positive and negative.

Also in the framework of a slightly different theoretical approach one expects the expressions for the $[J]^{(2)}$ contribution¹¹⁾ to remain valid in first approximation. These expressions are:

$$\begin{aligned}
 -\frac{\eta_1 - \eta_0}{\eta_0} &= 0, \\
 -\frac{\eta_2 - \eta_0}{\eta_0} &= \frac{1}{2}\psi_{02} \frac{4\xi_{02}^2}{1 + 4\xi_{02}^2}, \\
 -\frac{\eta_3 - \eta_0}{\eta_0} &= \psi_{02} \frac{\xi_{02}^2}{1 + \xi_{02}^2},
 \end{aligned}$$

where

$$\psi_{02} = \frac{\mathfrak{S}_{(2000)}^{(0200)2}}{\mathfrak{S}_{(2000)}^{(2000)} \mathfrak{S}_{(0200)}^{(0200)}}, \quad (15)$$

$$\xi_{02} = \frac{1}{\langle v_{\text{rel}} \rangle \mathfrak{S}_{(0200)}^{(0200)}} \frac{g\mu_N kT}{\hbar} \frac{H}{p},$$

$$\eta_0 = \frac{kT}{\langle v_{\text{rel}} \rangle \mathfrak{S}_{(2000)}^{(2000)}}.$$

g is the molecular g factor, μ_N the nuclear magneton, $\langle v_{\text{rel}} \rangle = (8kT/\pi\mu)^{1/2}$ with μ the reduced mass, the \mathfrak{S} 's are the effective cross sections as defined in ref. 12. These are discussed in some detail in an appendix to this article.

The results of a fit of the experimental curves for $\Delta\eta(\zeta)$ are given in tables II and III. The quality of the fit which emphasizes the central part

TABLE II

	Values for ψ_{02} and $(H/p)_{\xi_{02}=1}$ from the analysis for $[J]^{(2)}$					
	$\psi_{02} \times 10^3$			$(H/p)_{\xi_{02}=1}$ (kOe/torr)		
	This exp.	Ref. 2	Ref. 7	This exp.	Ref. 2	Ref. 7
N ₂	2.78	2.71	2.7	3.65	3.7	3.5
CO	3.63	3.60	3.7	5.25	5.25	5.35
CH ₄	0.79	0.81	0.9	5.9	6.15	6.2
CF ₄	3.1		4.05	49		51
HD	1.90	1.87		0.46	0.48	

TABLE III

	$\mathcal{E}_{(2000)}^{(2000)}$ (\AA^2)	$ \mathcal{E}_{(0200)}^{(2000)} $ (\AA^2)	$\mathcal{E}_{(0200)}^{(0200)}$ (\AA^2)
N ₂	35	1.46	22
CO	35	1.97	31
CH ₄	42	1.01	30
CF ₄	63	3.4	59
HD	19	0.28	2.2

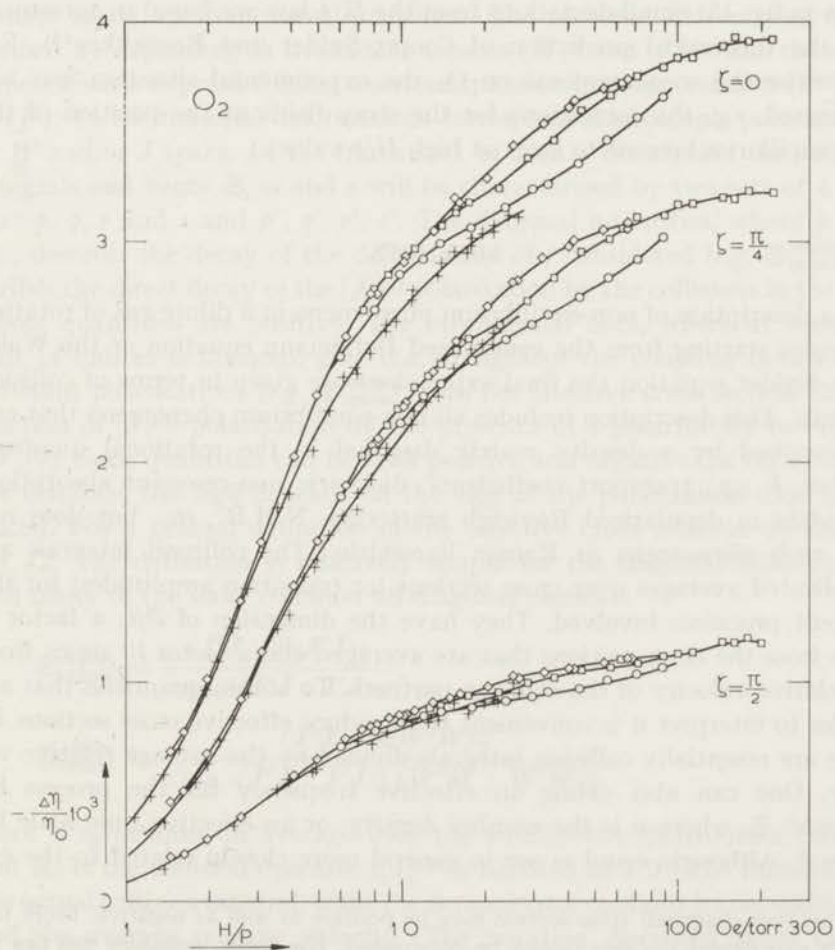


Fig. 15. The viscosity changes for O₂ as functions of H/p for $\zeta = 0, \pi/4$ and $\pi/2$.
 ○ 40.6 torr; ◇ 275 torr; □ 100 torr; + 817 torr.

of the curve can be seen in figs. 4-14 where the drawn curves correspond to the theoretical expressions. For the fitting procedure one prefers the results for the directly measured quantities $\Delta\eta(\zeta)$ to those for η_2 and η_3 which are calculated from these, since the accuracy of $\Delta\eta_3$ is relatively low. In table II the results for ψ_{02} and for the value of H/p for which $\xi_{02} = 1$, i.e. $(H/p)_{\xi_{02}=1}$, are compared with existing data. These have been obtained from different experiments, viz. in ref. 2 measuring η_4 and η_5 and in ref. 7 performing experiments on η_3 and $2\eta_2 - \eta_1 - \eta_3$. It is seen that the agreement between data from different sources is excellent. In table III the results are given in terms of the generalized cross sections $\mathfrak{S}_{(0200)}^{(0200)}$ and $|\mathfrak{S}_{(2000)}^{(2000)}|^\ddagger$. For comparison $\mathfrak{S}_{(2000)}^{(2000)}$ which follows from the field-free viscosity coefficient has been included.

Finally, some measurements have been performed on O_2 . The results are shown in fig. 15. Small deviations from the H/p law are found in agreement with the theoretical prediction of Coope, Snider and Beenakker¹⁴). For more extensive measurements on O_2 the experimental situation was not well suited, e.g. the corrections for the stray fields at the position of the other capillaries become too large at high H/p values.

APPENDIX

In a description of non-equilibrium phenomena in a dilute gas of rotating molecules starting from the generalized Boltzmann equation or the Waldmann-Snider equation the final expressions are given in terms of collision integrals. This description includes all non-equilibrium phenomena that can be described by a density matrix diagonal in the rotational quantum number J , e.g., transport coefficients, dielectric non-resonant absorption, linewidths in depolarized Rayleigh scattering, N.M.R., etc., but does not treat such phenomena as Raman linewidths. The collision integrals are complicated averages over cross sections (or transition amplitudes) for the different processes involved. They have the dimension of l^3/t ; a factor l^2 arises from the cross sections that are averaged and a factor l/t stems from the relative velocity of the collision partners. To obtain quantities that are simpler to interpret it is convenient to introduce effective cross sections \mathfrak{S} . These are essentially collision integrals divided by the average relative velocity. One can also define an effective frequency for the process by $\omega = n\langle v \rangle \mathfrak{S}$, where n is the number density, or an effective time scale by $\tau = \omega^{-1}$. Although τ and ω are in general more closely related to the ex-

[†] This (non-diagonal) cross section may be positive as well as negative. From the present experiment the sign cannot be determined. For linear molecules this can be done from measurements of flow birefringence. Such experiments have been performed by Baas¹³).

perimental results, they have the disadvantage of being density dependent, so that \mathfrak{S} is preferred. The collision integrals and hence \mathfrak{S} , ω and τ are different for the different transport processes. For a monatomic gas the different collision integrals that occur in the transport properties are distinguished by the two indices that label the well-known $\Omega^{(l,s)}$ integrals. For linear molecules the situation is more complicated because of the presence of angular momentum. Here, too, the use of a systematic notation has become necessary to be able to correlate the effective cross sections that occur in widely different physical phenomena. To obtain a systematic notation one observes that a non-equilibrium situation in a gas in the binary collision region is characterized by the deformation of the distribution function f . For rotating molecules f can depend on two vector quantities, the velocity \mathbf{W} and the internal angular momentum \mathbf{J} . Further it can depend on the scalars made up from these quantities. The tensorial deformation is described by expanding in irreducible tensors $[\mathbf{W}]^p$ and $[\mathbf{J}]^q$ while the scalar dependence is expressed using a series expansion in polynomials $S^r(W^2)$ and $R^s(J^2)$. To the tensorial deformations correspond macroscopic polarizations in \mathbf{W} and/or \mathbf{J} space. In the framework of such a description the collision integrals and hence \mathfrak{S} , ω and τ will be characterized by two sets of 4 indices: p, q, r and s and p', q', r', s' . The diagonal quantities, where $p = p'$ etc., describe the decay of the deformation of f considered (e.g. $\mathfrak{S}_{(0200)}^{(0200)}$ describes the direct decay of the $[\mathbf{J}]^{(2)}$ polarization by the collisions in the gas). These quantities are positive. The off-diagonal ones, where at least one pair of indices is unequal, give the strength of the coupling between the different polarizations (e.g. $\mathfrak{S}_{(2000)}^{(0200)}$ gives the effective cross section for production of $[\mathbf{J}]^{(2)}$ polarization by the presence of a polarization in velocity $[\mathbf{W}]^{(2)}$). Such quantities can be both positive and negative. In the example, for instance, the sign depends on the sign of the polarization that is produced. For a general definition of the effective cross sections we refer to ref. 12. The definition is relatively simple for the diagonal elements^{7,15}) and many of the more common off-diagonal elements

$$\mathfrak{S}_{(0200)}^{(0200)} = \frac{\langle \mathbf{J}^\circ \mathbf{J} : \mathfrak{R}_0 \mathbf{J}^\circ \mathbf{J} \rangle_0}{\langle v_{\text{rel}} \rangle \langle \mathbf{J}^\circ \mathbf{J} : \mathbf{J}^\circ \mathbf{J} \rangle_0},$$

$$\mathfrak{S}_{(2000)}^{(0200)} = \frac{\langle \mathbf{J}^\circ \mathbf{J} : \mathfrak{R}_0 \mathbf{W}^\circ \mathbf{W} \rangle_0}{\langle v_{\text{rel}} \rangle \langle \mathbf{J}^\circ \mathbf{J} : \mathbf{J}^\circ \mathbf{J} \rangle_0^{\frac{1}{2}} \langle \mathbf{W}^\circ \mathbf{W} : \mathbf{W}^\circ \mathbf{W} \rangle_0^{\frac{1}{2}}}.$$

Here $\langle \rangle_0$ denotes an average over the equilibrium distribution function and \mathfrak{R}_0 is the collision operator ($[\mathbf{J}]^{(2)}$ is denoted as $\mathbf{J}^\circ \mathbf{J}$.) The numerator is the actual collision integral, while the denominator contains its normalization and the average relative velocity. The notation discussed above can be simplified when there is no risk of confusion: a) for the diagonal elements one can write only one row of indices; e.g. $\mathfrak{S}(0200)$, b) if no problems with the scalar

dependence can arise, one can omit the last two zeros in the rows, *e.g.* $\mathfrak{S}_{(20)}^{(02)}$. Waldmann, Hess and collaborators use for the description of the viscosity in a magnetic field the notation σ_η , σ_T and $\sigma_{\eta T}$ for the cross sections $\mathfrak{S}_{(2000)}^{(2000)}$, $\mathfrak{S}_{(0200)}^{(0200)}$ and $\mathfrak{S}_{(2000)}^{(0200)}$ respectively. Such a notation is only suitable for simple cases and not for general use.

REFERENCES

- 1) De Groot, S. R. and Mazur, P., Non-Equilibrium Thermodynamics, North-Holland Publ. Comp. (Amsterdam, 1962) p. 311.
- 2) Hulsman, H., van Waasdijk, E. J., Burgmans, A. L. J., Knaap, H. F. P. and Beenakker, J. J. M., *Physica* **50** (1970) 53 (Commun. Kamerlingh Onnes Lab., Leiden No. 381c); this thesis, chapter II.
- 3) Hulsman, H., Burgmans, A. L. J., van Waasdijk, E. J. and Knaap, H. F. P., *Physica* **50** (1970) 558 (Commun. Kamerlingh Onnes Lab., Leiden No. 382b); this thesis, chapter III.
- 4) Beenakker, J. J. M. and McCourt, F. R., *Ann. Rev. Phys. Chem.* **21** (1970) 47.
- 5) Hulsman, H. and Knaap, H. F. P., *Physica* **50** (1970) 565 (Commun. Kamerlingh Onnes Lab., Leiden No. 383b); this thesis, chapter I.
- 6) Cornish, R. J., *Proc. Roy. Soc. A* **120** (1928) 691.
- 7) Korving, J., *Physica* **50** (1970) 27 (Commun. Kamerlingh Onnes Lab., Leiden No. 381b).
- 8) Vestner, H., *Verhandl. Deut. Physik. Ges. (VI)* **6** (1971) 539.
- 9) Burgmans, A. L. J., *et al.*, *Physica*, to be published.
- 10) Coope, J. A. R. and Snider, R. F., to be published.
- 11) McCourt, F. R. and Snider, R. F., *J. chem. Phys.* **47** (1967) 4117.
- 12) McCourt, F. R. and Moraal, H., *Chem. Phys. Letters* **9** (1971) 39.
- 13) Baas, F., *Phys. Letters* **36 A** (1971) 107.
- 14) Beenakker, J. J. M., Coope, J. A. R. and Snider, R. F., *Phys. Rev.* in press.
- 15) Hermans, L. J. F., Schutte, A., Knaap, H. F. P. and Beenakker, J. J. M., *Physica* **46** (1970) 491 (Commun. Kamerlingh Onnes Lab., Leiden No. 375b).

CHAPTER V

THERMOMAGNETIC SLIP IN RAREFIED POLYATOMIC GASES

Synopsis

We have verified experimentally that in a rarefied polyatomic gas the combination of a magnetic field and a temperature gradient can give rise to a slip velocity tangential to the wall. In a channel formed between two parallel plates at different temperatures this slip velocity gives rise to a pressure difference Δp . For not too low pressures, p , the quantity $p\Delta p/\Delta T$ is approximately a function of H/p only. Preliminary results are shown for N_2 .

In the discussion of the thermomagnetic torque discovered by Scott and coworkers¹⁾ the possibility of the existence of a "thermomagnetic slip" has become apparent. This slip is caused by the action of a magnetic field on a rarefied polyatomic gas when a temperature gradient perpendicular to the wall is present. The slip manifests itself as a velocity of the gas tangential to the wall. According to Waldmann^{2,3)} such a boundary layer phenomenon gives an important contribution to the Scott torque. In his explanation the slip is created by the interaction of molecular angular momentum with the wall. The magnitude and the sign of this slip are unknown, as very little is known on the interaction of the internal angular momentum of a rotating molecule with a surface. Levi and Beenakker^{4,5)} have suggested the presence of another slip contribution originating from transverse heat flow. Their mechanism is the same as the one that causes the, so called, thermal creep. This contribution to the torque can be calculated. It is small and has the opposite sign. In the view of these authors the major contribution to the torque stems from a bulk effect associated with the influence of a magnetic field on the Maxwell stress⁴⁻⁶⁾. In rarefied gases

this stress is associated with the occurrence of $\nabla \nabla T$. Theoretically, it is part of the second order Chapman-Enskog theory. In the torque experiment it is very difficult to distinguish between these three contributions. The experimental torque data available by now (e.g. refs. 7, 8) seem to point to the presence of both a stress and a slip contribution of opposite sign, the thermal stress being the larger³). As the Scott effect is one of the few cases where one can test the second-order Chapman-Enskog theory in a stationary situation, it is important to obtain the contributions separately. Following a suggestion by Waldmann²), we have made measurements under experimental conditions where no $\nabla \nabla T$ is present. Hence our results give direct information on the boundary layer effects.

The experimental setup is the following. The gas is contained in a channel formed between two parallel plates that are held at different temperatures. When a field is applied perpendicular to both the temperature gradient and the length l of the channel it causes a slip velocity along the wall in the direction of l . This gives rise to a pressure gradient along the channel. To get a measurable pressure difference under circumstances where Knudsen effects are not too important, it is necessary to work with a long channel. This has been achieved by placing 20 "elementary cells" in series between the poles of the magnet. In fig. 1 the actual arrangement is shown schematically: a hot plate is sandwiched between two cold plates, and the channel runs like a spiral around the hot plate. In such an arrangement the slip direction follows the spiral and the effects of upper and lower channels

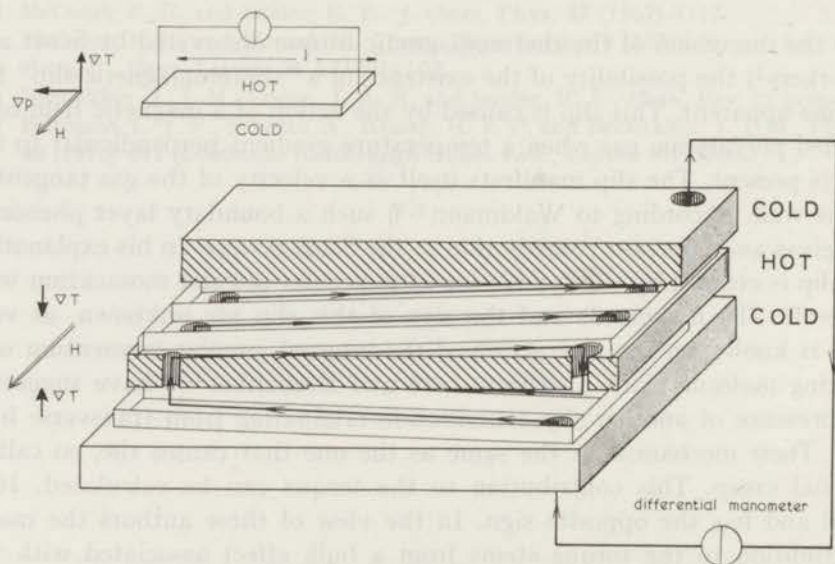


Fig. 1. Schematic diagrams of the apparatus.

add up, making a total length of 20×170 mm. The walls separating the channels are made of low-thermal-conductivity polyester of a 0.3 mm thickness; they are glued into slots cut into the plates. The distance of 1.8 mm between the plates is fixed by means of glass spacers. To guaranty the homogeneity of the temperature the hot plate is heated by means of 18 heaters distributed through the plate. The cold plates are water cooled. Typical temperature differences are between 5 and 40°C . The apparatus is surrounded by a vacuum jacket.

Measurements have been performed for N_2 , CO, HD and CH_4 . As an example, the results for N_2 are shown in fig. 2, where the quantity $p\Delta p/\Delta T$ has been plotted vs. H/p . Here p is the pressure, Δp the pressure difference over the channel, H the magnetic field and ΔT the temperature difference between hot and cold plates corrected for the temperature jump at the walls. In the figure one sees that for these (relatively high) pressures $p\Delta p/\Delta T$ is nearly a function of H/p only. This is to be expected, as for a boundary-layer effect Δp should be proportional to $1/p$, while the H/p dependence indicates that this effect belongs to the Senftleben-Beenakker class of phenomena (for a survey see e.g. ref. 9). The small deviations from the H/p behaviour are essentially the same as the deviations observed in the measurement of the ordinary (*dilute gas*) transport coefficients. All curves for different pressures can be brought to coincidence by application of Knudsen corrections $(1 + K/p)$ both on the magnitude of the effect and on the position of the curves on the H/p axis (see e.g. ref. 10). The extra-

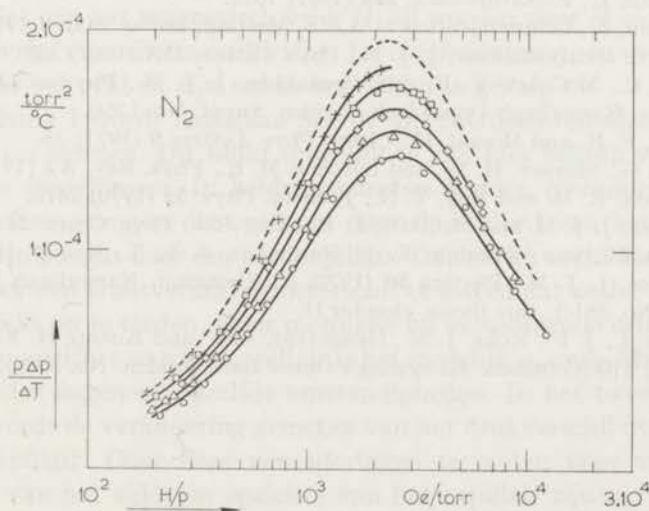


Fig. 2. $p\Delta p/\Delta T$ vs. H/p for N_2 .

+ $p = 9.27$ torr; \square $p = 5.43$ torr; \triangle $p = 2.26$ torr; \diamond $p = 3.21$ torr;
 \circ $p = 1.63$ torr; ----- extrapolated curve corresponding to $p = \infty$.

polated curve, corresponding to $p = \infty$ has been included in the figure. The absolute value of the effect, as determined in this preliminary experiment is still rather uncertain: a scale factor of at most 1.5 cannot be excluded. The direction of the pressure gradient is for N_2 and CO as indicated in fig. 1, while for HD and CH_4 , which have opposite g factors, the opposite direction is found. In all cases this slip would produce a torque opposite to the one measured in the Scott effect. This is in agreement with a picture that two contributions of opposite sign are present in the Scott effect. The magnitude of the slip effects encountered here is such that these should contribute significantly to the Scott torque. The slip mechanisms discussed above predict that the effect should occur at values of H/p associated with the Kagan polarization in the heat flow. Experimentally, however, one observes that for N_2 , CO and CH_4 the value of H/p for which the maximum is reached in this experiment is approximately a factor two lower than the values occurring in heat-conductivity measurements¹¹). For HD the difference is smaller, but there the curve spreads over such a range of H/p values that the presence of a contribution at lower H/p values is suggested. More experimental and theoretical work will be needed to clarify the situation. Further experiments are now in progress, detailed information will be published in due course.

REFERENCES

- 1) Scott, G. G., Sturner, H. W. and Williamson, R. M., Phys. Rev. **158** (1967) 117.
- 2) Waldmann, L., Z. Naturforsch. **22a** (1967) 1678.
- 3) Waldmann, L., Communication at A.P.S. Meeting, Dallas, March 1970.
- 4) Levi, A. C. and Beenakker, J. J. M., Phys. Letters **25A** (1967) 350.
- 5) Levi, A. C., McCourt, F. R. and Beenakker, J. J. M., Physica **42** (1969) 363 (Commun. Kamerlingh Onnes Lab., Leiden, Suppl. No. 126e).
- 6) McCourt, F. R. and Moraal, H., Chem. Phys. Letters **9** (1971) 35.
- 7) Scott, G. G., Sturner, H. W. and Larchez, M. E., Phys. Rev. **A2** (1970) 792.
- 8) Williamson, R. M. and Roy, T. N., J. chem. Phys. **53** (1970) 2478.
- 9) Beenakker, J. J. M. and McCourt, F. R., Ann. Rev. Phys. Chem. **21** (1970) 47.
- 10) Hulsman, H., van Waasdijk, E. J., Burgmans, A. L. J., Knaap, H. F. P. and Beenakker, J. J. M., Physica **50** (1970) 53 (Commun. Kamerlingh Onnes Lab., Leiden, No. 381c); this thesis, chapter II.
- 11) Hermans, L. J. F., Koks, J. M., Hengeveld, A. F. and Knaap, H. F. P., Physica **50** (1970) 410 (Commun. Kamerlingh Onnes Lab., Leiden, No. 378a).

SAMENVATTING

In dit proefschrift worden experimenten beschreven over de invloed van een uitwendig magnetisch veld op de viscositeit, η , van meeratomige gassen. In het algemene geval van een visceus medium wordt het verband tussen impulsstromen en snelheidsgradiënten bepaald door een vierde rangs viscositeits tensor. Voor een gas in een homogeen magnetisch veld kan men met behulp van symmetrie relaties aantonen dat deze tensor zeven onafhankelijke elementen bevat. Vijf van deze elementen zijn schuif viscositeits coëfficiënten en worden η_1, \dots, η_5 genoemd. Van deze coëfficiënten zijn η_1, η_2 en η_3 even functies van het magnetisch veld, H , zij worden voor $H = 0$ gelijk aan η_0 , de veldvrije viscositeits coëfficiënt. De coëfficiënten η_4 en η_5 zijn oneven functies van het veld en zijn nul in het veldvrije geval.

In hoofdstuk I wordt nagegaan hoe de vijf coëfficiënten afzonderlijk bepaald kunnen worden. Dit blijkt mogelijk te zijn met behulp van twee experimentele opstellingen. In beide apparaten worden (veranderingen van) drukverschillen gemeten die ontstaan door de invloed van het veld op de stroming van het gas door een plat capillair. De oneven coëfficiënten worden bepaald door een transversaal drukverschil te meten dat onder invloed van het veld blijkt op te treden. Door metingen bij verschillende oriëntaties van het veld ten opzichte van het capillair is het mogelijk η_4 en η_5 afzonderlijk te bepalen onder nagenoeg dezelfde omstandigheden. In het tweede type experiment wordt de verandering gemeten van het drukverschil over de lengte van het capillair. Door deze veranderingen te meten voor verschillende oriëntaties van het veld ten opzichte van het capillair zijn η_1, η_2 en η_3 afzonderlijk te bepalen.

In hoofdstuk II en III worden resultaten gegeven van experimenten ter bepaling van de oneven coëfficiënten. Eerst wordt nader ingegaan op de be-

rekening van η_4 en η_5 uit de waargenomen transversale drukverschillen. Met name wordt de afhankelijkheid van het drukverschil van de dimensies van het apparaat experimenteel nagegaan, verschillende correcties worden bepaald en systematische fouten worden afgeschat. Vervolgens worden resultaten gegeven voor de gassen N_2 , CO, HD en CH_4 bij kamertemperatuur. Bij een vergelijking met de theorie blijkt dat de dominante bijdrage tot het effect afkomstig is van de $[J]^{(2)}$ anisotropie van de verdelingsfunctie van de impulsmomenten J . In hoofdstuk III worden resultaten gegeven voor η_4 en η_5 van O_2 . Deze coëfficiënten vertonen een zeer ingewikkelde afhankelijkheid van veldsterkte en druk.

In hoofdstuk IV worden experimenten aan de even coëfficiënten beschreven. Hierbij worden η_1 , η_2 en η_3 bepaald voor de gassen N_2 , CO, HD, CH_4 en CF_4 . De resultaten blijken consistent met die voor η_4 en η_5 : ook hier blijkt de $[J]^{(2)}$ bijdrage dominant te zijn en de waarden voor de effectieve botsingsdoorsneden, waarin de resultaten zijn uit te drukken, komen zeer goed overeen met die bepaald uit η_4 en η_5 . De kleine afwijkingen van een zuiver $[J]^{(2)}$ gedrag, die in alle gevallen gevonden zijn, worden besproken. In een appendix wordt nader ingegaan op het gebruik van effectieve botsingsdoorsneden.

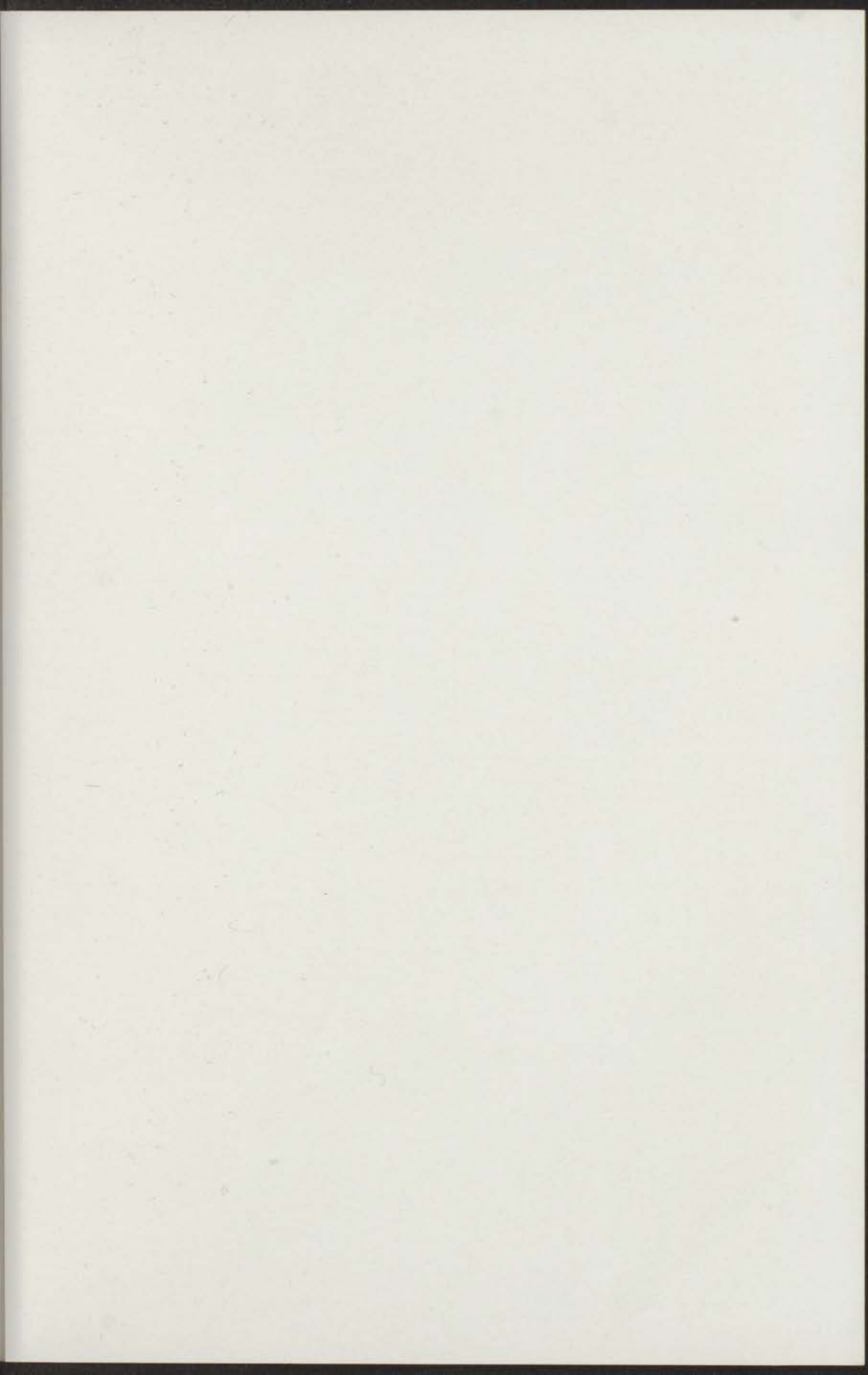
In hoofdstuk V worden enkele voorlopige resultaten gemeld van metingen aan een nieuw verschijnsel: de thermo-magnetische slip. Het blijkt dat in een sterk verdund gas onder invloed van een magnetisch veld en een temperatuurgradiënt een stroming van het gas langs de wand ontstaat.

Op verzoek van de faculteit der Wiskunde en Natuurwetenschappen volgen hier enkele gegevens over mijn studie.

Na mijn Gymnasium- β opleiding van 1952 tot 1959 aan het Huygens Lyceum te Voorburg begon ik in september 1959 mijn studie aan de Rijksuniversiteit te Leiden, waar ik in 1963 het kandidaatsexamen Natuurkunde en Wiskunde met als bijvak Sterrekunde aflegde. Sindsdien ben ik op het Kamerlingh Onnes Laboratorium werkzaam in de werkgroep voor Molecuulfysica onder leiding van Prof. Dr. J. J. M. Beenakker en Dr. H. F. P. Knaap. Veel experimentele ervaring deed ik op onder leiding van Dr. J. Korving. In 1965 werkte ik gedurende enkele maanden in het "Instituut voor Lage Temperaturen en Technische Fysica" te Leuven. Vanaf 1964 ben ik werkzaam op het natuurkundig practicum en vanaf 1966 assisteer ik voorts bij het college moleculaire natuurkunde. In 1966 legde ik het doctoraalexamen experimentele natuurkunde af en begon aan het in dit proefschrift beschreven onderzoek. Sinds mei 1966 ben ik als wetenschappelijk medewerker in dienst van de Stichting voor Fundamenteel Onderzoek der Materie (F.O.M.).

De experimenten werden verricht in samenwerking met achtereenvolgens de heren Drs. A. M. Vossepoel, Drs. E. J. van Waasdijk, Drs. A. L. J. Burgmans, K. W. Walstra en F. G. van Kuik. Het apparaat, beschreven in het laatste hoofdstuk, werd ontworpen in samenwerking met Drs. A. Schutte. De technische realisering van de verschillende apparaten was bij de heren J. M. Verbeek en P. Zwanenburg in bekwame handen. De technische voorzieningen kwamen tot stand dankzij inspanning van velen, van wie ik hier de heren J. Turenhout, J. Dunsbergen en T. A. van der Heijden met name wil noemen. De tekeningen van dit proefschrift zijn verzorgd door de heren

W. F. Tegelaar en J. Bij, terwijl mej. A. M. Aschoff en mej. S. M. J. Ginjaar zorgden voor het uittypen van het manuscript. De verschillende hoofdstukken werden op Engels taalgebruik gecorrigeerd en van kritische opmerkingen voorzien door Dr. F. R. McCourt, Dr. V. G. Cooper, Dr. N. D. Hamer en Prof. Dr. C. M. Knobler.



W. J. Dreyer en J. M. G. van der Meer, A. M. A. van der Meer en J. M. J. G. van der Meer
deelden met het schrijven van het manuscript. De voorbladzijde is het
aan schrijven op Engels taal- en literatuurwetenschap en de afsluitende opmerkingen
zijn geschreven door Dr. P. H. M. G. van der Meer, Dr. V. G. van der Meer, Dr. H. D. van der Meer en
Prof. Dr. C. M. Koster.

